ADVANCED MASTERS IN STRUCTURAL ANALYSIS
OF MONUMENTS AND HISTORICAL CONSTRUCTIONS

Master's Thesis

Marina Polónia Rios

Structural performance of shells of historical constructions: The Municipal Theatre of Rio de Janeiro.

This Masters Course has been funded with support from the European Commission. This publication reflects the views only of the author, and the Commission cannot be held responsible for any use which may be made of the information contained therein.

Portugal | 2017

DECLARATION

Name: Marina Polónia Rios

Email: mariprios@gmail.com

Title of the Msc Dissertation: Structural performance of shells of historical constructions: The Municipal Theatre of Rio de Janeiro

Supervisor(s): Nuno Mendes, Deane Roehl

Year: 2017

I hereby declare that all information in this document has been obtained and presented in accordance with academic rules and ethical conduct. I also declare that, as required by these rules and conduct, I have fully cited and referenced all material and results that are not original to this work.

I hereby declare that the MSc Consortium responsible for the Advanced Masters in Structural Analysis of Monuments and Historical Constructions is allowed to store and make available electronically the present MSc Dissertation.

University: University of Minho

Date: 27/07/2017

Signature: _____

ACKNOWLEDGEMENTS

Firstly, I would like to thank my supervisors, Professor Nuno Mendes and Professor Deane Roehl, for their guidance and support during this process. Especially, I express my gratitude to Dr. Mendes, for the hard work and for always being there for me when I needed.

I acknowledge the SAHC Consortium for granting me the opportunity to attend this Master and providing financial support.

I would like to present also my thankfulness for Danielli Cintra and Giorgos Karanikoloudis for their support throughout this process. Besides, I would like to thank Geraldo, Juliana and Marisa, for sharing their knowledge and enthusiasm regarding the structure object of this study.

I present also my deep appreciation to all the SAHC lecturers, for their teaching and assistance during the master, particularly to Professor Pere Roca and Professor Luca Pelá for their guidance in the first part of the master.

To my SAHC colleagues and friends, for making this year unforgettable.

My eternal gratitude to my family, for their unconditional support and encouragement, who made enormous effort to reduce the distance and always be close to me. I would like to remember especially Felipe, who came into world bringing joy and love.

An especial thanks to Raoni, who shared this amazing experience with me.

ABSTRACT

Heritage construction must be object of special care due to its historical and cultural value. In the modern concept, conservation of these structures should mainly respect their authenticity. With this in view, prior to any intervention on the structure, a detailed study should be carried out to guarantee full understanding on the structure conditions, allowing the minimum intervention to be applied. The analysis of these structures should gather most information as possible on the structural conditions, involving historical research, visual inspection, non-or minor destructive tests, monitoring and numerical modelling. The structural analysis by numerical simulation is crucial for understanding the structural behaviour under different conditions, allowing evaluate causes of damages, capacity of the structure and the efficiency of strengthening techniques.

The object of this study is the Municipal Theatre of Rio de Janeiro, built in the beginning of the 20th century and considered a masterpiece of the Brazilian eclectic style. This work is mainly focused on the structural analysis of the shells located on the front part of the theatre, namely a barrel vault and two lateral domes. In general, the structure presents itself in good conditions. However, important damages were reported in the 1970s, that led to an intervention in order to guarantee the structural safety.

The study is divided in four main parts, namely (i) a study on the state of the art of structural analysis of shell elements made of masonry together with a historic and architectonic review on the theatre, (ii) in-situ investigation by NDT tests, such as dynamic identification tests, (iii) preparation of the numerical model, including its calibration and validation by comparison with experimental data, (iv) non-linear structural analysis, aiming at identifying the possible cause of reported damage and evaluation on the structural capacity.

According to the results obtained in this study, the differential soil settlements can be one of the causes for the damages identified in the 1970s, namely settlements at the base of the main façade and towers. The shells present a considerable safety level under vertical loads and the strengthening intervention performed in 1970 increased significantly the load capacity of the barrel vault. Even though the study carried out allows a good understanding on the structural behaviour of the shell elements, further analysis is recommended in order to improve the current conclusions.

RESUMO

Análise estrutural de cascas em construções históricas: Theatro Municipal do Rio de Janeiro

As construções históricas devem ser tratadas com especial cuidado devido ao seu valor histórico e cultural. De acordo com os conceitos atuais, essas estruturas devem ser conservadas respeitando a sua autenticidade. Desta forma, é necessário um estudo detalhado antes de qualquer intervenção no edifício, permitindo um conhecimento detalhado sobre as propriedades estruturais, garantindo assim que a intervenção seja mínima. A análise dessas estruturas deve reunir a maior quantidade de informação possível. Deste modo, deve-se realizar uma pesquisa histórica, inspeção visual, ensaios não ou semi-destrutivos, monitoramento e a execução de análises numéricas. A análise estrutural através de simulações numéricas é essencial para entender o comportamento da estrutura sob diferentes condições, permitindo avaliar as causas de danos, a capacidade da estrutura e avaliar a eficiência de técnicas de reforço.

O objeto desse estudo é o Theatro Municipal do Rio de Janeiro, construído no início do século XX, considerado uma obra-prima do estilo eclético no Brasil. Esse trabalho tem por objetivo principal a análise estrutural das cascas localizadas na parte frontal da construção, incluindo uma abóboda de berço central e dois domos laterais. Em geral, a estrutura apresenta-se em boas condições de conservação. No entanto, na década de 1970 foram detetados danos que levaram a uma intervenção nas cascas para garantir a sua estabilidade estrutural.

Este trabalho está divido em quatro partes, incluindo: (i) uma pesquisa do estado da arte sobre a análise estrutural de elementos de casca, em conjunto com uma investigação sobre a história e arquitetura do teatro; (ii) investigações das condições estruturais *in-loco* através de testes não destrutivos, abarangendo ensaios de identificação dinâmica; (iii) preparação de um modelo numérico, englobando a sua calibração e validação através da comparação com os resultados obtidos experimentalmente; (iv) execução da análise estrutural não-linear estática, tendo por objetivo identificar possíveis causas para o dano relatado nos anos 1970 e avaliar da capacidade da estrutura.

De acordo com os resultados deste estudo, os assentamentos diferencias do solo são uma das causas prováveis para os danos observados em 1970, particularmente assentamento diferenciais na base da fachada principal e da torres laterais. A análise da capacidade de carga da estrutura comprovou que as cascas apresentam um considerável nível de segurança para ações verticais. Por fim, foi concluído que as intervenções realizadas em 1975 aumentaram substancialemente a capacidade estrutural da abóbada de berço. Os estudos realizados permitem obter um bom nível de conhecimento a cerca do comportamento estrutural dos elementos de casca. Porém, são recomendados outros estudos complementares com o objetivo de aprimorar as conclusões atuais.

TABLE OF CONTENTS

LIST OF FIGURES

LIST OF TABLES

1. INTRODUCTION

1.1 Motivation

Historical constructions are an important aspect in the formation of different cultures. Due to limited exchange of information between countries in ancient years, each culture developed its own constructive techniques leading to different typologies of construction according to the location and period in history. Hence, these structures must be object of special care in order to guarantee its conservation through time, including a careful process of diagnosis and reliability assessment in order to define efficient and appropriated intervention when necessary.

Structural analysis by numerical modelling is a powerful tool in order to better understand the structural behaviour of these buildings, contributing to all phases of project, from diagnosis to definition of intervention (Mazziotti, 2016). However, it requires several input information with details regarding structural geometry, material properties, internal morphology, existing damage and construction techniques that usually are not available in the case of historical constructions (Roca et al., 2010). Historical investigation together with inspection techniques, known as non or minor destructive tests, such as thermography, GPR, monitoring, flat-jack tests, are necessary to overcome this problem (Elyamani, 2015).

The structural analysis of masonry buildings is a great challenge, since masonry is a composite material with units and joints, for which the characterization of its material properties is difficult. The material properties of masonry depend on several aspects, such as the techniques applied during the construction. Furthermore, masonry presents a highly non-linear behaviour. Hence, it is fundamental to calibrate numerical models with in field information to achieve reliable results.

Among the techniques that can be used for model calibration, dynamic identification is a method that presents relevant information for the historical constructions. It consists in measuring the acceleration in different points of the structure to estimate the dynamic properties, namely natural frequencies, mode shapes and damping ratios, which can be used for the modal updating of models.

This study aims to evaluate the structural behaviour of masonry shells of the Municipal Theatre of Rio de Janeiro. This theatre is an impressive example of the eclectic architectonic movement in Brazil, from the beginning of the 20^{th} century. The eclecticism is characterized by the mix of different architectural styles from the past, in order to create a new architectonic language. This movement was only recognized by its cultural value in the 1970s. Hence, there are few constructions left with these characteristics. With this in view, the Municipal Theatre of Rio de Janeiro becomes even more important, since it is a representative piece of this architectonic style with refined decoration and great variety of construction techniques and materials (Machado, 2012).

The structure of the theatre consists in load bearing masonry walls in the perimeter with metallic structure in the interior. The construction is divided in three main parts: (i) the foyer, which consists in the entrance hall, the main stairs and two lateral resting rooms, (ii) the concert hall, with the audience divided in four levels and (iii) the stage together with the structure that holds the equipment and scenarios. The object of this study are the three shells located in the first part: a barrel vault over the foyer room and two spherical domes, over the lateral resting rooms. These shells are made of masonry and have been object of a strong intervention in the 1970s, in which a layer of reinforced concrete was applied over the existing masonry. There are few documents of such intervention, increasing the difficulty in identifying the structural characteristics of these elements.

In order to have a fully understanding on the structural behaviour of the mentioned shell elements, the structural analysis by means of numerical modelling was performed. NDT tests to gather information related to the structural elements were carried out. The numerical model was calibrated and validated according to the results of the in-situ tests and the non-linear analysis was performed to simulate the structural behaviour of these elements.

1.2 Objectives

The main objective of this dissertation is to evaluate the structural behaviour of shell elements in the Municipal Theatre of Rio de Janeiro, identifying the possible causes of previous damage, evaluate the structural capacity and the effectiveness of reinforcement intervention applied on the shells. Furthermore, this work involves the following task and particular objectives:

a) In situ dynamic identification tests and visual inspection, aiming at estimated the dynamic properties, geometric properties, types of structural elements and damage.

b) Preparation of a numerical FEM model, including calibration based on the experimental dynamic properties.

c) Performance of non-linear analysis, aiming at identifying the possible cause of the damage that led to the intervention in 1975, namely a study for the soil-structure interaction.

d) Assessment of the load capacity of the shell elements based on non-linear static analysis for the unstrengthened configuration.

e) Evaluation of the effectiveness of the strengthening intervention applied on the shells.

1.3 Thesis outline

This thesis is organised in seven chapters, which are described in this Section. Chapter 1 explains briefly the motivation of the work, the main objectives of the thesis, and the overall organisation of the thesis.

Chapter 2 presents an overview on the structural behaviour of vaults and domes, including a review of the state-of-the-art of structural analyses for these elements and masonry construction in general.

Chapter 3 presents the historical and architectural survey regarding the Municipal Theatre of Rio de Janeiro, together with the main structural aspects of the shells under study and the description of previous intervention works carried out in the building.

Chapter 4 summarizes the inspection works carried out in the Municipal Theatre of Rio de Janeiro, namely visual inspection, thermography, pachometry and dynamic identification tests. The structural properties and the current condition of the building are discussed based on these works.

Chapter 5 introduces the main aspects considered in the development of the numerical model, such as geometrical and material features. A preliminary linear static and eigenvalue analyses are presented. The numerical model was calibrated, based on the experimental results obtained from the dynamic identification tests. The modal updating was performed assuming the moduli of elasticity of the materials as variables of calibration.

Chapter 6 presents the non-linear analysis of the theatre. The interaction between soil and structure was evaluated in order to estimate the possible cause of the previous damages. Additionally, a study on the load capacity of the shells was performed. Finally, the improvement of the structural behaviour provided by the layer of concrete introduced in the intervention of 1975 was assessed.

Chapter 7 presents the conclusions. Discussion on the results and recommendations for further studies are also stated.

2. OVERVIEW OF VAULTS AND DOMES

2.1 Introduction

In the early history, constructions were mainly made of stones, with most of them made of piers and lintels as structural elements. However, this led to the need of enormous pieces, being hard to transport and limiting the construction span. Applying several small pieces of stones in an arched shape proved to be a successful solution that allowed not only the increase of spans but also the reduction in costs with transport and facilitating the construction. In general, arches are constructed by the assemblage of stones, one beside the other over a centering. Once the last piece on the top – the crown – is placed, the centering can be removed. If the geometry of the arch is correct, the reaction between the pieces and the loads acting on the structure will be in equilibrium, resulting in a self-stable structure (Huerta, 2004). Ceilings could be provided by the construction of continuous arches, being named as vaults.

Vaults and domes can be defined as curved structures used to provide ceiling to spaces, being especially applied in important constructions, such as palaces and churches due to their valuable aesthetic features. They can assume different shapes, which vary according to their use, type of structure, location, period in history and others. Their structural behaviour and construction techniques may differ according to their shape.

The main characteristic of a vaulted structure is stability, provided solely by mobilizing compression forces at the cross-sections. These forces transfer the applied loads to the supports in the vault base by inclined components. Hence, these structures have an important horizontal reaction at the base. For this reason, they need to present adequate support conditions provided by elements capable of resisting such thrusts. This is the most crucial aspect to guarantee stability.

Most vaults and domes are made of masonry, which is a complex material due to its composite character of units and mortar. It presents great strength under compression, with brittle response in tension and frictional response in shear, being characterized by its heterogeneity and anisotropy (Roca et al., 2010). Hence, structural analysis methods for masonry structures should consider the parameters mentioned above for evaluating in-plane and out-of-plane failure mechanisms (Tralli, Alessandri, & Milani, 2014).

2.2 History

Distinct cultures constructed vaults and domes using a variety of local materials such as wood, mud-brick and stones. They have been built from pre-history until modern times, being the predominant type of roof for large constructions until the middle of the 19th century, with the advent of metallic and reinforced concrete structures, resistant to tensile stresses. The earliest structures of this type were likely domed huts made from saplings, reeds, or timbers and covered with thatch, turf, or skins.

Materials may have transitioned to rammed earth or more durable ones like stone as a result of the local conditions, being the most common one masonry – with brick or stone units (Mainstone, 2001).

The main difficulty in building vaults was the need for centering, which was highly expensive and time-demanding. One possible solution was the false-vault, which consists in a sequence of self-stale cantilevers. This solution, however, allowed only small spans at a high cost of material and height. Timber centering was the most usual technique for vault construction, which could be substituted by rubble fillings and mounds or smart construction techniques that avoided the use of centering, such as the Catalan vaults.

The Romans were responsible for truly spreading this technique, since they made extensive use of arches, vaults and domes in their construction. The use of pozzolan concrete made it easier to build this type of structure, since it was adaptable to curved shapes. Its high strength also allowed large spans of up to 20m for vaults and 40m for domes. Examples of famous vaulted and domed constructions made by Romans are the Basilica Nova (Figure 1) – built between 308 and 312 AD having the main nave covered by vaults of 25m span – and the Pantheon (Figure 2) – built in 125 AD with a dome of 43.3m, being the biggest span until the 15th century.

Figure 1 - Basilica Nova's vaults

Figure 2 - Pantheon's Dome ("Great Buildings Image - Pantheon," n.d.)

The Byzantines also built several vaulted and domed constructions. They developed further the technology from the Romans, adapting the structure to the trajectory of forces with the use of ribbed domes and buttresses instead of massive walls. This lead to lighter structures and reduction in the material consumption. The main material used in byzantine construction is masonry made of rubble material with lime mortar. The main example of byzantine building is the Hagia Sophia Church, with an impressive dome with 31m of span and several vaulted and arched elements.

The Romanesque construction style prevailed in Europe from the 10th to 12th centuries and are much simpler than the ones mentioned previously, with extensive use of barrel vaults and massive three-leaf walls. These structures are characterized by their redundancy and ductility.

The Gothic construction is characterized by the skeletal type of construction, with use of arches, ribs, flying arches, piers and buttresses. The path of the load was well worked, channelling the loads towards the buttress and foundation, leading to clear spaces and material safe. One great advantage of this construction period was the development of gothic cross vaults (Figure 3), since it only requires centering in the arches and ribs. Another convenience of this type of vault is the confinement provided by the arches and ribs, presenting less cracks than the unconfined Roman domes.

Figure 3 – Gothic Vaults in Saint Chapelle ("Sainte Chapelle: The Radiating Cathedral," n.d.)

During the Renaissance period (15th and 16th centuries), domes were recovered as roofing solution for important buildings. The construction typology combines Roman and Gothic techniques, as is easily recognized in the dome of Florence (Figure 4) - the most emblematic dome in the world, with a span of 43.6m and 33m rise. It is characterized by the pointed geometry that leads to smaller horizontal thrust and ribbed structure with double membrane.

Figure 4 – Florence Dome – outside view ("Brunelleschi's Dome: Florence Cathedral, Florence Duomo," n.d.)

In the 17th and 18th centuries the idea of double vaults was developed. This allowed the clean spaces inside the buildings with an outstanding structure outside. The true dome that behave as a shell is the internal one, while the external one is considered a false dome, supported in a trussed structure. This type of structure was widely used in India and Europe, with the emblematic examples of the Taj Mahal and Saint Paul's Cathedral.

2.3 Mechanical properties

Masonry is a composite material made by the assemblage of units – stone, brick or adobe – usually connected by mortar joints. The global mechanical properties of masonry depend on the dimensions and mechanical properties of each element, and the behaviour of the interface between units and mortar joints. Moreover, the arrangement of units and the constructive techniques also influence the final behaviour of the material, leading to a wide range of values for the mechanical properties of masonry. Furthermore, the material properties depend on the conservation status, since masonry can present alterations associated to different types of damage. Hence, mechanically characterizing historical masonry is a complex task that depend on many factors. Some guidelines, such as the Italian code "*Circolare sul nuove norme tecniche per le costruzioni*" (2008), present estimations of

material properties as function of the main characteristics of masonry (Table 1). These values should be altered by confidence factors according to the level of knowledge of the structure and material.

Table 1 – Mechanical properties for masonry according to masonry typology (Addapted from NTC-08, 2008)

Type of masonry	f_m	τ_0	***E***	***G***	***w***
	(N/cm^2)	(N/cm^2)	(N/cm^2)	(N/cm^2)	(kN/m^3)
	min-max	min-max	min-max	min-max	
Irregular stone masonry (cobblestone, erratic and irregular stones)	100 180	2.0 3.2	690 1050	230 350	19
Stone masonry with voids, limited thickness and inner core	200 300	3.5 5.1	1020 1440	340 480	20
Masonry with shaped stone units with good texture	260 380	5.6 7.4	1500 1980	500 660	21
Soft stone masonry (tuff, calcarenite, etc.)	140 240	2.8 4.2	900 1260	300 420	16
Stone masonry with square shaped units (ashlar)	600 800	9.0 12.0	2400 3200	780 940	22
Solid brick masonry with lime mortar joints	240 400	6.0 9.2	1200 1800	400 600	18
Semi-solid brick masonry with cement mortar joints (volume of voids ≤ 40%)	500 800	24 32	3500 5600	875 1400	15
Hollow brick masonry (volume of voids ≤ 45%)	400 600	30 40	3600 5400	1080 1620	12
Hollow brick masonry with dry vertical joints (volume of voids ≤ 45%)	300 400	10 13	2700 3600	810 1080	11
Masonry with concrete brick units or expanded clay (volume of voids between 45% and 60%)	150 200	9.5 12.5	1200 1600	300 400	12
Masonry with semi-solid concrete brick units (volume of voids < 45%)	300 440	18.0 24.0	2400 3520	600 880	14

Borri, Corradi, & Castori (2015) present an alternative method for the mechanical characterization of masonry based on qualitative information obtained by visual inspection and on in-situ non-destructive tests. The Masonry Quality index method defines quantitative values according to seven aspects related to mechanical and geometrical properties of the elements as well as construction techniques.

Masonry presents highly different behaviour under tension and compression. While in compression it presents high strength and limited ductility, in tension the strength is almost null with brittle behaviour.

In both tension and compression, as well as in shear, masonry presents non-linear stress-strain relation with softening behaviour (Figure 5), described by progressive damage (Pelà, 2009). In general, it is also an anisotropic material, presenting different behaviour for each direction.

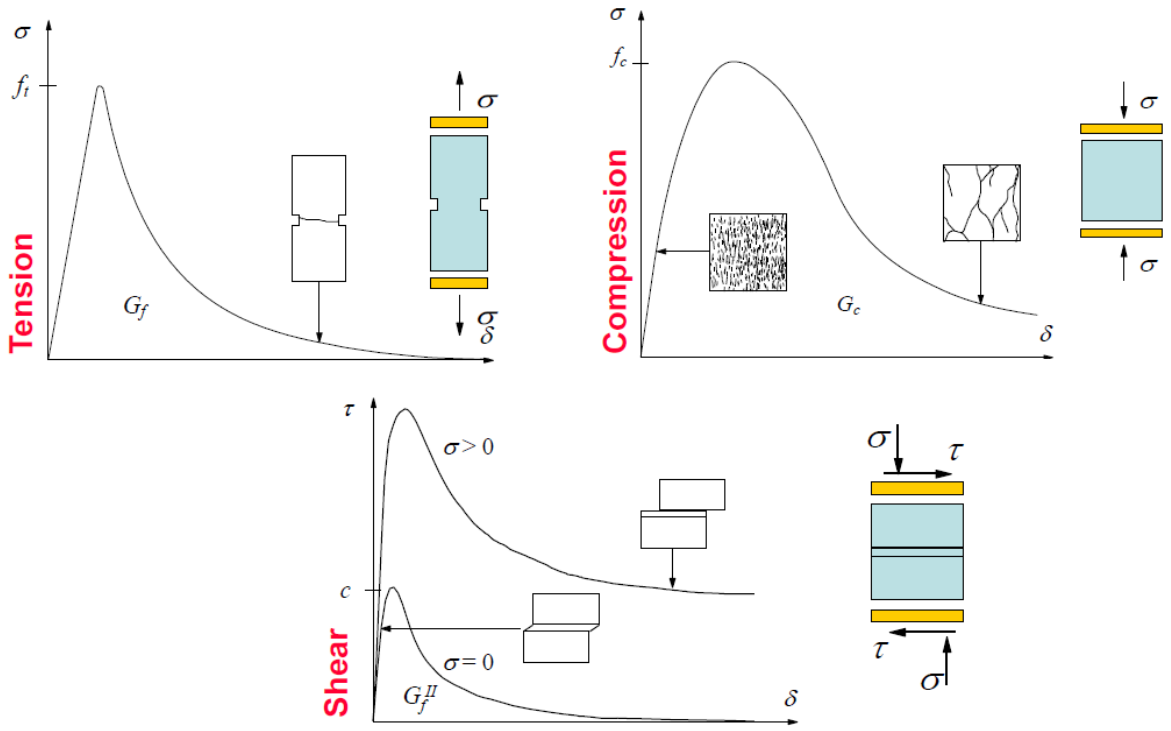

Figure 5 – Stress-strain relation of masonry under tension, compression and shear

2.4 Structural behaviour

Vaults are structures characterized by mobilizing only compression forces in order to reach stability. In general, the structural behaviour of vaults can be idealized as a 2D structure with behaviour similar to arches. The strength of the vault depends on the way units are assembled during its construction, which can be by arch assemblies or by enchainment of units as continuous surfaces (Arun, 2006). Self-weight as well as distributed loads over the vault follow thrust lines formed by inclined components that result not only in a vertical reaction but also in a horizontal reaction (Figure 6), that must be resisted by the supporting elements. Due to the self-weight, their vertical component increases from the crown to the base. If only vertical forces are applied to the vault, the horizontal component will be constant and its value depends on the thrust line shape, which is defined by the vault geometry – for the same span, it is greater when the rise of the arch decreases.

The vault supports may be provided by thick walls, buttresses or adjacent vaults to react the horizontal force. Furthermore, horizontal ties may be added to help the equilibrium of the horizontal forces at the base of the arch (Figure 7).

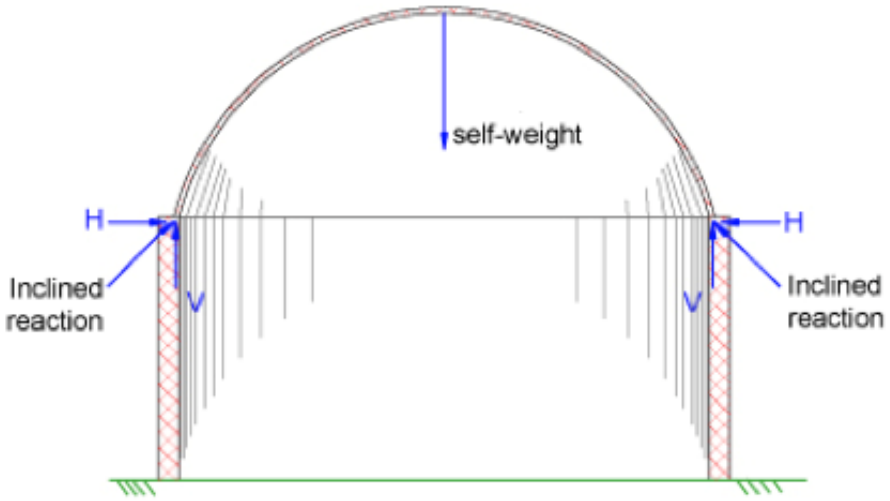

Figure 6 – Reactions at supports of arches (Low, 2011)

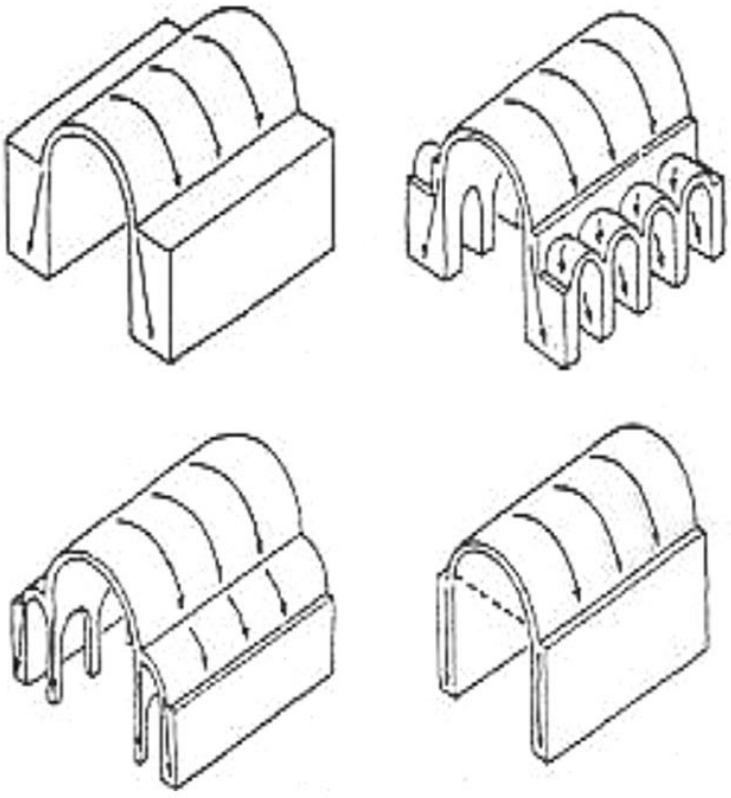

Figure 7 – Types of supports to transfer the horizontal thrust to the base of the structure (Feilden,1982)

The presence of loose fill (non-structural material) or structural backing (structural material) also influences considerably the vault behaviour. Filling material increases the self-weight, creating extra compression in the vault, reducing the horizontal thrust, while the structural backing rises the range where the thrust line can pass and decrease the span, increasing the stability of the structure. These elements are especially relevant when vaults are submitted to non-symmetrical loads, leading to a high increase in the bearing capacity (Santos, 2014). However, this increment is only meaningful in cases of semi-circle cross-section. If the vaults present segmental cross section with angle smaller than 158º the presence of infill is not meaningful for the structural behaviour (Canhão, n.d.). Hojdys & Krajewski (2014) performed non-symmetrical load tests in barrel vaults with filling materials presenting different levels of lateral constraints and the results are presented in Figure 8.

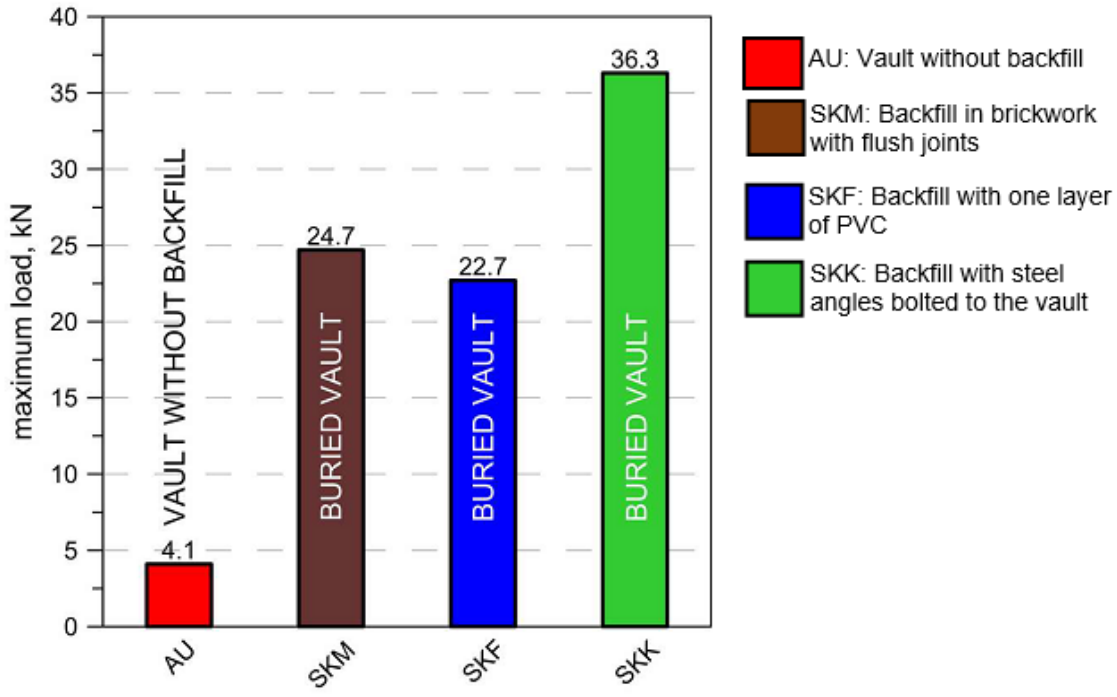

Figure 8 – Maximum capacity of non-symmetrically loaded barrel vaults with different types of filling material (Hojdys & Krajewski, 2014)

The boundary conditions of the vaults are also an important aspect of the vault behaviour and is highly dependent on the quality of the connection between adjacent elements, determined especially by the interlocking of units (Cattari, Resemini, & Lagomarsino, 2008).

The load path in vaults results in thrust lines shaped as arches, hence vaults can be analysed by slicing it in several arches, for which the pattern depends on the vaults shape. The three main shapes of shells are presented in Figure 9 and are further detailed in this Section.

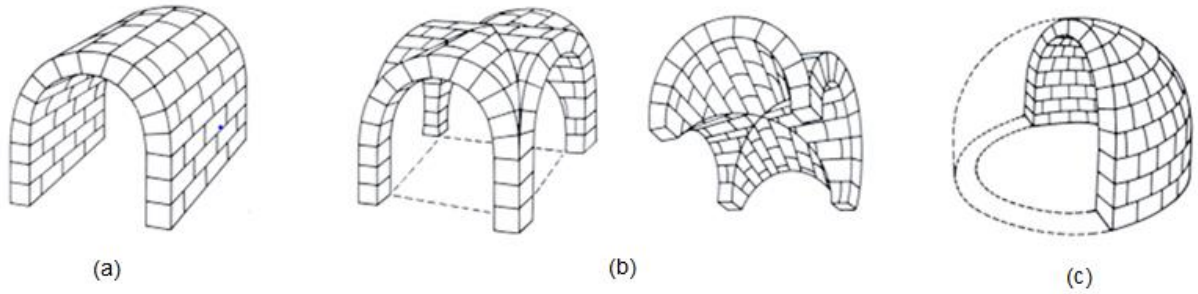

Figure 9 – Main types of shells: (a) barrel vault, (b) groin vault, (c) dome (Addapted from "Humanities I Test 1 Images," n.d.)

- **Barrel vault**

Barrel vaults are single curved vaults, with a cylindric shape, consisting in continuous arched sections along two parallel lines. These lines are considered the springs of the vault and usually are also defined by the supporting walls. They can have various shapes according to the different possible forms of arches presented in Figure 10.

The behaviour of barrel vaults depends mainly on the supporting conditions. In general, they are supported continuously in the longitudinal directions. In these cases, the vaults present the principal stresses in the transverse directions, as a series of parallel arches. If the support condition is not continuous, bending stresses will appear, with compression at the top and tension at the bottom and the loads being transmitted to the boundary conditions by shear (Arun, 2006).

The masonry morphology has also influence on the structural behaviour of the element, since in this type structures the equilibrium is ensured by the mutual thrust of the blocks. In barrel vaults the pattern is especially important, where it can behave as a set of adjacent arches in case of orthogonal pattern or as a 3D element in case of parallel pattern (Cattari et al., 2008).

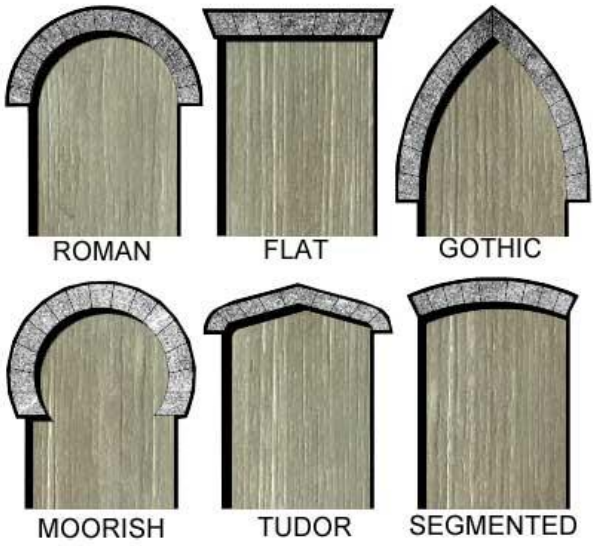

Figure 10 – Shapes of arches (Gelms, 2015)

- **Groin vaults**

Groin vaults are formed by the intersection between two barrel vaults. The main difference between this type of vault and the barrel vault is the support, since groin vaults are supported by piers while barrel vaults are supported by walls, leading to lighter structures. However, the lack of continuous support requires the use of stiffeners like arches in the periphery of each barrel vault (Arun, 2006).

The joint between the two vaults can be thicker than the other parts of the vault, defining the shape of the arches. In such cases, the element is then called ribbed vault. The main advantage of ribbed vaults is that the ribs impose a greater resistance to the structure and allow a reduction of thickness of the vaults itself, saving material and reducing self-weight.

Masonry pattern in groin vaults can assume several shapes (Figure 11), which also influences the stress distribution on the vaults. Two possibilities for load distribution in cross vaults are presented in Figure 12.

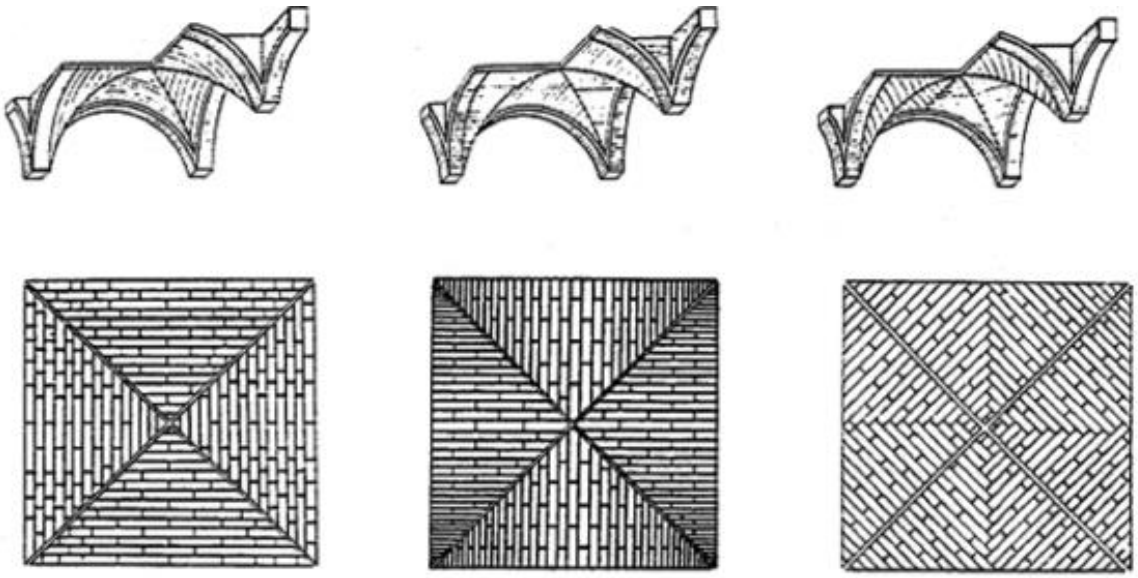

Figure 11 – Masonry patterns for groin vaults (Cattari et al., 2008)

Figure 12 – Distribution of loads in groin vaults (O'Dwyer, 1999)

- **Domes**

Domes can be considered doubly curved surfaces, made from the rotation of an arch around its central vertical axis. Domes are frequently used in historical architecture, especially in religious constructions, due to its visual impact. The symbolism associated with domes includes mortuary, celestial, and traditions that have developed over time. Historical domes can be made in many different shapes according to the region and culture (Figure 13):

- Hemispherical dome: this is the most common type of dome and consists in a semi-sphere;
- Onion dome: it is made of a horseshoe arch, with the springing smaller than the biggest span and has a pointed top (Hourihane, 2012);
- Oval dome: it has an oval shape profile in plan, for which the geometry consists of a combination of circular arches, transitioning at points of tangency (Huerta, 2007).
- Parabolic dome: this is a unique shape for an arch where the uniform load is in equilibrium leading to no bending stress in the arch. The first domes with this shape date from the 18th century;
- Segmental dome: it is characterized by a profile of less than half a sphere.

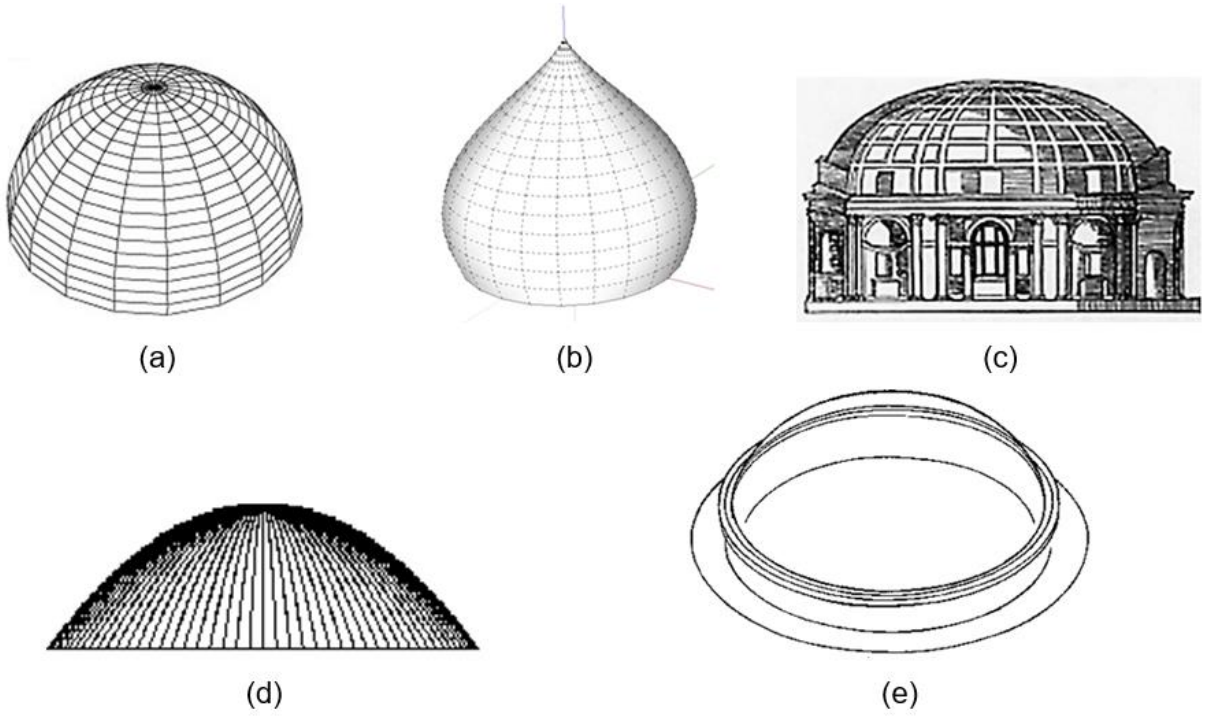

Figure 13 – Shapes of domes: (a) hemispherical dome (“Long Life of Catenary,” n.d.), (b) onion dome (“SketchUp Extension Warehouse,” n.d.), (c) oval dome (Huerta, 2007), (d) parabolic dome (“Geometrica,” n.d.), (e) segmental dome (“What is saucer dome? definition and image,” n.d.)

Domes have similar behaviour to vaults, with the meridian forces responsible for the vertical transfer of thrusts. However, they also develop internal horizontal thrusts – the hoop forces (Figure 14), which

form parallel rings responsible for resisting the out-of-plane bending moment from the meridians, acting as lateral support. The rings are in compression near the crown until an angle of 52º from the top and in tension at the bottom part of the dome, below this angle. The domes are usually stiffened in its bottom part, subject to tensile stresses, by thickening the masonry (Arun, 2006). The hoop forces allow the dome to work as a self-stable structure, hence it is possible to work in a ring-by-ring construction without centering (Hourihane, 2012).

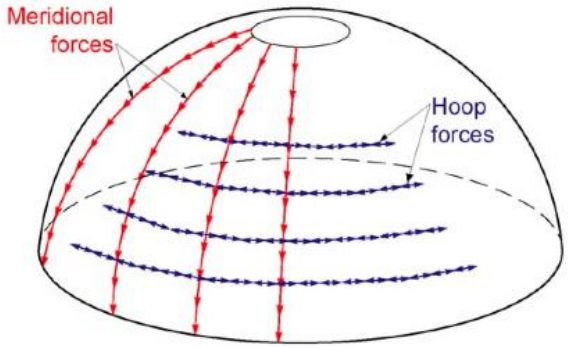

Figure 14 – Internal forces acting in a dome (Low, 2011)

As for the arches, domes also produce an inclined reaction force, but with smaller magnitude, since the hoop forces acting at the bottom part work as a ring helping to reduce the stresses. Therefore, the supporting structure must be able to resist not only vertical loads but also horizontal loads. Thus, the boundaries of such elements are usually continuous as walls or closely spaced columns, changing the tensile stresses in the hoop forces at the bottom into compression (Arun, 2006).

The masonry pattern in vaults can also assume different shapes, being usually circular. The influence of different masonry patterns in the structural behaviour of domes has been studied by Calderini (2004).

2.5 Typical damage and collapse mechanisms

One of the main tools to identify causes and mechanisms of decays in historical buildings is visual inspection, with a detailed mapping of existing cracks together with a geometric survey. Through the analysis of crack maps, it is possible to highlight major structural problems and acquire information about the present level of safety of the building. Crack patterns are associated to force distribution, since cracks propagate perpendicular to tension lines. However, it must be considered that the increase of the stresses may lead to changes in crack pattern as the cracks may progress to different directions (Arun, 2006). Cracks may be analysed in terms of thickness, width and age, since the damage in the vaults may substantially change the stiffness of vaults and the distribution of horizontal loads to vertical elements (Cattari et al., 2008).

Since vaults can be analysed by being sliced in arches, the collapse mechanisms for arches are similar to the collapse mechanisms of vaults. Arches have high capacity of deformability due to the formation of hinges. If an arch develops three hinges, it becomes a statically determined structure and may deform. Depending on the depth and friction in the joints between the voussoirs, arch can accommodate small inward and outward movements of the supports (Arun, 2006). If four hinges are formed alternately in intrados and extrados for an eccentric point load, a kinematic admissible mechanism is formed, leading the structure to collapse. The collapse due to formation of hinges usually involves large deformation of the structure. Figure 15 presents different types of collapse mechanisms with four hinges. If the load is symmetrical, five hinges are necessary to form a kinematic admissible mechanism.

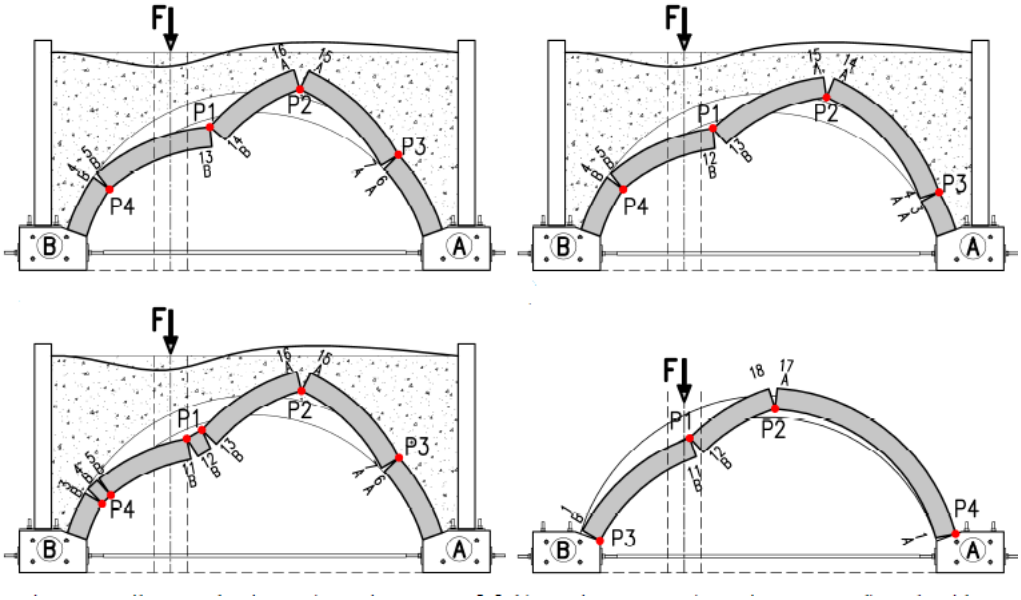

Figure 15 – Different collapse mechanisms involving four hinges (Hojdys & Krajewski, 2014)

In barrel vaults, longitudinal cracks usually indicate changes in the span, as previously mentioned for arches. In the same way, the formation of four longitudinal cracks means the development of a collapse mechanism. Transversal cracks in these vaults usually mean movement of the extreme supports and are typically related to soil settlements.

In groin vaults, generally two mechanisms are possible. The first mechanism is related to the outward movement of the abutment, leading to the detachment of one of the webs and hinges formation at the springing and at the crown. The second mechanism can be considered a shear failure due to the differential movements of the two opposite sides of the bay, creating typical diagonal cracks (Gaetani, 2016), as presented in Figure 16.

The typical crack pattern in domes is meridional cracks that appear due to tensile hoop stresses in the bottom part (Figure 17). The formation of such cracks on the surface of the dome means loss of hoop forces' effect, and consequently loss of the property of self-stability. The structure behaves as several

arches, leading to an increase in the horizontal reaction. If the walls are strong enough to resist this additional stress, the structure can be considered stable. The cracks in domes may also present circumferential shapes, which in this case are related to movements of the supports (Arun, 2006).

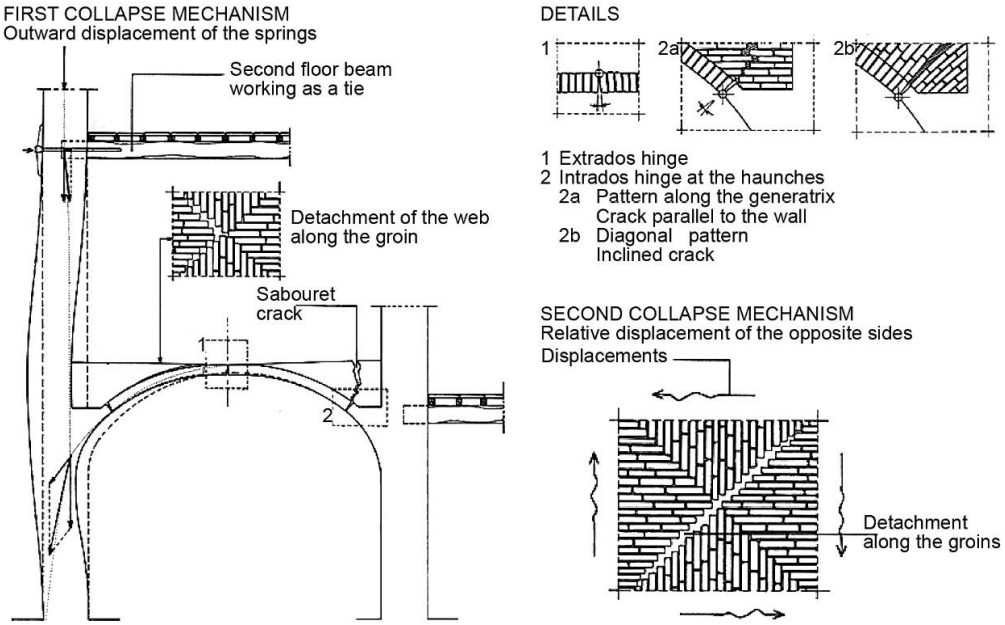

Figure 16 – Typical collapse mechanisms for groin vaults (Giovanetti, 2000)

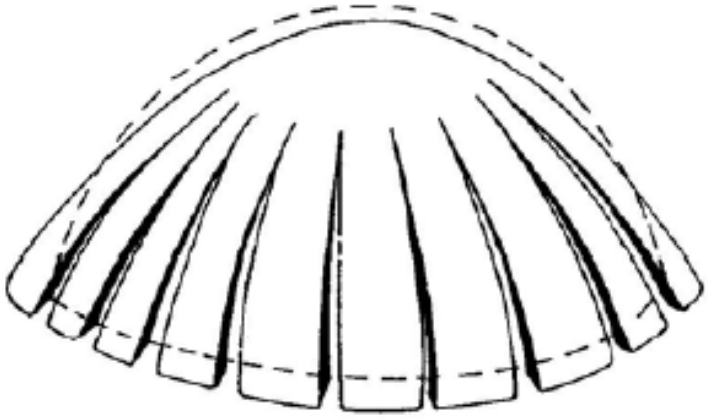

Figure 17 – Typical crack pattern in domes with the formation of concentric arches

One typical reason for the development of cracks in vaults is the compatibility between elements. These cracks occur due to differences in strength and stiffness in adjacent elements, causing their separation. In gothic vaults, this phenomenon is known as *Sabouret* cracks. This type of crack usually occurs in the parallel direction to the support lines.

One example of deeply studied crack pattern is Brunelleschi's dome, which presents a complex crack pattern that appeared soon after its construction, possibly due to a strong earthquake in 1453. Such cracks have increased and changed through years and are object of several monitoring studies. They caused changes on the structural behaviour of the dome which does not work anymore as a monolithic element, acting as eight concentric independent arches (Ottoni et al., 2010).

Among main causes of damages in masonry vaults in historical structures are earthquakes. These damages are related to movement of the base and differ according to the shape of the vault. Domes are significantly stronger to earthquake action than gothic vaults. This is due to the double curvature of domes, making their weakness related mainly to support conditions and stiffness. Gothic vaults are usually slender and may have poor connections between ribs and webs. Besides, they are supported by slender columns that are only partially compensated by the abutments (Croci, 2006).

Examples of damages caused by earthquakes in vaults are presented by Binda, Chesi, & Parisi (2010), based on the survey of damages carried out after L'Aquila earthquake in Italy in 2009 at the Saint Biaggio Church. Two main types of damage were observed, namely the partial collapse of a barrel vault due to debris failure (Figure 18) and the parallel circular cracks close to the base of spherical vaults in the lateral naves, that are connected to the cracking over the arches between chapels (Figure 19).

Figure 18 – Partial collapse of the barrel vault in Saint Biaggio Church from L'Aquila earthquake (Binda et al., 2010)

Figure 19 – Circular cracks in spherical vaults of lateral naves in Saint Biaggio Church from L'Aquila earthquake (Binda et al., 2010)

Croci (2006) associated the collapse mechanism of some ribbed vaults in St. Francisco de Assisi Basilica, during an earthquake in 1997 to the presence of loose fill material in the extrados of the vault close to the base, that followed the movement of the roof opposing their recovery. Another reason presented is the progressive loss of curvature of the ribs, forming a hinge in its middle leading to collapse, which was also observed in other vaults that did not collapse. In these cases, it is possible to observe the detachment between webs and ribs (Figure 20).

Figure 20 – Detachment between ribs and webs in a vault in St. Francisco de Assissi Basilica (Croci, 2006)

2.6 Structural analysis

The main challenge in the structural analysis of arches is to define the horizontal thrust acting on the supports in order to design properly the buttresses. Nowadays, the thrust is associated to the concept of force and can be estimated according to the theory of structures, defined by mechanical laws and strength of materials. However, this scientific knowledge began to be developed in the 17th century, being widely spread in the 19th century (Huerta, 2004). Before this period, geometrical rules based on proportion between the pieces were defined, permitting the construction of safe structures.

With the beginning of scientific approach, the geometrical rules were improved resulting in the theory of Limit Analysis, which is a simple and accurate tool to assess stability of arched structures. An alternative to Limit Analysis is the Finite Elements Method (FEM) combined with non-linear materials for masonry. Modern theories were developed to further understand masonry structures behaviour, allowing to describe anisotropy, low tensile strength, softening behaviour and finite compression strength of masonry (Tralli et al., 2014).

It must be remarked that a detailed description of the vault geometry is of main importance for the success of the structural analysis. Due to the non-elastic behaviour of masonry material, equilibrium conditions play a key role in the stability of these structures, being defined mainly by the geometry. Hence, existing deformations and cracks together with the presence or not of infill are crucial in the analysis of such structures (Tralli et al., 2014).

In this section, an overview of the different techniques used to evaluate the behaviour of masonry vaults along history is presented.

2.4.1. Ancient geometrical rules

In the ancient times, there was no knowledge of mechanics of structures. However, several buildings succeeded with sophisticated construction techniques and impressive structural capacity. This prosperity is mainly due to empirical design rules spread between build masters based on the

geometry and proportion between elements, defined mainly by the observation of successful structures. In these rules it is applied the principle of proportion: if a building with a given proportion between the size of elements worked well, another one with different scale but with same relation between dimensions will also work (Huerta, 2004).

The first rules related to vaults in history are from the Hellenistic era, in which Herón from Alexandria have written several treatises around 60 A.C. which were lost in time. The Byzantines also have technical treatises, which included not only the knowledge from practice of construction, but also some concepts related to mechanics and equilibrium (Huerta, 2004).

There are two main geometrical rules from the late gothic period. The first one consists in dividing the arch in three equal parts from which the width of the buttress can be geometrically obtained as presented in Figure 21 (Gaetani, 2016). This rule is mostly known as Blondel's rule, who have published it in the Traité d'Architecture (Blondel, 1675). However, previous to that other authors have already mentioned it such as Baccojani (1546), Martinez de Aranda (1590) and Derand (1643) (Huerta, 2004). It is known that this rule was applied to the Saint Chapelle and to the Girona Cathedral. The second rule differs from the first one as it considers the thickness of the arch, taking into account the weight of the structure in the geometrical proportions. It was proposed by Hernán Ruiz in 1560 (Navascués Palacio, 1974).

Between the 15th and 18th centuries, several rules based on proportions between different parts were defined by different authors. One example is the rule provided by Palladio (1570), known as rule of the third, in which the width of the buttress should be 1/3 the span of the vault. Fray Lorenzo (1639) defined a similar rule in 1639. However, the proportion changes according to the material of the units in the masonry.

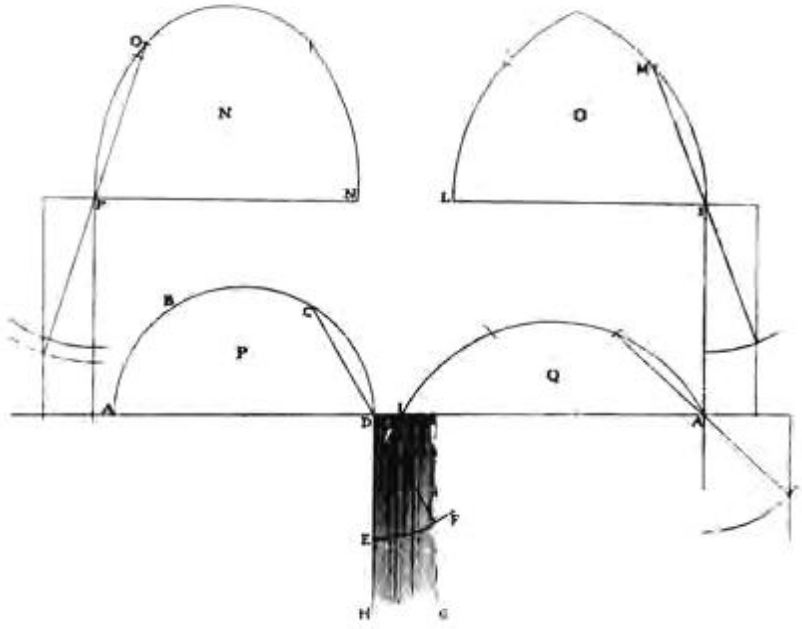

Figure 21 – Application of Blondel's rule to distinct types of arches (Derand, 1643)

2.4.2. Rational approaches and limit analysis

The first advance based in rational approaches was made by Wren (1750), in the design of Saint Paul's Cathedral, where the equilibrium of moments involved in the half part of the arch was considered. However, this approach was wrong, since it did not consider the horizontal thrust of the arch.

The catenary concept was presented in Robert Hooke's Latin anagram (1675), stated that a stable arch would have the shape of a hanging rope (Gaetani, 2016). This principle was used by Antonio Gaudi, who created 3D hanging models (Figure 22) to design vaults according to the catenary shape in the Church of Colònia Güell (Roca et al., 2010).

Figure 22 – Gaudi's hanging model for Colònia Guell (Ràfols, 1929)

In the 18th and 19th centuries, several researchers, such as De La Hire (1712) and Rankine (1858), studied geometrical solutions based on equilibrium. These studies resulted later in the graphic static analysis, for which the different formulations were presented by Méry (1840) and Moseley (1833) during the 19th century, being the last formulation the most complete. The graphic statics is based on the principle that the arch is stable if it is possible to fit a thrust line inside its boundaries. Numerous

thrust lines can be found for a structure, and it is enough that at least one of them fits in order to guarantee the safety of the structure (Figure 23). One example of this theorem is presented in Figure **24**, in which the safety of the arch is assured by the presence of the thrust line even in a very thin section, in the case of erosion simulation.

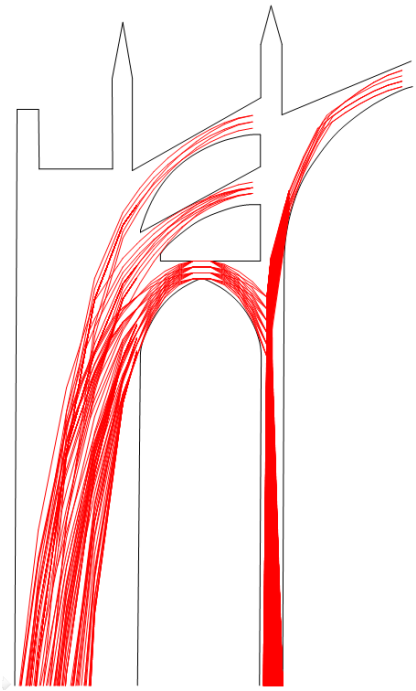

Figure 23 – Several solutions for thrust lines – Mallorca Cathedral (Maynou, 2001)

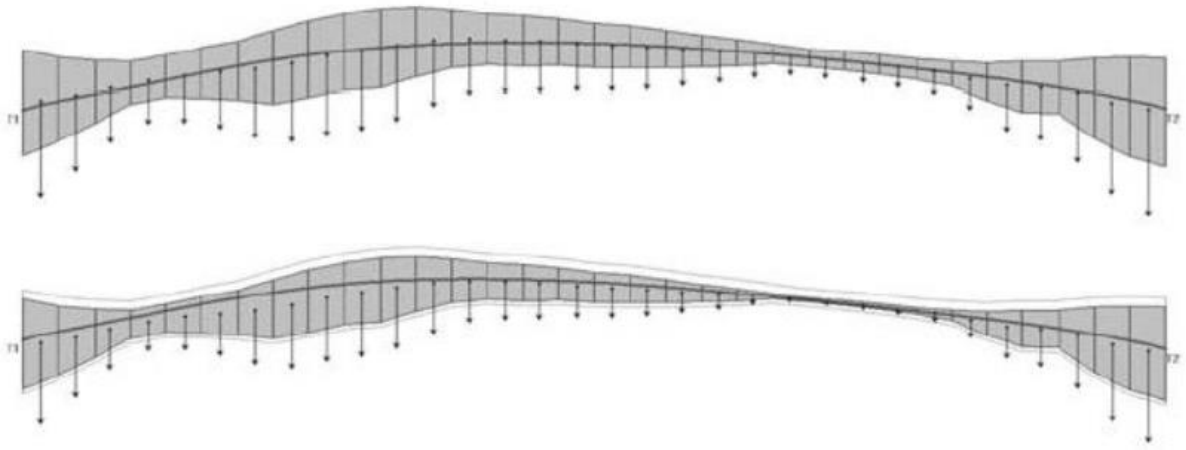

Figure 24 – Reduction of arch thickness in Limit Analysis as erosion simulation (Block, 2005)

Another theory to assess the safety of arches is related to the configuration of kinematic mechanisms due to the formation of hinges (Figure 25). This first concept was developed by Leonardo da Vinci in the 15th century, however it was only further studied by Couplet (1729), assuming that there was no sliding between the voussoirs, and was mathematically stated by Coulomb in 1773 (Roca et al., 2010).

Figure 26 presents a collapse mechanism due to the formation of four hinges in an arch during an experimental campaign.

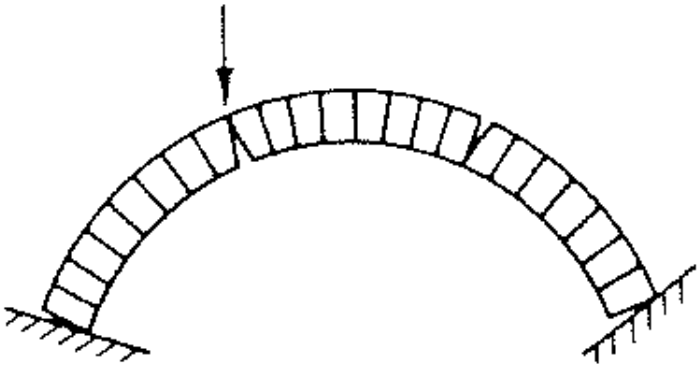

Figure 25 – Kinematic mechanism due to formation of plastic hinges

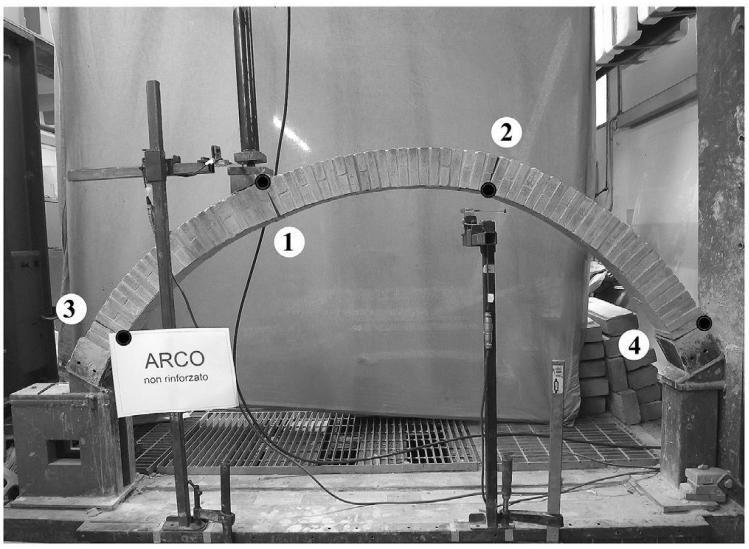

Figure 26 - Sequence of hinge formation creating a collapse mechanism (Misseri et al., 2016)

In the 19th century, the research was focused on finding the real thrust line based on the elastic theory. Winkler (1880) presented the first deep discussion on the subject, where he understood that deformations of the centering during construction or yielding of the buttresses would generate hinges in the structure that would change the position of the thrust line (Huerta, 2001).

Heyman (1966) identified that the thrust line in fact moved abruptly from one position to another according to the emergence of cracks in the arch. Hence, it is impossible to define the actual thrust line in the structure, being only possible to define its value within certain limits (Huerta, 2001). Thus, Heyman developed the Limit Analysis theory, based on the concepts of plasticity besides the well-known ideas of thrust line and equilibrium. This theory consists in the combination of the graphic statics, which is the first theorem and gives a lower bound estimation of the ultimate load (static

approach or lower limit theorem), together with the kinematic approach (upper limit theorem), which presents the upper bound estimation of the ultimate load. When the solutions obtained from both theorems are equal, the solution is unique (third theorem or unique theorem). It is noted that the original limit analysis presents three main assumptions: (a) the infinite compressive strength; (b) the null tensile strength; (c) sliding failure does not occur. (Jacques Heyman, 1982).

Heyman (1995) proposed subsequently an advance in the original Limit Analysis theory, in which finite compressive strength of masonry could be modelled by a reduction in the thickness of the arch. This simulation is especially important in the case of very shallow arches (Tralli et al., 2014).

Limit analysis is a powerful tool to assess the safety of structures and to be considered at least as a complementary tool for structural analysis of arched constructions. It must be remarked that it is capable only of defining the ultimate capacity of structures, without providing information related to service load levels (Roca et al., 2010). Hence, several researches dedicated their work to improve and facilitate their application.

O'Dwyer (1999) presented a new technique named the Thrust Network Method (TNM) that consists in modelling the principal stresses in a masonry vaults as a discrete network of forces with optimization techniques to define the optimum network shape. This approach is limited to vertical forces with the layout of the network being fixed in plan, incapable of dealing with horizontal indeterminacies. An extension of this method was proposed by Block & Lachauer (2014), introducing the Maxwell reciprocal force diagrams to describe the horizontal equilibrium (Tralli et al., 2014). With the nonlinear analysis, this method is able to analyse the structural redundancy of unreinforced masonry.

Another approach is proposed from an analogy to the catenary principle, which led to the adoption of a cable element allowing the method to deal with complex and multiple hanging nets composed of virtual strings subjected to arbitrary loading (Andreu et al, 2006).

Lucchesi and co-workers (2007) developed a numerical approach for the structural analysis of masonry vaults based on the concept of maximum modulus eccentricity surface, generalizing the static approach used for arches to vaults (Roca et al., 2010). Vouga and co-workers (2012) presented an efficient algorithm to find target surfaces, based on the thrust network and the lumped stress method.

All these methods are based on the original limit analysis formulation, considering an associated flow-rule, which assumes a dilatancy between blocks under friction effect. However, this is a simplification to allow the application of plasticity theorems (Roca et al., 2010). This simplification is correct only in cases of failure due only to tensile cracking or in cases where the volume generated by the sliding of units is irrelevant. For other cases, this may lead to severe underestimation of the ultimate collapse load (Gaetani, 2016).

To overcome this problem, Orduña & Lourenço (2005a and 2005b) proposed a load-path following procedure. With the same objective, Gilbert and co-workers (2006) proposed an iterative procedure

considering a non-associative frictional joint model to obtain a converging solution. In addition, the limit state analysis considering finite friction between blocks allows to study the importance of three-dimensional stress fields in equilibrium of complex vaults (D'Ayala & Casapulla, 2001).

2.4.3. Finite element method (FEM)

Although limit analysis can provide a simple and fast estimation of collapse loads, it is often not sufficient for a full and detailed structural analysis (Milani et al., 2007). More sophisticated approaches are frequently necessary to better characterize the structural behaviour not only for collapse as the limit analysis, but at different stages of its history or load path. However, modelling historical structures is usually a hard effort due to its complex shapes with curved elements. The Finite Element Method (FEM) is a tool to overcome this problem, affording realistic and accurate description of geometry, providing detailed non-linear analysis (Roca et al., 2010). One example is presented in Figure 27, in which due to FEM modelling it was possible to describe in details the curved shapes of gothic vaults in Santa Maria del Mar (Mazziotti, 2016).

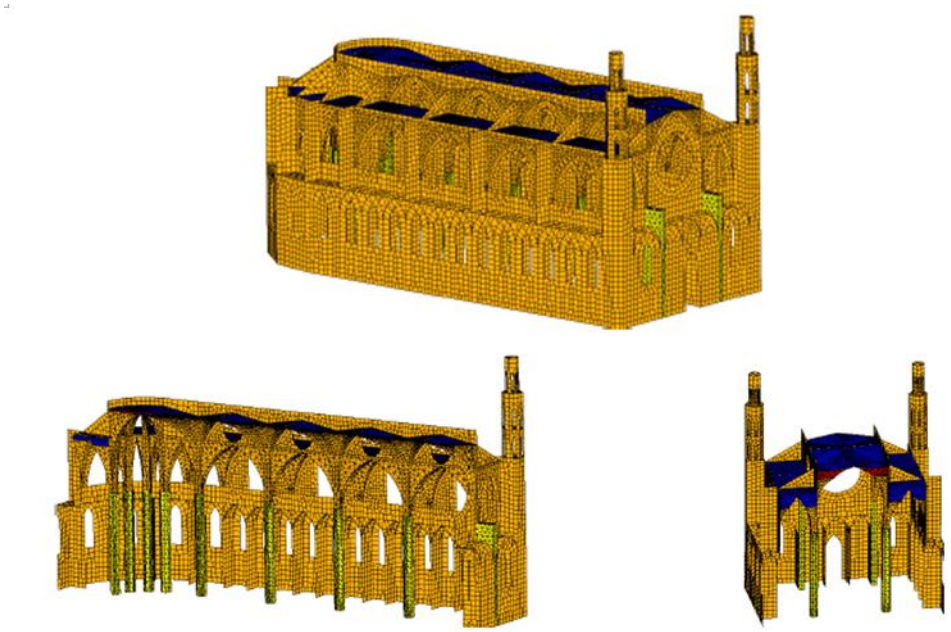

Figure 27 – FEM Modelling of the Santa Maria del Mar Church (Mazziotti, 2016)

The FEM numerical modelling for masonry can be divided into two main approaches: macro-modelling and micro-modelling, being the last one divided in detailed or simplified micro-modelling. Detailed macro-modelling consists in modelling separately the units and the mortar joints – represented by continuous elements, and the unit/ mortar interface – represented by discontinuous elements, with specific properties for each of these elements. The simplified micro-modelling is considered a discontinuous model, in which units are modelled together with the mortar-joints in size, but with the mortar properties being defined together with the interface characteristics in discontinuous elements.

Finally, in macro-modelling analysis, masonry is regarded fictitiously as a homogeneous continuous material, without distinction between units and joints (N. Mendes et al., 2017). Hence it demands less computational effort being recommended for the analysis of large structural members or entire structures. Figure 28 presents the three numerical modelling approaches for masonry.

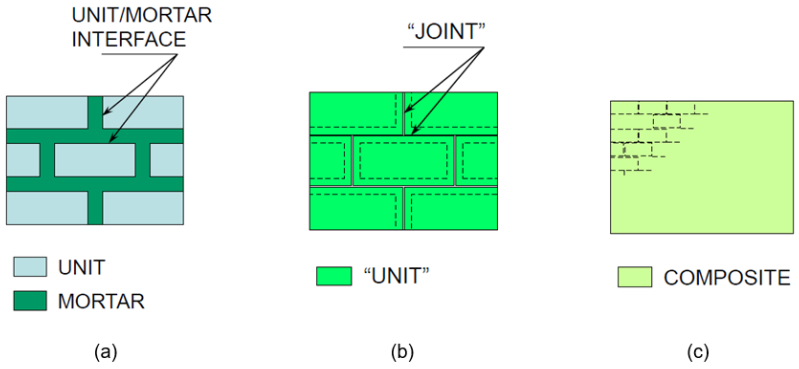

Figure 28 – Numerical modelling approaches for masonry: (a) detailed micro-modelling, (b) simplified micro-modelling, (c) macro-modelling (Lourenço, 1996)

In general, FEM programs are mainly developed for analysis of concrete and steel structures, considering the damage through the plasticity and smeared cracks material models. They do not consider heterogeneity or orthotropic behaviour of masonry (Tralli et al., 2014). Lourenço (1996) proposed a non-linear constitutive model in which the material presented different yield criteria under tension and compression, with softening characteristic that describe the gradual decrease of strength according to the increase of deformation (Roca et al., 2010 and Tralli et al., 2014).

Detailed micro-modelling is the most accurate tool to describe the real behaviour of masonry, since it considers separately the units, joints and interfaces between both. However, the computational effort required to perform the structural analysis is too high, limiting its applicability to analyse local response of material or small elements and structural details. Hence, it is preferable to use the homogenized modelling, which is a balance between micro and macro-modelling, consisting in a detailed FEM modelling of a so called "macroblocks" which is a characteristic part of the structure, generating the whole structure by repetition. This approach was developed in parallel by Pluijm (1999), Lopez and coworkers (1999) and Zucchini & Lourenço (2009).

A technique of micro-mechanical homogenized model was developed by Milani et al. (2007) and further researched by Milani et al. (2008) to apply the kinematic theorem of limit analysis, providing an upper bound of the collapse load. This approach was then applied for linear and non-linear problems (Zucchini & Lourenço, 2009).

Multi-scale modelling is another approach to substitute the homogenization technique. It consists in observing the same phenomena in two different scales, namely macro and micro-models, in which the two models interact and exchange information during the analysis. However, this technique requires substantial computational effort, being more suitable for small elements (Pettraca, 2016).

The main non-linear analyses techniques are developed for 2D problems. Domes and vaults are 3D curved spatial elements, creating an additional difficulty to the analysis. There are few studies published with this aim, some of them made by Oñate et al. (1995), Croci (1998), Barthel (1993) and Cauvin & Stagnitto (1993). Further formulation of spatial curved shell was proposed by Lourenço (1997), being the only micro-modelling technique for this type of structure (Roca et al., 2010).

2.4.4. Discrete element method (DEM)

Discrete element method is the modelling of structures by an assemblage of distinct blocks connected by its boundaries. It was developed by Cundall & Hart (1971) and is based on two concepts: finite displacements and rotations of discrete bodies is allowed, including the complete detachment of parts and it can recognize new contacts between blocks automatically (Roca et al., 2010). Its formulation considers blocks with polyhedral shapes, assumed to be rigid or deformable, with the discontinuities being treated as boundary conditions between blocks (N. Mendes et al., 2017).

The main advantages of this method are the possibility to modelling different sources of nonlinear behaviour, typically large displacements, which is not appropriated for FEM analysis. It is also suitable to study not only failures in static range but especially in dynamic range (Roca et al., 2010). Another possibility of the method is the ability to simulate the progressive failure associated with crack propagation and significant deformation (Gaetani, 2016).

The method was initially developed to study jointed rock, but was extended to masonry structures. Azevedo and coworkers (2000) examined the suitability of the method for masonry structures together with analysis of collapse patterns. Studies related to practical examples in masonry construction have been performed by Pagnoni (1994), Lemos (1998) and Sincraian (2001). Mamaghani and coworkers (1999) studied the failure mode of masonry arches with DEM method as presented in Figure 29.

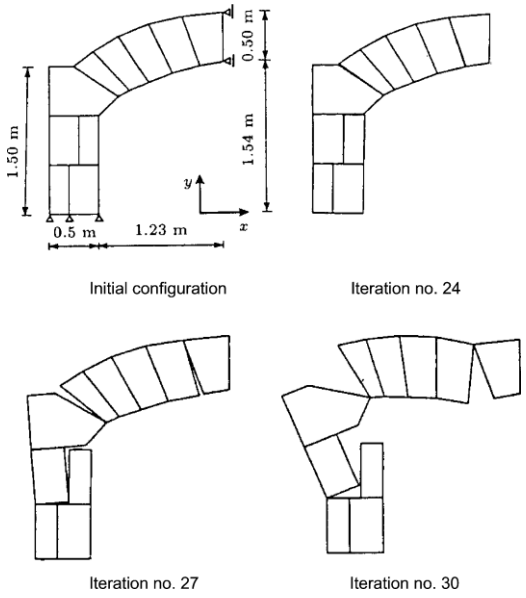

Figure 29 – Failure mode of masonry arches defined by DEM analysis (Mamaghani et al., 1999)

3. THE MUNICIPAL THEATRE OF RIO DE JANEIRO

3.1 Historical overview

In 1902, the Rio de Janeiro's mayor Pereira Passos remodeled the city center of Rio de Janeiro, especially the Central Avenue – known nowadays as Rio Branco Avenue – where the theatre is located. The need for modernizing the city came from the changes in the politics, since Brazil had just become a republic and wanted to be noted internationally. Besides, the rich population of the city wanted a place for socialization, and supported the construction of a new theatre (Simeone, 2002). Pereira Passos included the construction of the theatre as part of this renovation plan, hence the design of *"Theatro Municipal do Rio de Janeiro"* was opened to competition in 1903. The final layout was result of a merge between the two winners of the competition: Oliveira Passos (Figure 30) and Albert Guilbert (Figure 31). The two models had the same typology and were both inspired in the design of Paris' Opera from Charles Garnier (Fundação Theatro Municipal do Rio de Janeiro, 2016).

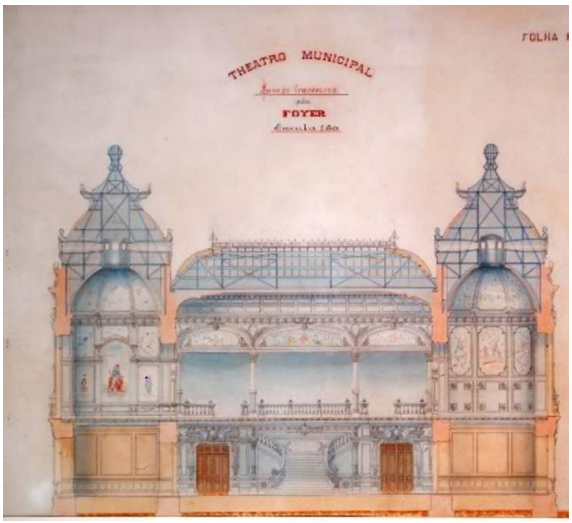

Figure 30 – Design project of Oliveira Passos for the Municipal Theatro (SkyscraperCity, 2011)

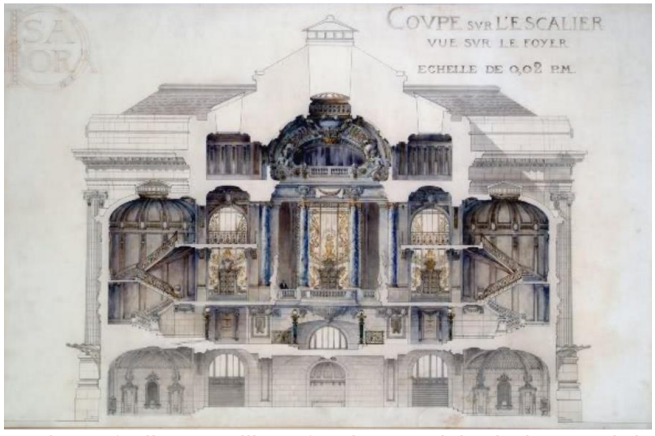

Figure 31 – Design project of Albert Guilbert for the Municipal Theatro (SkyscraperCity, 2011)

Some renowned artists were invited to work in the decoration of the theatre, namely Eliseu Visconti, Rodolfo Amoedo and the Bernardelli brothers. Stained glasses windows and mosaic finishing were imported from European artists (Fundação Theatro Municipal do Rio de Janeiro, 2016).

The Municipal Theatre of Rio de Janeiro was built between 1905 and 1909 (Figure 32), being inaugurated in July 14, 1909 by Brazil's president Nilo Peçanha and Rio de Janeiro's mayor Sousa Aguiar. It is considered nowadays one of the most important concert halls not only in Brazil but also in South America (Fundação Theatro Municipal do Rio de Janeiro, 2016).

The theatre was one of the first constructions made with electricity, phone connection, firefighting system and air conditioning. Therefore, it is also considered an example of the technological advances in the period after the industrial revolution (Machado, 2012).

Figure 32 – Construction of Theatro Municipal do Rio de Janeiro (Fundação Theatro Municipal do Rio de Janeiro, 2016)

3.2 Description of the theatre

3.2.1. Location

The theatre is situated in the city center of Rio de Janeiro, in the Floriano square. This neighbourhood is popularly known as Cinelândia (Figure 33), due to several theatres, cinemas, restaurants and bars close to this location in the 1930s. The region is also famous for its remarkable constructions in eclectic style, such as the National Library, The National Museum of Fine Arts, the former Supreme Court and the theatre itself, which is located in the corner formed by the headboard of the square and the Rio Branco Avenue (Figure 34).

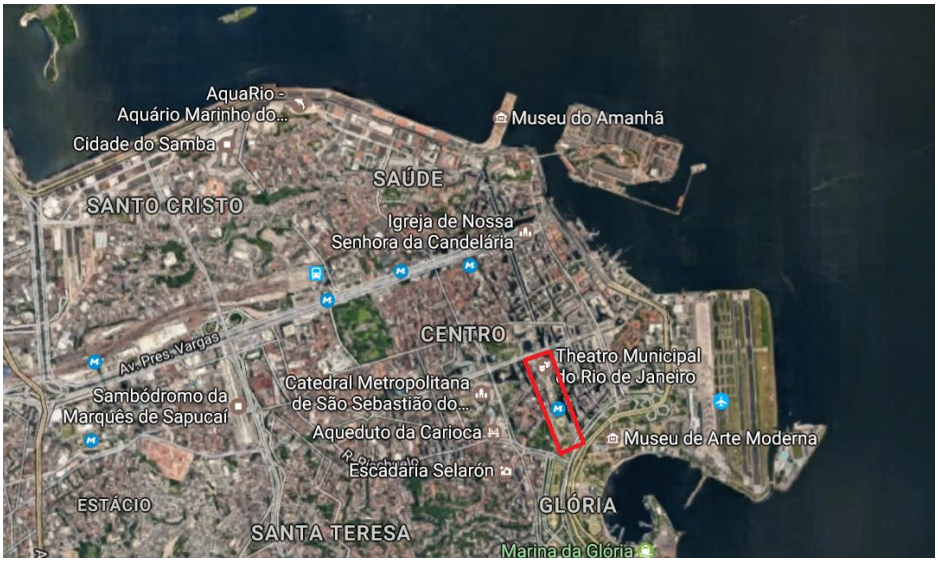

Figure 33 – Cinelândia square (adapted from “Google Maps,” 2017)

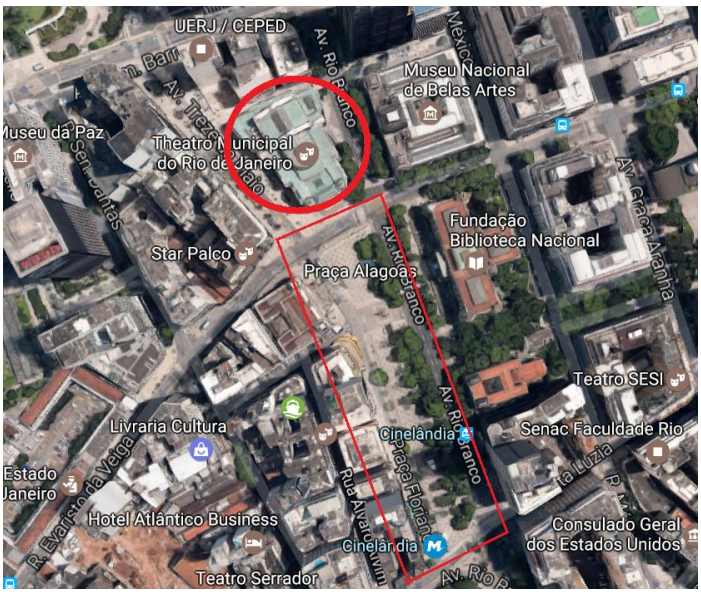

Figure 34 – Theatre Location (adapted from “Google Maps,” 2017)

3.2.2. Architecture

The Municipal Theatre of Rio de Janeiro is a masterpiece in eclectic style and is considered an ikon of the modernization plan for the Rio de Janeiro’s city center in the beginning of 20th century. The eclectic style is predominant in the main buildings from the end of 19th century and beginning of 20th century in Brazil, and symbolizes the end of colonial period by the construction based on the foreign architecture as a way to present the city as one of the main capitals of the world (Simeone, 2002). The design of the theatre is result of the works from Oliveira Passos and Albert Guilbert, strongly based in the Paris’ Opera, as mentioned previously.

With total of 4220m^2, the original capacity of the theatre was of 1739 spectators. However, due to the increase of interest from the public, an intervention was made in 1934 that raised its capacity to 2361 places. Nowadays, the theatre can receive a public of 2252 people due to current legislation.

The main architectonic features of the building are following described.

- **Façades**

Figure 35 presents the main façade of the building. The access to the theatre is possible by stairs made of granite together with the bottom part of the walls and main columns. The façade is characterized by the six main columns in the central body, which are made of marble in Corinthian style. Above the columns there is a cornice that holds an inscription with the theatre's name followed by a pediment sided by two sculptures authored by Rodolpho Bernardelli. These sculptures are part of a set of six sculptures placed along the theatre's façades. The design lines are of classic style, but the varied decorative elements of the façade resembles the baroque architecture (Secretaria de Cultura, 2017). The lateral façade (Figure 36) is marked by balusters made of six columns in marble with golden capitals. Arched windows over the columns allow the light to come into this part of the Theatre, while three arched doors in the bottom allow access to the theatre. In the side of Treze de Maio Avenue, these doors lead to a private garden.

Figure 35 – Main façade - Municipal Theatre of Rio de Janeiro (Mapa de Cultura RJ, n.d.)

Figure 36 – Lateral façade - Municipal Theatre of Rio de Janeiro (Panoramio, 2014)

- **Interior of the theatre**

The interior of the theatre is divided in three parts, namely the main body, the showroom and the stage, as presented in Figure 37.

The first floor of the main body consists in the entrance lobby with two resting rooms in the laterals with circle shape. The famous stairs in the centre lead to the second level, which is considered the

noble level. There are also lateral stairs on both sides of the theatre that give access to all the floors of the theatre together with an elevator on the left side.

The second floor of the *foyer* is decorated in Luis XVI style, with two remarkable elements: the windows, composed of three panels in stained glass made by Fuerstein and Fugel in Stuttgart, and the barrel vault, that forms the ceiling of the room and was painted by Eliseu Visconti. The two lateral resting rooms have circled shapes and its ceilings are spherical vaults, painted by Henrique Bernardelli. The walls are covered with panels painted by Rodolfo Amoedo. At this floor there are also two lateral balconies, with impressive ceramic ceilings and floors in venetian mosaic (Secretaria de Cultura, 2017).

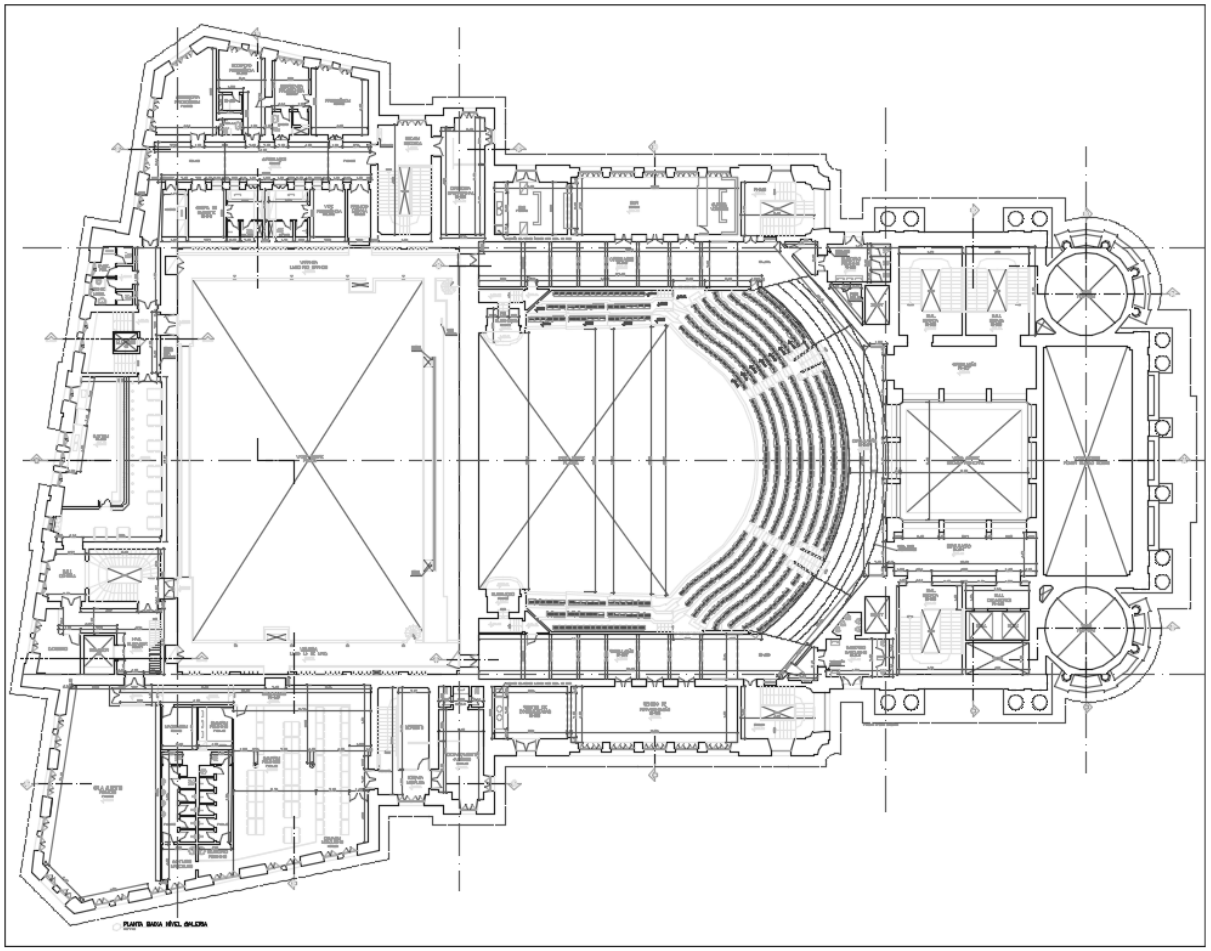

Figure 37 – Plan of the Theatre (Addapted from Fundação Theatro Municipal do Rio de Janeiro, 2006)

The audience of the showroom is divided in six categories: the central audience and the lateral houses located in the first level, the noble balcony and the cabins in the second level, the simple balcony in the third level and the galleries in the fourth level. The stage is located in the first level, with the moat for the orchestra underneath it. The technical room for lights and sounds is located over the noble balcony.

The lobby has access to the central audience and the lateral houses. From the lateral corridor is possible to reach the lateral stairs and elevators that will lead to the three floors and the restaurant Assyrio in the basement. The *foyer* gives access to the noble balcony and the cabins. The simple balcony and the galleries are located on the third floor and fourth floor respectively, which can be accessed by lateral stairs.

The most important artistic features of the showroom are a painting from Eliseu Visconti, located over the stage, the central chandelier made of crystal and the “As Oreadas”, the painting that surrounds the chandelier, also by Visconti, in an elliptical shape (Figure 38).

Figure 38 – Painting in the ceiling of the concert hall (“Eliseu Visconti - Site oficial do pintor,” n.d.)

The remarkable Assyrio restaurant is located at the underground of the building. It is characterized by a sudden change in the architectonic style, since its decoration is based in the Babylonian and Persian style (Fundação Theatro Municipal do Rio de Janeiro, 2016).

The stage consists in a huge open space in box shape, surrounded by two main walls that avoid the fire to expand to other parts of the theatre. There are corridors in the laterals of the stage on both sides and at five different levels. The stage machinery is located in the basement, while the supports for the scenery features are located on the top.

- **Roof**

The roof is the most impressive part of the building, extensively ornamented, made of noble materials and a morphology of high complexity (Figure 39). The original tiles were made of zinc. However, they were replaced later by copper tiles. The main parts are a barrel vault, two small domes in both sides of the main façade and half a dome at middle of the building.

Figure 39 – Roof of Theatro Municipal do Rio de Janeiro (SkyscraperCity, 2011)

The roof over the *foyer* is cylindrical, with an artistic type of fence over its ridge, while the lateral resting rooms are covered with spherical domes. The main stairs are covered by a roof with two levels. The first level is composed by four faces and the second level consists in a skylight of glass and metallic structure, which allows the entrance of natural light into the building. This part of the roof was modified in interventions along the theatre's history.

The great dome (*Grande Cúpula*) is the central element of the theatre, covering the showroom. It has a half-elliptical shape in the front part and a regular shape in the back. There is a globe in its higher point and on top of it rests the sculpture of an eagle measuring 6,98m wide and 3,72m height. The roof over the stage has a regular shape with two sides, being the tallest part of the building with 47m height.

3.2.3. Structure

The structure of the Theatre is supported by 1180 wood piles with length between 4 and 11m. It is known that the piles are immersed in water, once the water table in this region is close to the surface. The ground in this location is result of landfill over a lagoon (Fundação Theatro Municipal do Rio de Janeiro, 2016).

The structural system consists in load-bearing walls with the internal structure made of metallic beams and columns made of cast iron and marble, respectively. The roof is made of wood and metallic trusses that reach a span of 30m in some parts of the building, supporting the metallic tiles and wooden plates. The metallic structure is made of steel and wrought iron in preference of the cast iron (Cintra et al., 2017), which was used mainly in the piers of the showroom. The properties of the metallic elements are presented in Table 2. The walls are made of stone masonry in the first floor,

while the upper parts are made of solid brick masonry, the piers on the façade and around the stairs are made of marble (Figure 40). The joints of both of them are made with lime-cement based mortar.

Table 2 – Strength of metallic elements (Cintra et al., 2017)

Material	Type of stress allowed	Maximum stress (MPa)
Cast iron	Compression	100
Wrought iron	Tension and compression	80
Steel	Tension and compression	120

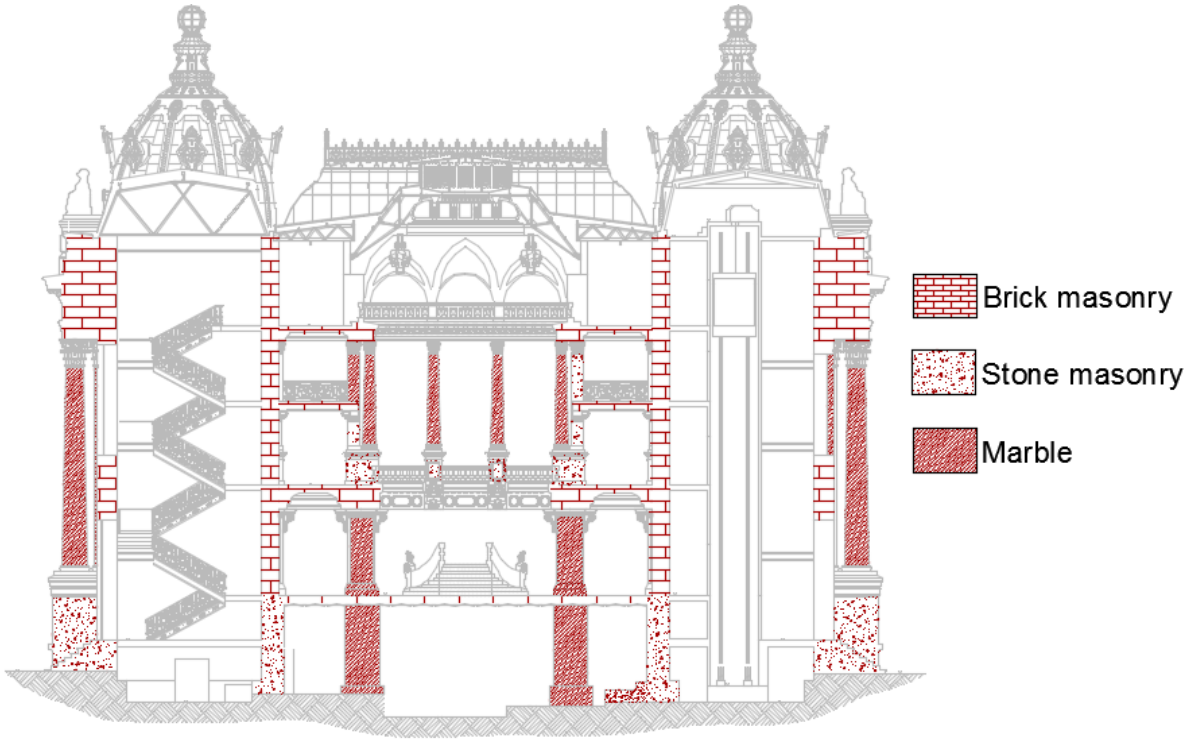

Figure 40 – Masonry types on walls piers and columns

The concert room is supported by marble piers, with granite bases together with 12 cast iron piers that support the roof and its dome (Cintra et al., 2017). The beams that support the slabs of the audience are made of steel and have spans reaching 7.6m, which support transversal beams made of laminated profiles with span of 4.9m and with a spacing of 1.3m. The slabs are made of ceramic bricks covered with cement based mortar (Cerne Engenharia e Projetos, 2006e). Some of the metallic piers were replaced afterwards by concrete trusses as described in Section 3.3.1.

The *foyer* and the lateral round rooms are supported by masonry walls and marble piers. Metallic beams were used to cross higher spans, such as the surrounds of the stairs, over the windows and under the main stairs. The slabs are made of pierced brick in small vaults that are supported in metallic beams spaced of approximately 1.0m.

The structure of the roof is highly complex and was designed in England by Shewing Steel Work & Frazzi in 1905 (Cintra et al., 2017). It consists of metallic trusses that support the most robust pieces, while timber structure was used to make complex shapes and support the most delicate pieces. The parts of the roof that were modified in the intervention of 1934 are supported by reinforced concrete structures. The timber structure is covered by wooden rules that are responsible for the shape of the roof, which are the base to fix the metallic tiles. A bitumen lining is placed under the tiles in order to guarantee the impermeabilization of the roof. The original tiles were made of zinc and were replaced later by copper tiles. The tiles are enough deformable so that they can follow the shape defined by the timber structure (Machado, 2012).

The roof is characterized by three main parts, which are detailed in this Section: (i) the part over *foyer* (ii) the lateral domes, (iii) the Great dome.

- **Roof over the *foyer***

The *foyer* is covered by a roof made of copper tiles, supported over composite trusses of wood and steel. In Figure 41, four trusses in the transversal direction of the vault can be observed, which are supported in stones joined to the masonry walls, together with four half trusses at the corners. The trusses are connected by horizontal beams in the bottom and in the top plans. The curvature of the roof is made by additional timber elements. The roof structure is supported by the lateral walls and do not have any connection with the internal vault.

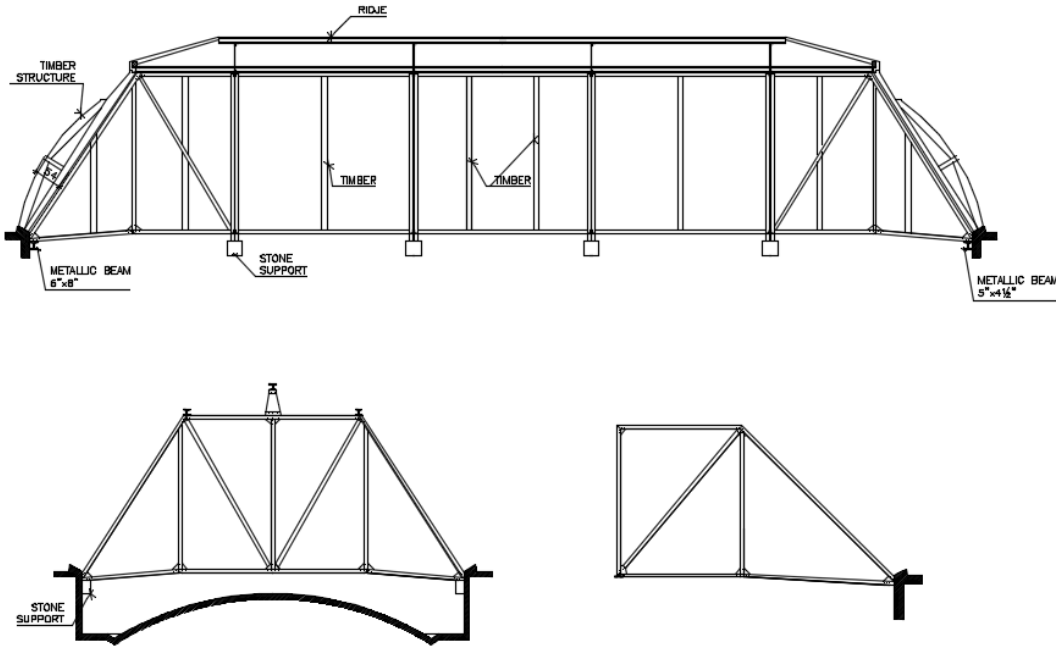

Figure 41 – Structure of the roof over the barrel vault (Cerne Engenharia e Projetos, 2006c)

- **Lateral domes of the roof**

The domes of the roof have a varying curvature making a peak shape and is made of copper tiles with a globe of glass on its top. It is supported in a metallic structure that consists in a square pier

composed on double “L” profiles with bracings along it measuring 9.2m long. From this pier start eight radial bracing profiles in three levels. Each level is made of horizontal and inclined pieces, except for the first level, in which the bottom pieces are also inclined to reach the supporting masonry walls. These bracings are connected to their external extremes, as presented in Figure 42.

These structures are supported only in lateral walls, and do not apply any load in the internal vault, with a spacing between the metallic structure and the dome of more than 1,20m.

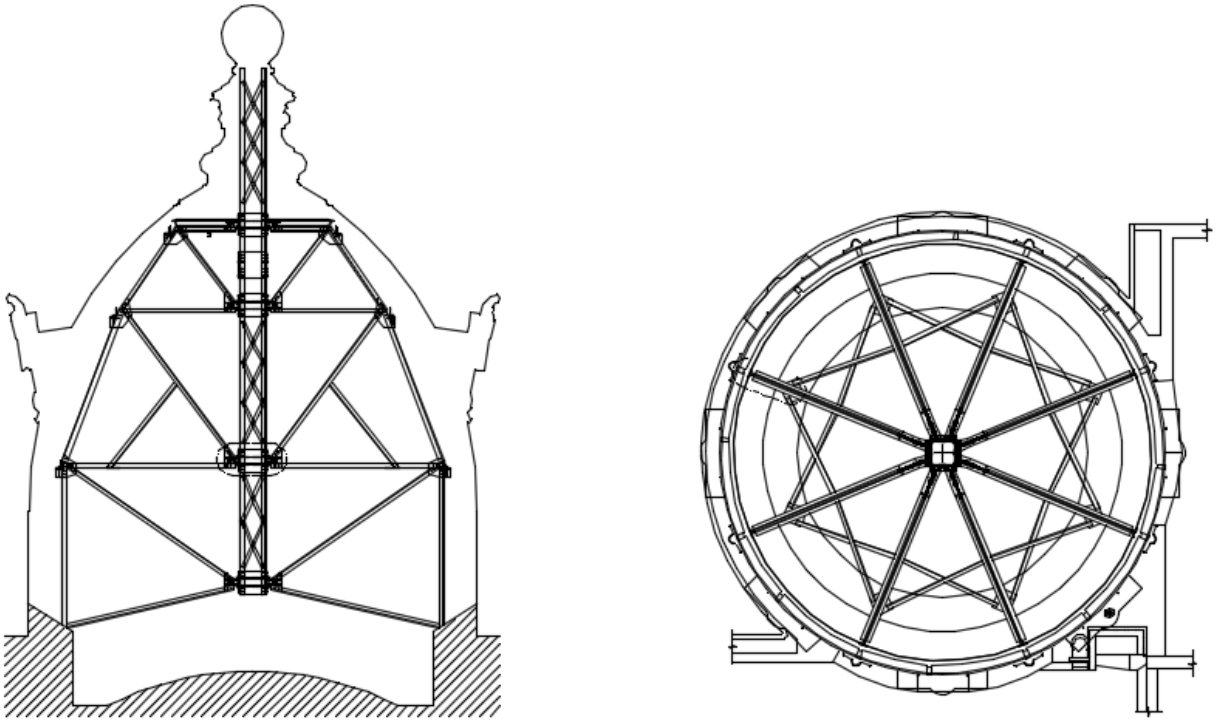

Figure 42 – Metallic structures of the lateral domes (Cerne Engenharia e Projetos, 2006b)

- **Great dome**

The great dome is part of the roof over the elliptical ceiling in the showroom. It is made of copper tiles in the shape of half a sphere in the front part and by a regular triangular roof in the back part. It has a lantern on top of the spherical part close to the connection with the regular part. On top of this lantern, there is a globe that holds the magnificent eagle.

The metallic structure that holds the roof is presented in Figure 43 and Figure 44. The structure of the curved part is made of seven radial trusses forming the shape of the vault, and the top chord follows this variation. The trusses are connected at the center to the main truss, which divides the spherical part from the rectangular part, which crosses a span of 22.5m and supports the weight of the lantern. The radial trusses are supported in the external perimeter of the vault in metallic trusses embedded in the masonry walls. Small profiles make an approximation for the curved shape of the vault, in which timber pieces are supported making the final shape of the vault, to receive the copper tiles. The rectangular part of the roof is supported by three metallic trusses connected by horizontal bracings.

The transversal metallic trusses are supported by the reinforced concrete trusses built in 1934, as well as by the small cantilever trusses.

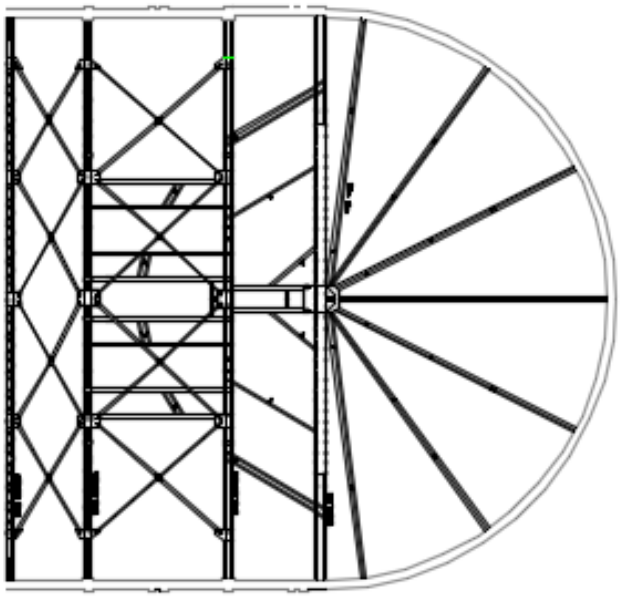

Figure 43 – Plan of the metallic structure of the roof over the main vault (Addapted from Cerne Engenharia e Projetos, 2006a)

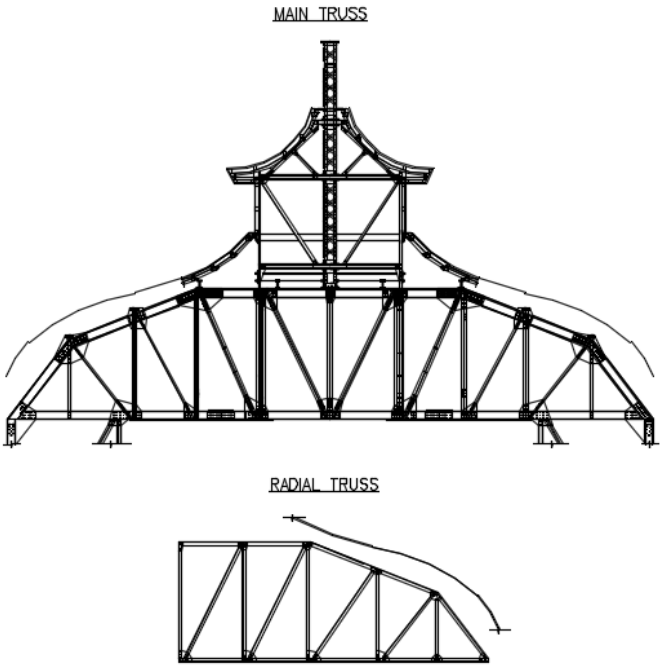

Figure 44 – Trusses of the metallic structure of the roof over main vault (Addapted from Cerne Engenharia e Projetos, 2006a)

The elliptical ceiling consists in a reticulated metallic structure covered with panels made of stucco – a mortar made of gypsum, lime and water – that support the canvas for the Viconti's painting. The reticulated structure is made of meridional elements displaced radially surrounded by three rings,

being one of them in the base. The stucco panels consist in plates of plaster with 25cm width, reinforced with textile mesh. Even though this element resembles a vault, it does not behave structurally as a shell.

The ceiling is supported by metallic ties fixed in the metallic structure of the roof, which distribution can be observed in Figure 45.

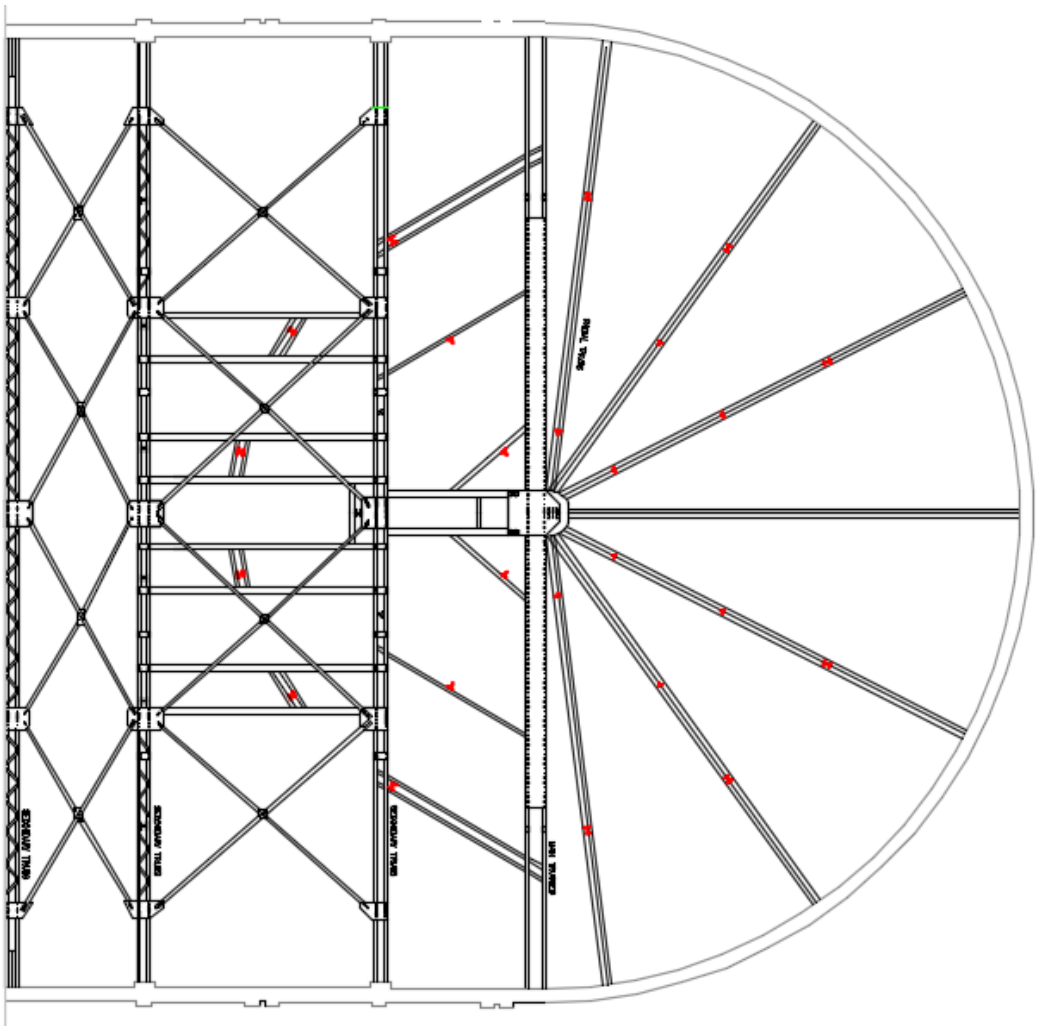

Figure 45 – Position of the ties that support the main internal vault (Addapted from Cerne Engenharia e Projetos, 2006a)

3.3 Anamnesis

Since its construction, the Theatre passed through four main interventions in 1934, 1975, 1996 and 2008, which will be described in the following Sections together with other important events in the surroundings that may have affected the Theatre's structure.

3.3.1. Intervention in 1934

In 1934, a great renovation work was performed in the theatre to increase its capacity with design by Paulo Fragoso and Bjarne Ness (Cintra et al., 2017). The internal divisions in the central audience and the noble balcony were removed, increasing the number of chairs. Aiming at increasing the visibility, the cast iron piers in the noble balcony were removed and replaced by three reinforced concrete trusses with six meters height to cross a span of 30m, which are supported by masonry walls, as presented in Figure 46. In the opposite side of the stage cantilever trusses were built to support the new arrangement of the space with spans of 6m (Cerne Engenharia e Projetos, 2006e).

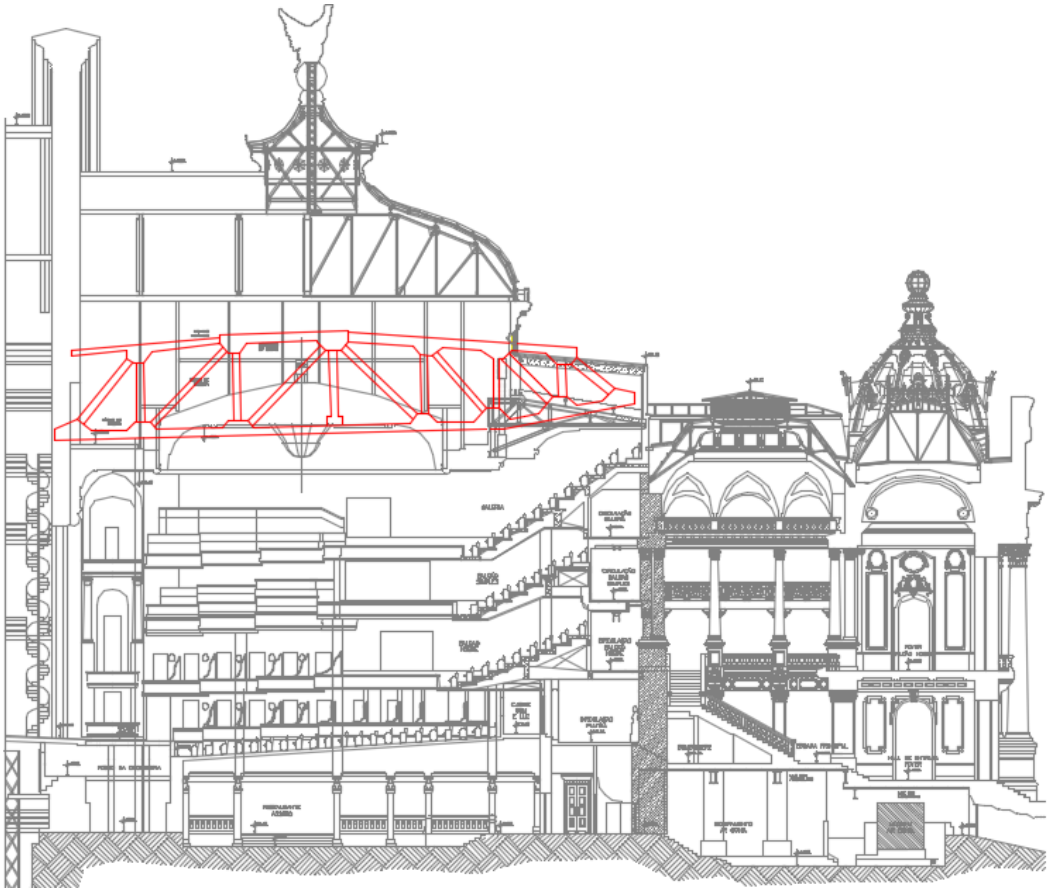

Figure 46 – Concrete truss that replaced the cast iron piers (Cerne Engenharia e Projetos, 2006d)

This intervention resulted in considerable volumetric changes in the part of the roof over the stairs. A masonry wall between the main vault and the main stairs was built to support these trusses, which divided the roof over the stairs in two levels, creating a new volume of rectangular shape presented in Figure 47. A new structure of reinforced concrete and beams was built and can be seen in the corridor of the galleries, with the apparent sequential beams (Machado, 2012). Nowadays, the original structure is only responsible for supporting the ceiling (Cerne Engenharia e Projetos, 2006e).

Figure 47 – Volumetric change due to the intervention of 1934 (Machado, 2012)

3.3.2. Construction of metro station in the end of 1970s

The metro of Rio de Janeiro was inaugurated in 1975 with 5 stations: Praça Onze, Central, Presidente Vargas, Cinelândia and Glória, which construction carried out in the previous nine years. The Cinelândia station is located very close to the theatre. Figure 48 shows the construction of the station and the proximity of the ditch to the theatre can be observed. These excavations led to instability issues in the structure of the theatre, causing the appearance of cracks. It is notable especially the cracks in the vault over the *foyer*, which had to be reinforced as presented in Item 3.3.3.

Figure 48 – Construction of the Cinelândia metro station (O Globo, 1996)

3.3.3. Intervention in 1977-1979

The intervention that carried out between 1977 and 1979 included the restoration of the theatre as a whole, from replacement of damaged copper tiles at the roof to recovery of artistic elements. Hydraulic and electrical installations were also reviewed and updated when necessary (Fundação de Teatros do Rio de Janeiro (FUNTERJ), 1977).

At the time of this intervention, an inspection of the theatre was performed, where the main problem observed in this occasion was related do moisture coming from the roof in poor state of conservation. The humidity led to strong deterioration of the metallic structure of the lateral stairs and severe damage of some artistic elements, mainly in the paintings from Visconti, Amoedo and Bernardelli located in the *foyer* and the lateral spherical rooms (Figure 49). The repair was made by replacement of some of the zinc tiles by copper ones and recover of parts of the metallic and timber trusses that support the roof (Machado, 2012).

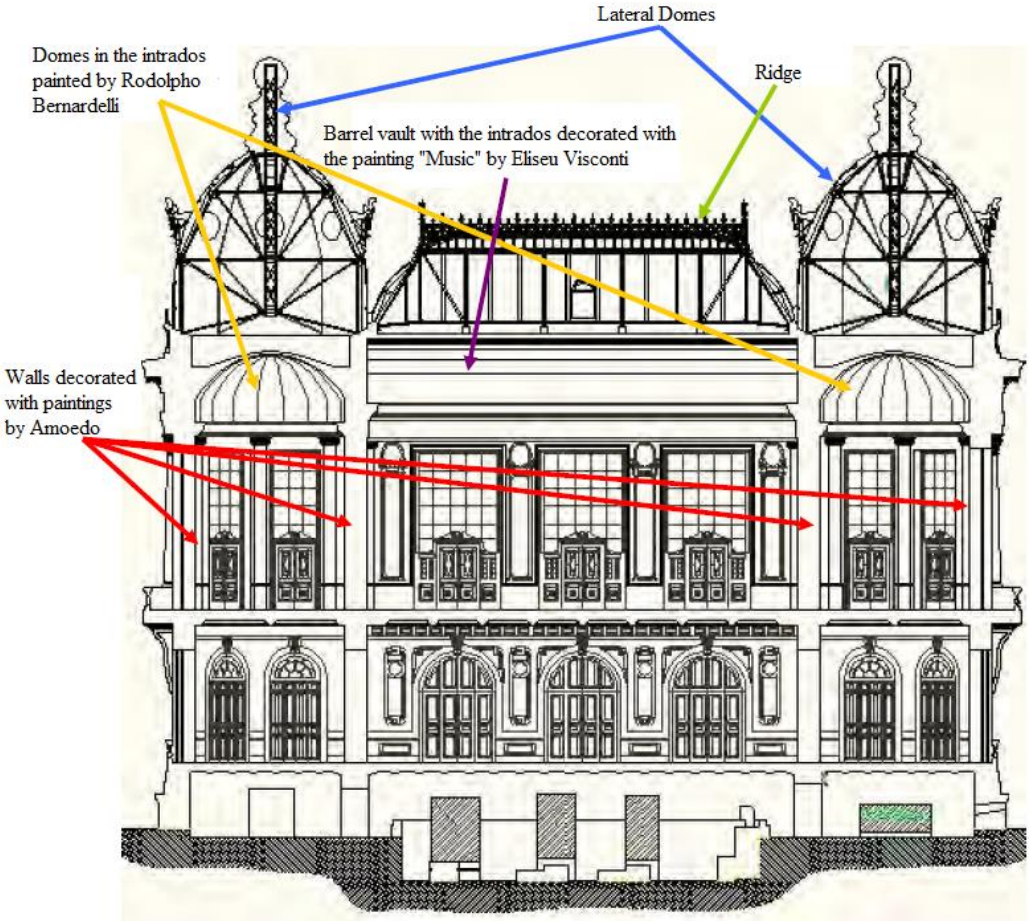

Figure 49 – Decorative elements with damage identified in 1975 (Machado, 2012)

A report made by FUNTERJ (1977) describes the paintings of the spherical vaults as in a desperately state of conservation due to humidity and fungi attacks. The vault over the *foyer* was also in a critical condition, as consequence of differential soil settlements due to the construction of a metro station

close to the theatre together with humidity caused by the poor conditions of the roof. Severe cracks were observed at all the three vaults (Figure 50 and Figure 51). It was concluded by the time of this inspection that the structure need to be reinforced (Schiros, 1975).

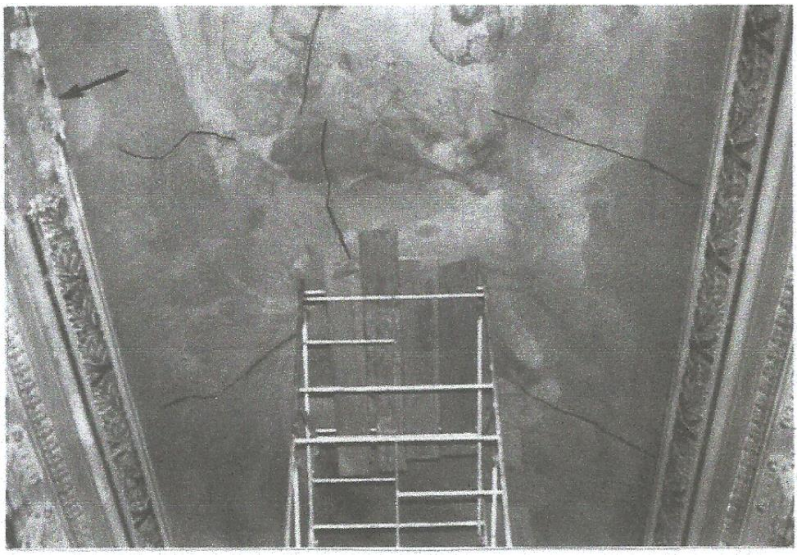

Figure 50 – Cracks in the vault over the *foyer* (Schiros, 1975)

Figure 51 – Cracks in the lateral dome (Schiros, 1975)

An intervention was performed at the barrel vault, in which a layer of projected concrete was built over the existing vault with a reinforcement mesh of 3mm diameters rebars each 10cm in two layers. In addition, two beams of reinforced concrete were built on top of the load bearing masonry walls that

supported the vault in order to help the absorption of the horizontal thrusts created by the vault. The reinforced concrete layer was connected to the masonry vault by metallic elements positioned in each of the bricks of the masonry vault. The existing cracks were sealed, recovering the monolithic behavior of the masonry and finally the Visconti painting was restored (Cintra, 2018).

Even though there is no evidence in the literature mentioning reinforcement of the lateral domes, it is possible to observe the presence of a concrete layer also at these vaults. Hence, it is expected that the reinforcement performed for the barrel vault was extended to the two domes, with the use of similar material and technique.

3.3.4. Intervention in 1987-1989

Even though the last intervention in the roof had been only ten years before, the roof presented poor conditions of conservation leading to some leakage issues. This was due to lack of a maintenance plan. Therefore, the main goal of the intervention between 1987 and 1989 was to cover the areas that present leakage problems.

The architect Jean-Loup Roubert, who previously worked in the roof of Paris Opera, was responsible for the diagnosis and definition of the necessary intervention. The original plan also included restoration of the façade, interior parts, artistic elements and modernization of the electrical installation and air conditioning. However, due to the limited amount of money available for this intervention, only a small part of the scope was made. The bad state of conservation of the roof remained and the leakage continued in several areas. After this, punctual actions were made but were not enough to completely solve the damages (Machado, 2012).

3.3.5. Intervention in 2008-2010

The restoration work carried out between 2008 and 2010 was one of the greatest interventions in heritage buildings ever made in Brazil. It included works to recover and modernize the installations and restoration of artistic elements. The intervention involved a multidisciplinary team with careful supervision by Iphan (Institute of National Historical and Artistic Heritage), which has detailed documentation of the works performed (Machado, 2012).

The main objective of this intervention was to recover the conditions of the roof. The theatre had suffered with problems related to bad maintenance of the roof along all its history. Even though some intervention were made previously, they were minor and localized works, not capable of solving this issue conclusively. In the inspection made previously to the execution of the works, the state of conservation of the roof was not different from past analysis, presenting several damages and leakage points that caused several damages inside the theatre related to presence of moisture.

The decays observed in the roof were similar in all its extension and were mainly related to weathering, such as solar irradiation, pollution, as well as biological attacks, such as the presence of fungi and excrements of birds. Some tiles were deformed and presented perforation and cracks,

probably due to the action of wind and the lack of a proper path for people to walk over the roof in the occasion of its maintenance. In some cases, bad intervention was performed such as addition of asphaltic waterproofing materials. The metallic structure of the roof did not present any severe damage, with exception of the oxidation of some points and without reduction on the structural capacity. The concrete structure added in 1934 was also in good condition. Some parts of the wood from the structure of the roof were deteriorated (Machado, 2012).

The works performed included recover of the roof structure with replacement of deteriorated elements of timber and metal from the trusses, the wooden ceiling and the bitumen lining. In addition, all the water drainage system was reviewed.

Most of the original zinc tiles were replaced along history by copper tiles. Since zinc tiles were not fabricated anymore, it was decided to use copper tiles in this intervention and eliminate the original zinc from the structure. However, the original zinc tiles had a width of 90cm, which is not a regular size for copper tiles and could not be fabricated in time to fit the schedule of the works. Hence, it was decided to replace all the tiles of the roof by new tiles of 52cm, changing the pagination. Furthermore, the greenish color of the roof was due to the natural oxidation patina of the copper. Thus, the new tiles would not have this coloration, with the reddish color of the copper instead. Therefore, it was decided not only to change the original pagination, but also to apply an artificial patina in the material in order to maintain the greenish aspect. The simple plates were entirely substituted, but the ornaments were fully maintained (Machado, 2012).

3.3.6. Collapse of buildings in the neighborhood in 2012

In January 25, 2012, the “Liberdade” building with twenty stories collapsed, taking with it two more buildings of four and ten stories. The construction is located in Treze de Maio Avenue, 44, in a distance close to 20m from the rear of the Theatre. No important damage was observed in the structure of the Theatre associated to this event, apart from the detachment of part of the plaster in the façade.

3.4 Shells

The main object of this study are the three vaults, namely the barrel vault on top of the *foyer* and the two spherical vaults over the lateral resting rooms. The vaults are crucial parts for the architecture and characterization of the eclectic style of the theatre, being the most important decorative feature in each room where they are located. The vaults have artistic paintings at the intrados. The barrel vault was painted by Eliseu Visconti between 1913 and 1916 in canvas, placed on the surface of the vault. The two lateral vaults were painted by Henrique Bernardelli in 1908 directly over the regularization plaster that covers the masonry (Cintra, 2018).

3.4.1. Barrel vault over the *foyer*

The barrel vault over the *foyer* (Figure 52) is characterized by its cylindric shape with dimensions in plan of 6.20 x 17.40m and rises 2.60m. The intrados section is not a perfect segment of circle, it has varying radius, being bigger on the top part than in the basis. In the extrados the radius is continuous, with same dimension as the biggest one from the intrados. Hence, the intrados and extrados have different curvature, leading to a variation of the thickness of the element. The vault is fully supported in the longitudinal extremes by masonry load bearing walls, while in the transversal direction, it is supported by masonry piers with different cross-section and spacing in each side. In the internal side of the theatre, the vault is supported by four sets of columns with square and circular cross-sections (54cm of size and diameter). The external side is supported by the load bearing wall of the façade, which is characterized by three big openings with spans of 3.30m and 3.15m (Figure 53). Metallic beams cover the spans between columns (see Section 4.3). Reinforcement concrete beams in the lateral of the vault were included in the intervention made from 1977 to 1979, with estimated section of 40 x 40cm.

Figure 52 – Barrel vault over the *foyer* (Eder Santos Carvalho, 2012)

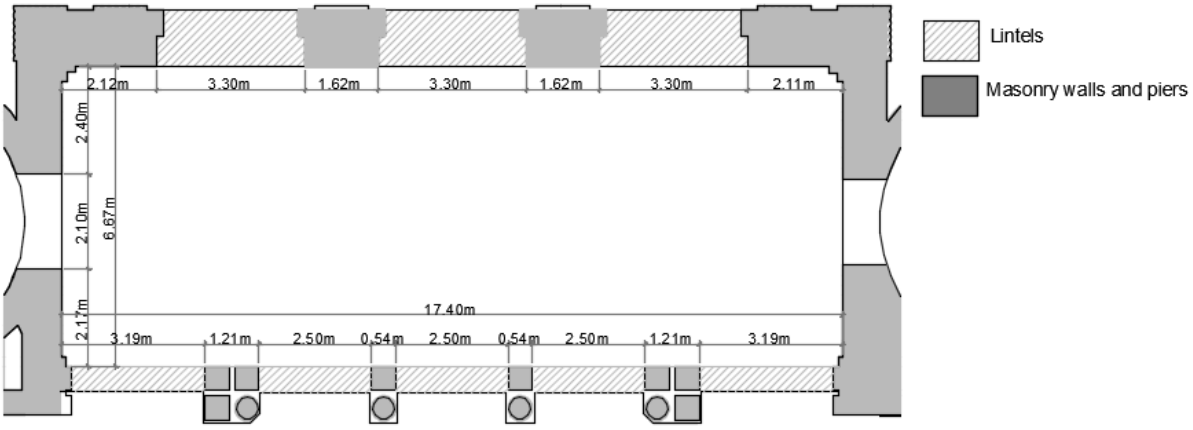

Figure 53 – Suporting conditions of the barrel vault

The vault was originally built with two layers of solid brick masonry and lime mortar joints, with a backing of 1.75m height in the laterals. The total thickness of the vault is estimated to be 30cm and the backing in the laterals with a height of 1.75m. In the 1970s a layer of projected concrete reinforced with 3mm steel rebars each 10cm was applied on top of the vault, in order to increase its stability (see Section 3.3.3). It is assumed that the concrete slab thickness is variable with 7cm in the center of the vault, leading to the different curvatures between the intrados and the extrados (Figure 54).

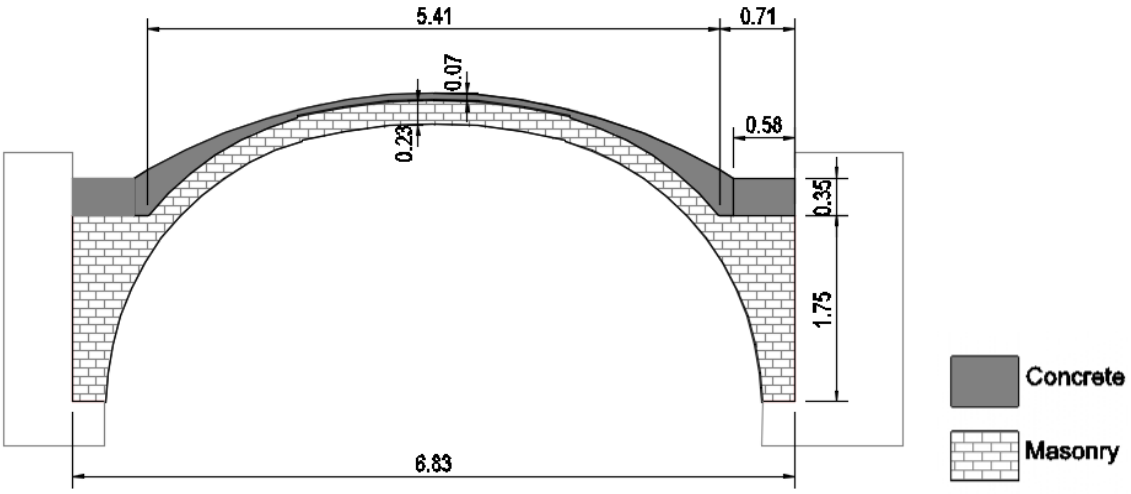

Figure 54 – Transversal cross-section of the barrel vault

3.4.2. Lateral domes

The lateral vaults (Figure 55) have round shape in plan with diameter of 6.00m and rise of 1.80m, being a segmental dome, with the rise smaller than the radius. The dome has double curvature with the radius of the extrados being 5.97m. The vault is supported by masonry walls. However, openings

in the walls due to the presence of windows and doors break the continuity of the support, as presented in Figure 56. Over the windows openings metallic, beams were placed to cover the span (see Section 4.3).

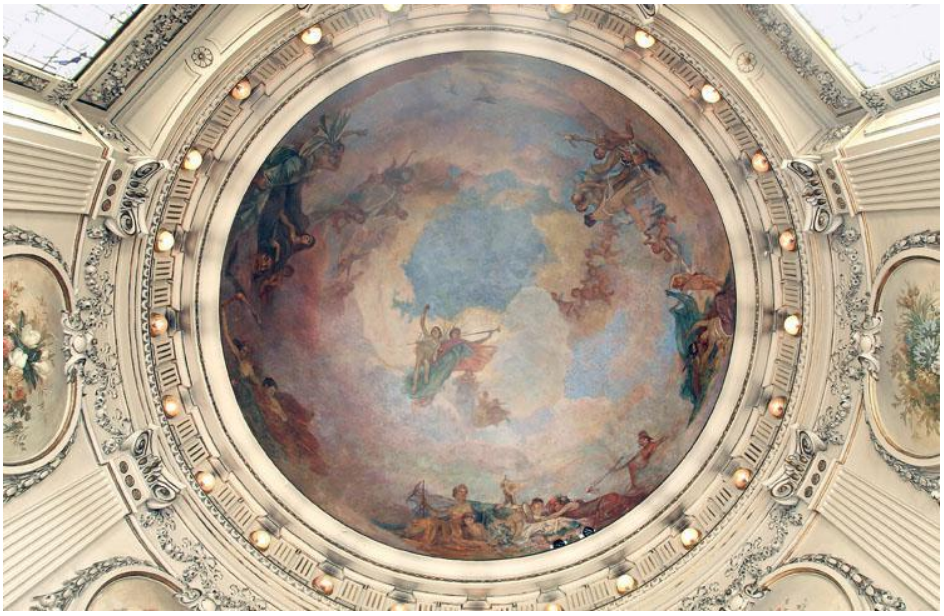

Figure 55 – Spherical vaults over the lateral rooms (Mapa de Cultura RJ, n.d.)

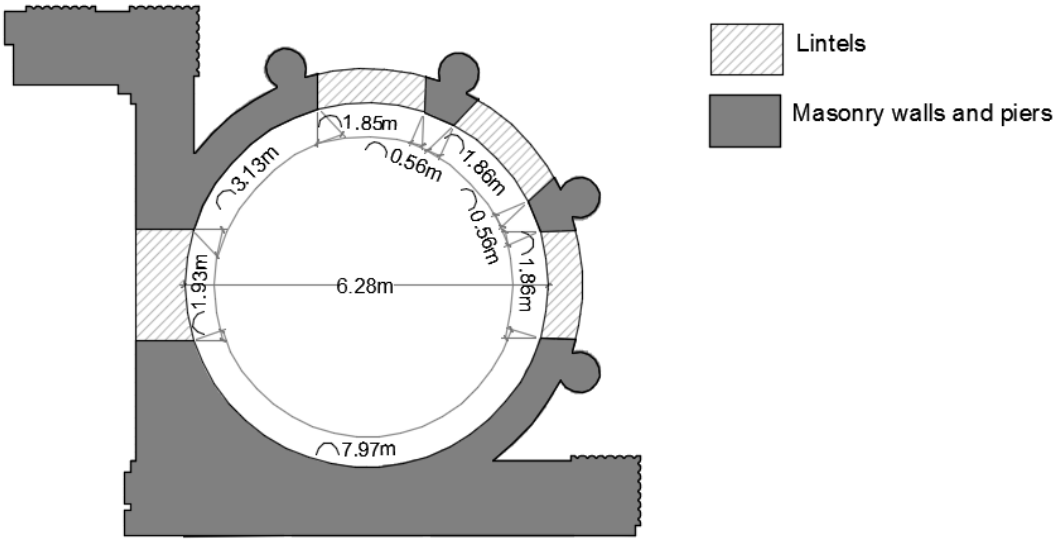

Figure 56 – Support conditions of the lateral domes

The material used for their construction is the same as for the barrel vault, namely masonry with solid bricks and lime mortar joints. However, in this case it is only one layer of bricks placed in the transversal direction. Due to lack of information, the same construction typology was assumed for the barrel vault and the dome, being considered a backing in the perimeter of the dome with 1.33m height. As mentioned in Section 3.3.3, the domes were also reinforced with concrete layer in the intervention

that carried out between 1977 and 1979. It is assumed that similar material and technique from the barrel vault was adopted. An estimation of the different layers is presented in Figure 57: a layer of reinforced concrete with thickness varying from 4cm to 10cm, and a 10cm layer of masonry material. The lateral of the dome is filled with perforated brick.

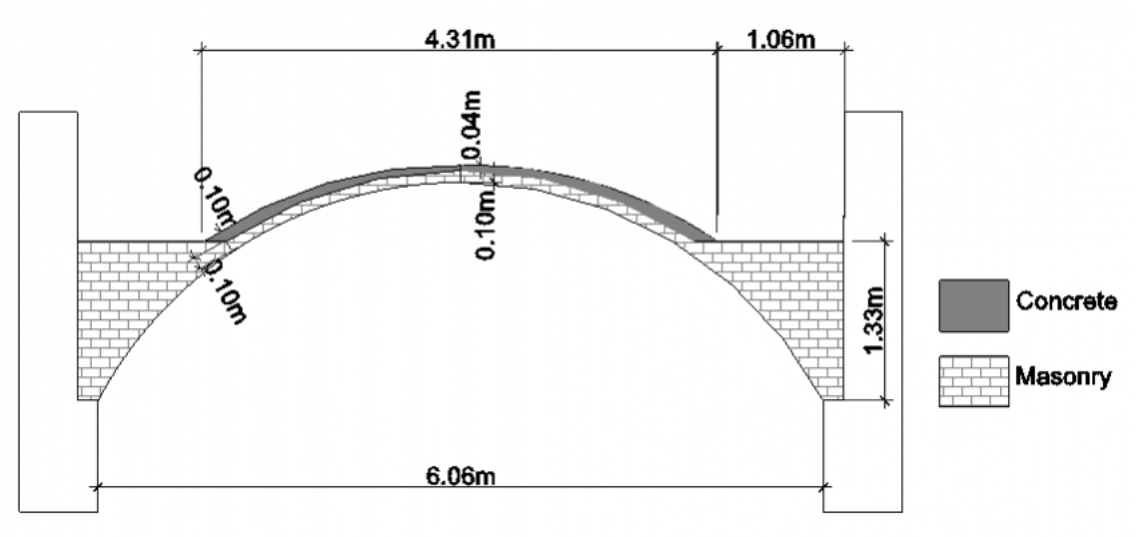

Figure 57 – Transversal cross-section of the lateral domes

4. NON-DESTRUCTIVE TESTS

4.1 Introduction

In order to have a proper understanding of any structure, it is necessary to know its elements, materials, morphology, structural features and conservation status. The Municipal Theatre of Rio de Janeiro is built in eclectic architectonic style, which is known for the extensive decoration, with no apparent parts of the structural materials. Hence, it is very difficult to identify the structural elements and conditions only by visual inspection. It is necessary to perform non-destructive tests to have a better understanding of the structure.

An investigation campaign has been carried including diverse NDT tests to gather information regarding structural conditions, morphology and materials that may affect the behaviour of the shells under study (Cintra, 2018). The results of thermography tests performed in the context of this study, are presented in Section 4.2.

Additionally, pachometry tests were carried out to identify metallic elements embedded in the masonry walls (Section 4.3). Also, dynamic identification tests were performed in order to estimate the dynamic properties of the structure (Section 4.4).

4.2 Thermography

The tests with thermographic camera were carried out on January 19, 2017 by a team from Catholic University of Rio de Janeiro and Federal Fluminense University. The conditions in situ were 26 to 28ºC of temperature with 59% humidity. It was used a camera FLIR T1020 with infrared sensor.

Figure 58 presents the thermographic pictures from the two extremes of the vault over the *foyer*, in which can be seen the layout of the ceramic bricks placed in the longitudinal direction of the vault. It was possible to estimate the size of the bricks in 20x10x5cm. Cracks can be observed in both pictures. These cracks are probably the same cracks that were object of repair in the 1970s, since they have similar description and location – longitudinal cracks in the middle of the vault.

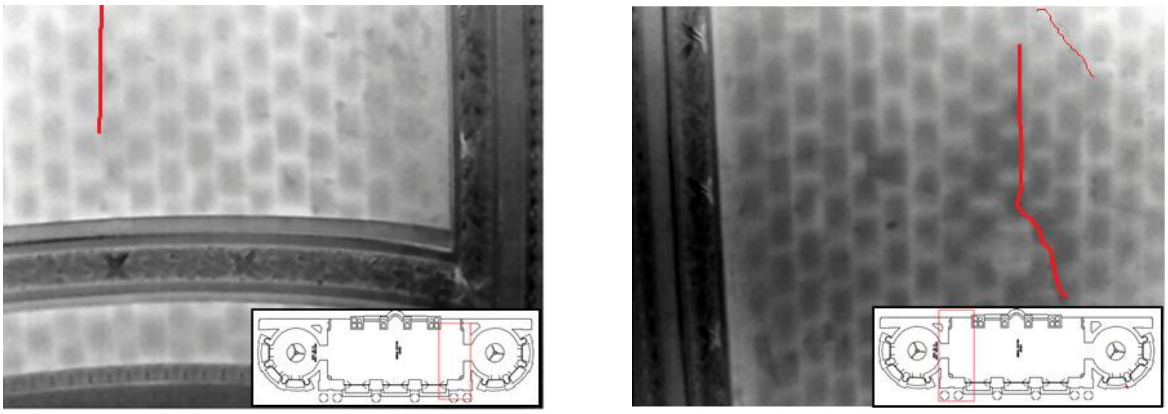

Figure 58 – Thermographic pictures of the vault over the *foyer* (Cintra, 2018)

Figure 59 and Figure 60 present the thermographic pictures for the lateral domes on each side of the *foyer*. In Figure 59, it is possible to see the layout of the bricks, which is different from the layout of the vault over the *foyer*. This confirms the information previously mentioned, namely that in these vaults it is only one layer of bricks set in the perpendicular direction. Cracks can be observed in both vaults, which probably were repaired in the intervention from 1977-1979.

Figure 59 – Thermographic picture of the vault on side of Rio Branco Avenue (Cintra, 2018)

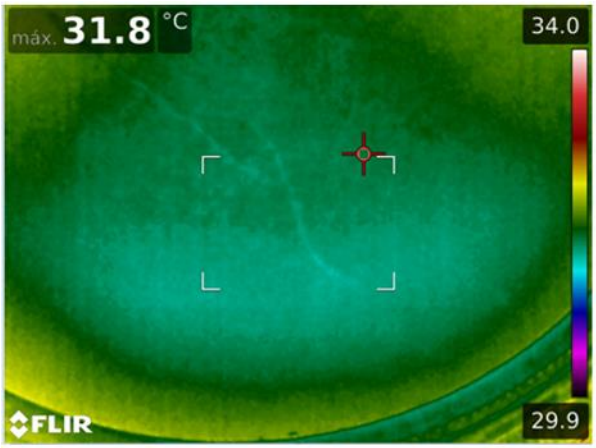

Figure 60 – Thermographic picture of the vault on side of Treze de Maio Avenue (Cintra, 2018)

4.3 Pachometry

It was known from historic and architectonic research that the concert hall and the roof are supported by metallic structures. However, there is little information regarding the presence of metallic structure in the *foyer*, apart from one drawing from the original design presenting metallic beams supported by a pier at the corner of the main stairs (Figure 61). Since the spans in this part of the structure are considerably high to be supported solely by flat masonry, it is highly possible that metallic beams embedded in the structure are present not only in the position specified in the drawing, but also in other parts of the structure. A pachometer was used to identify the location of metallic beams in the main spans of the structure.

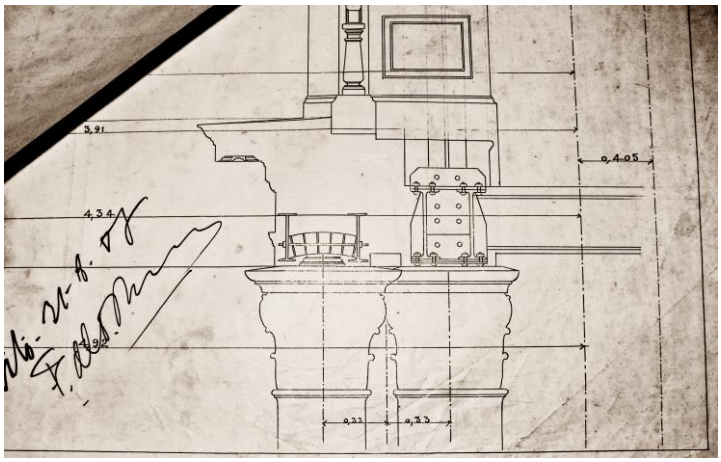

Figure 61 – Original drawing of the structure with the presence of metallic beams

The tests confirmed the presence of metallic beams in the perimeter of the opening of the main stairs in all levels – noble balcony, simple balcony and gallery. Metallic beams in the spans formed by the openings of the windows in the lateral resting rooms were also identified, but there is no evidence of metallic elements over the opening of the door or in other parts of this room. It was not possible to measure over the openings of the windows of the *foyer*, but due to the large span in this region, it is assumed the presence of metallic beams also in this part of the structure. Figure 62 presents the distribution of metallic beams in the structure.

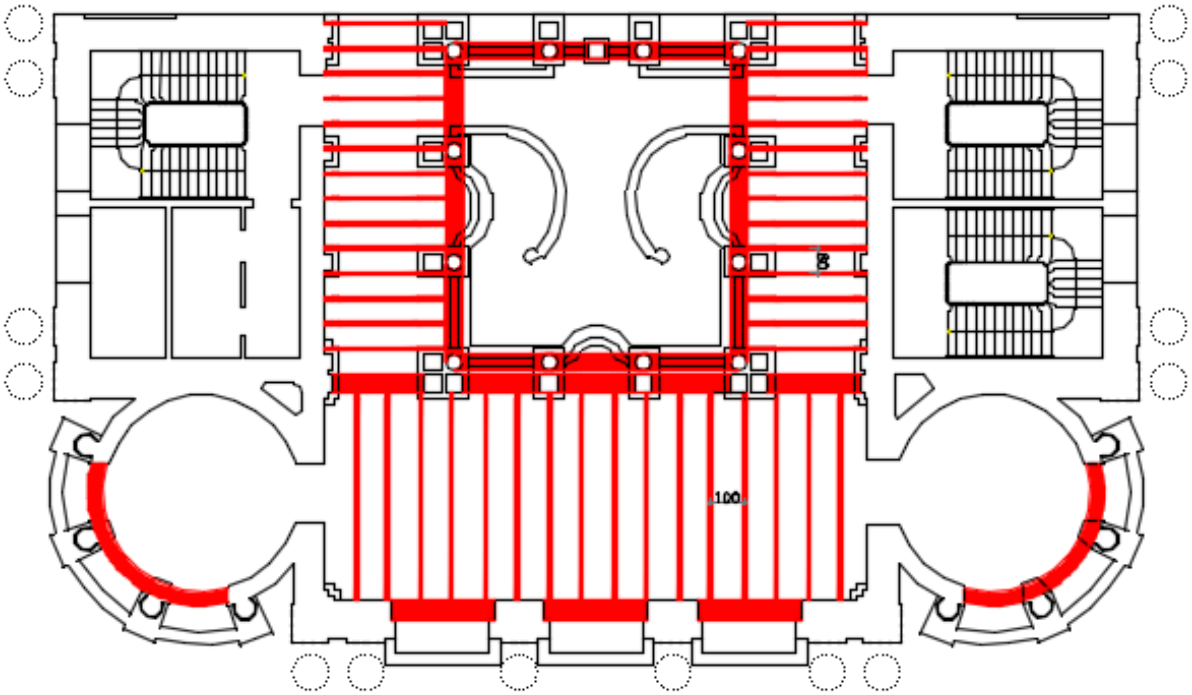

Figure 62 – Schematic distribution of metallic beams according to pachometer inspection

In the slab of the *foyer* beams were identified each one meter, while in the slabs in the lateral to the stairs the beams are spaced of 80cm (all floors). Since it is known that the slabs of the first level are made of small vaults supported by metallic beams, it is assumed that the same structural arrangement was used for the other levels.

4.4 Dynamic Identification

Dynamic identification tests were performed in the Municipal Theatre of Rio de Janeiro, aiming at estimating the dynamic properties (natural frequencies and mode shapes), mainly of the global modes of the structure and the local modes of the shells. There are three shell elements considered in this study, namely the barrel vault located over the main room of the *foyer* and two domes located over the lateral resting rooms. In this study, symmetry of the structure was assumed, hence only one of the domes was tested.

The tests performed in the Municipal Theatre of Rio de Janeiro were carried out by a team from University of Minho and Catholic University of Rio de Janeiro, from 15th to 19th May, 2017. The test planning, results and main conclusions are presented in the next Sections.

4.4.1. Test Planning

The main objective of the dynamic identification test is to estimate the dynamic properties of the structure: natural frequencies and mode shapes. These information can be used to validate and update numerical models, assess level of connection between parts of the structure, identify weak structural features and evaluate the influence of major damage on the structural response (Elyamani, 2015).

In this study, the output only technique was adopted, where only the output is measured and considers ambient vibration as source of excitation (wind, traffic). The ambient vibration tests are recommended for large structures, where application of an excitation is hard to be performed and can involve high costs. In this technique, the main assumption is that ambient excitation is stationary, considered a white noise (Ramos, 2007).

For the instrumentation of the structure eight piezoelectric accelerometers (sensitivity equal to 10 V/g, frequency range from 0.15 to 1000 Hz, dynamic range ± 0.5g) (Figure 63), coaxial cables and one 24 bits data acquisition system with two acquisition boards (Figure 64) were used. A piezoelectric accelerometer is a spring-mass-damper system, in which main advantage is that it does not need external power source, however is not able to measure the DC component – response at 0 Hz (N. A. L. Mendes, 2012). The accelerometers were attached to the structure by a cube made of wood, set with a polymeric paste, to guarantee the stability of the signals. The software used to acquire the data was developed by University of Minho.

The dynamic identification tests performed in the Municipal Theatre of Rio de Janeiro resulted in measurements of a total of 60 points of the structures, being 12 of these in two directions. These points were displaced in a total of 14 setups, with 30 minutes of data recording each and with a sampling frequency of 200Hz. A reference point was defined for all the setups (Figure 65), in which the transversal accelerations were measured. The tests were carried out in three parts, as presented in the following Sections.

Figure 63 – Piezoelectric accelerometer attached to the structure

Figure 64 – Data acquisition system

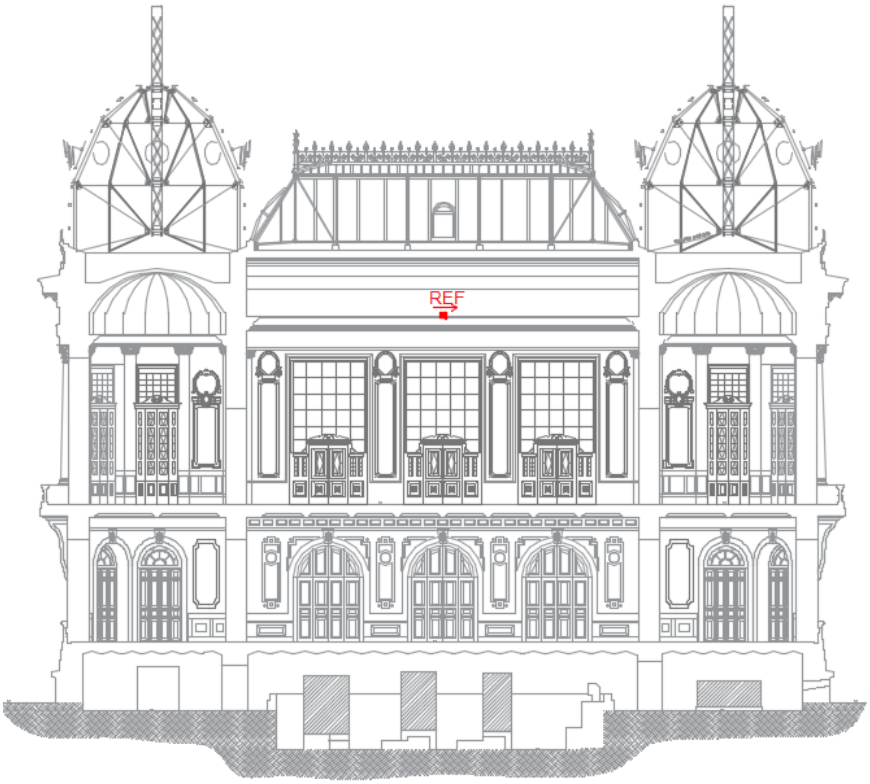

Figure 65 – Position of the reference accelerometer (REF)

- **Global modes of the structure**

Firstly, some accelerometers were set across the structure to estimate the global modes. Due to the large dimensions of the building and limited length of the cables available for the tests, these setups were performed with less accelerometers than the setups for estimating the local modes of the shells, leading to a total of seven setups for 17 points. The acceleration signals were performed in three directions as presented in Figure 66.

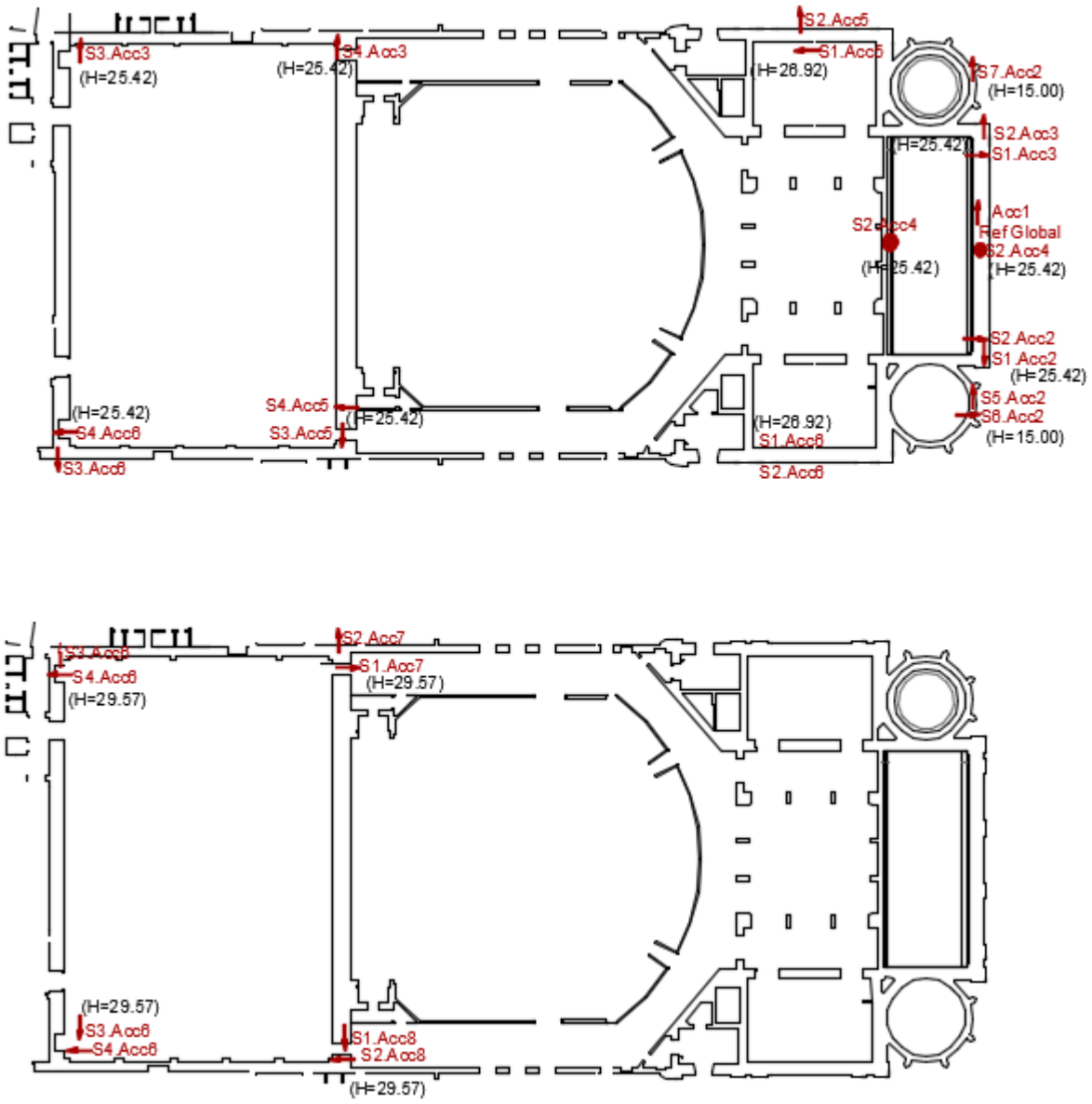

Figure 66 – Setups for estimating the global modes of the structure ("H" is the height of the building)

- **Vault over the *foyer***

A total of 25 points were measured in the vault over the *foyer*. The points were divided in four setups with seven accelerometers each, namely one reference and six varying points. A local reference was defined for these four setups, being identified by the accelerometer number one (Figure 67).

All the accelerometers were placed in the vertical direction – by using a level to guarantee the correct position – with the objective to identify the local modes of vibration of the shell. As presented in Figure 67, it is possible to observe that some points were also measured in the supporting beams, in order to assess the boundary conditions of these elements.

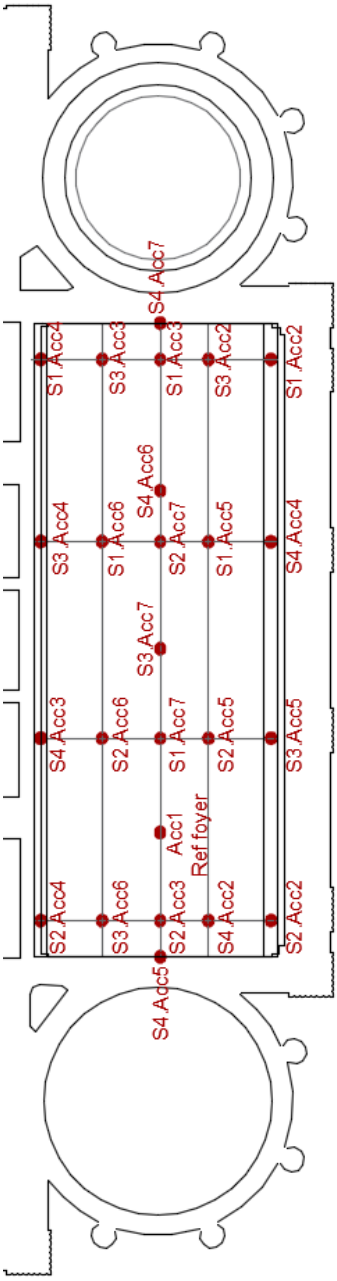

Figure 67 – Setups of the vault over the *foyer* (measurements in the vertical direction)

- **Lateral dome – facing Rio Branco Avenue**

Finally, in the lateral domes 17 points were measures in the vertical direction, including one at the center, which was adopted as reference, and 16 spread across the vault. Two extra accelerometers were placed at the base of the dome to evaluate the boundary conditions. Three setups were performed with seven accelerometers each, being one of them the local reference, and six varying according to Figure 68. Figure 69 presents the accelerometers for the Setup 1.

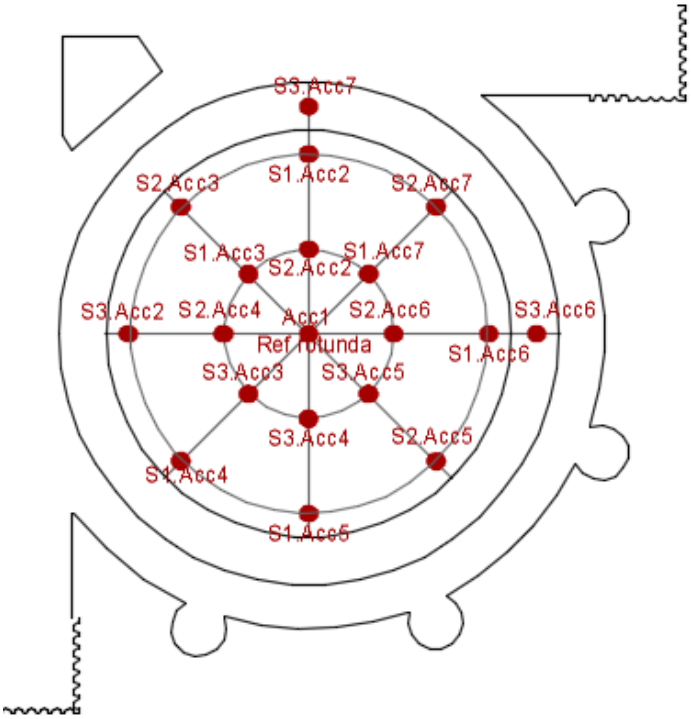

Figure 68 – Setups of the lateral dome on the side of Rio Branco Avenue (measurements in the vertical direction)

Figure 69 – View of the accelerometers for Setup 1 of the lateral dome

4.4.2. Results of the tests

There are several methods to identify the dynamic properties for structures, which can be divided in two main groups: (i) methods in the frequency domain decomposition; (ii) methods in the time domain decomposition. In this study, the FDD (Frequency Domain Decomposition) method was adopted. The FDD is based on the analysis of each measured point and in the correlation between signals, indicating the peaks in the FRF (Frequency Response Function). It assumes that the resonant frequencies are well spaced and the contribution of other modes in the vicinities is null (SVS, 2014). The software ARTeMIS (SVS, 2014) was used to process the data and estimate the dynamic properties of the structure. The mode shapes and their analysis for each part of the test carried out in the Municipal Theatre of Rio de Janeiro are presented below.

- **Global modes of the theatre**

Five modes of vibration were identified for the global behavior of the structure (Figure 70). The mode shapes related to each mode of vibration are presented in Figure 71, where the grey color represents the undeformed element while the blue the deformed shape.

The frequency of the first mode of the structure is equal to 2.82Hz and corresponds to the first transversal mode of the structure. At a frequency of 3.42Hz there is the second mode, which is also a transversal mode. However, in this frequency the front part of the structure moves in opposite direction of the back wall. The third frequency identified (4.32Hz) is the third transversal global mode of the structure. At frequency of 5.57Hz (fourth mode), only the front part (the *foyer*) is mobilized. Finally, the mode shape at the frequency of 6.51Hz corresponds to third global mode of the structural in the transversal direction with third curvature in plan.

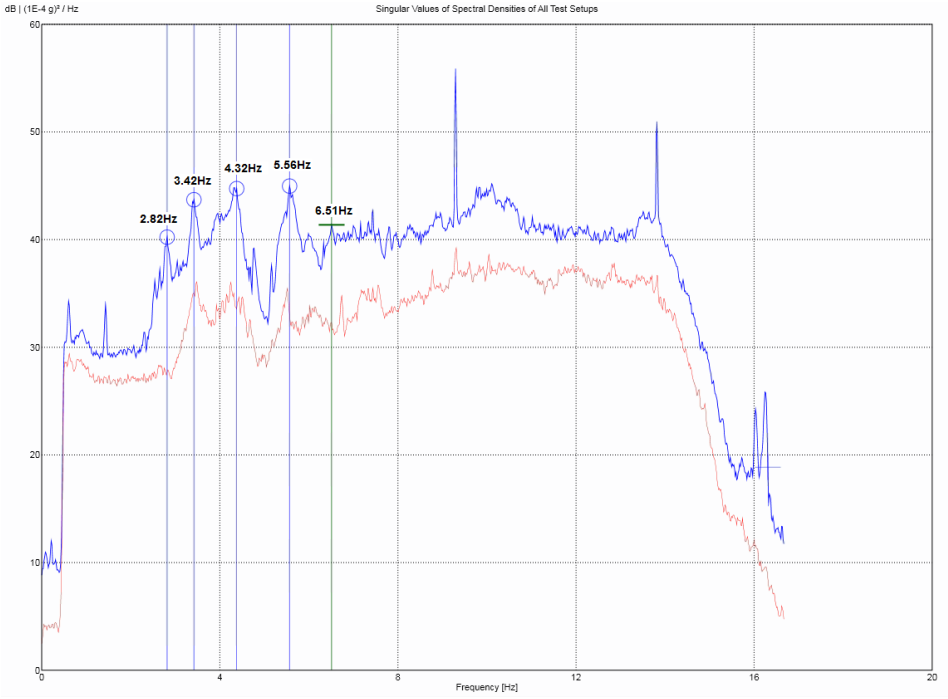

Figure 70 – Singular value of spectral densities of all global setups (FDD method)

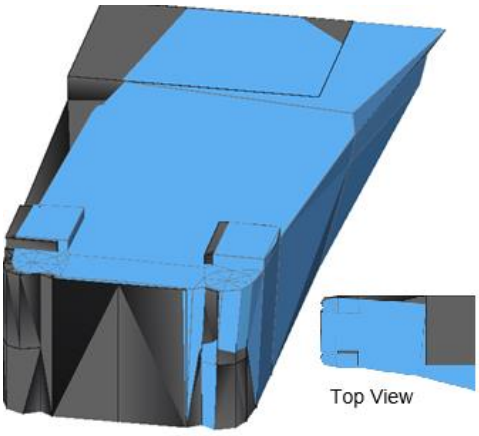

1st Mode [2.82Hz]

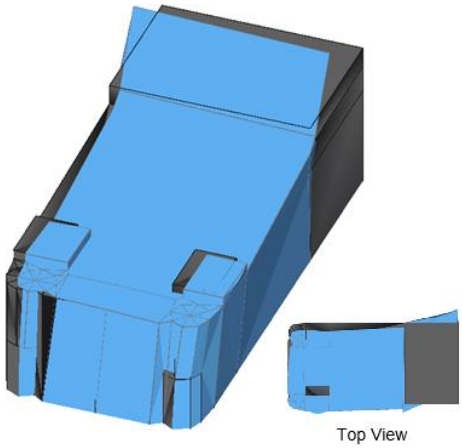

2nd Mode [3.42Hz]

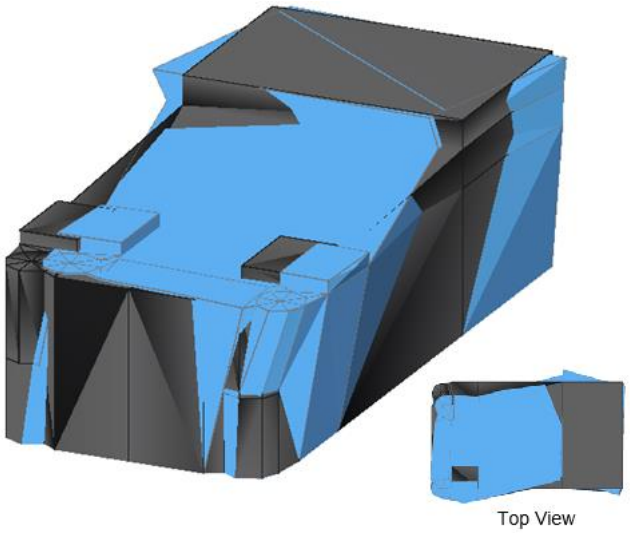

3rd Mode [4.32Hz]

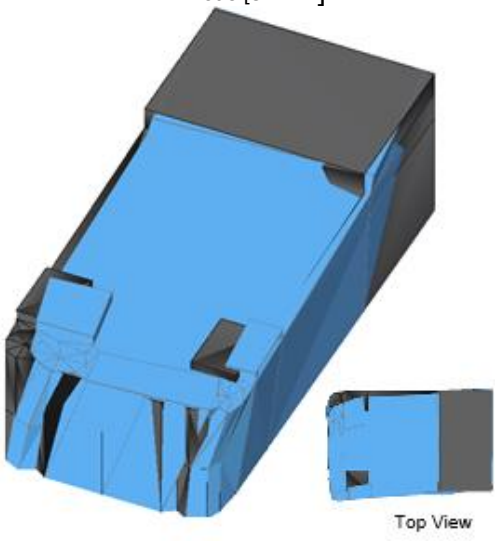

4th Mode [5.57Hz]

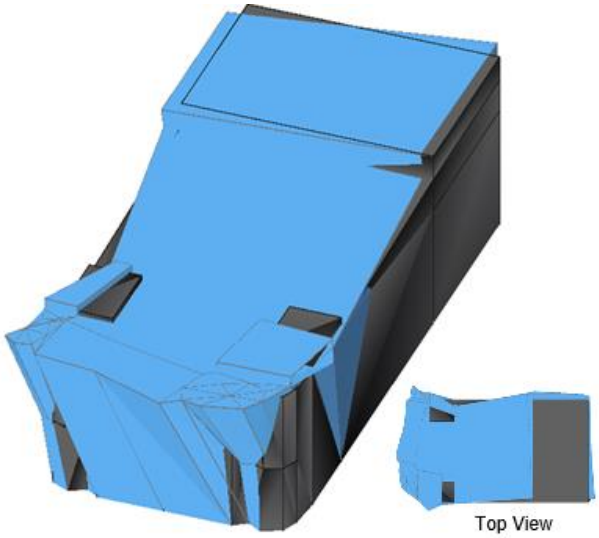

5th Mode [6.51Hz]

Figure 71 – Global mode shapes of the structure

- **Local modes of the vault over the *foyer***

In the dynamic identification tests of the *foyer*, nine modes were identified. Figure 72 presents the singular values of the spectral densities with the identified frequencies. Figure 73 and Figure 74 present the shapes of each mode shape, in which the grey color represents the undeformed element while the blue the deformed shape.

The mode shape at 6.31Hz represents the movement of the vault as a whole. This can be identified by the movement of the base together with the middle of the element. The mode shape at a frequency of 7.13Hz represents also the vertical movement of the vault. However, in this case the middle part moves with greater amplitude than the base. Thus, this mode is identified as the first local mode of the vault with small movement of the supports.

The first main local mode shape of the vault appears at a frequency of 9.57Hz. The boundary points move with very low amplitude, while the middle points present greater amplitude in the vertical direction. The mode shapes at frequencies 14.71Hz, 18.00Hz and 19.40Hz are related to the asymmetry in the boundary conditions of the vault. The modes of the frequencies equal to 14.71Hz and the 19.40Hz are due to transversal asymmetry (longitudinal supports), while the mode with frequency equal to 18.00Hz is asymmetry in the longitudinal direction. The mode shape with frequency equal to 26.04Hz corresponds to a mode in transversal direction with second curvature. The modes with frequencies equal to 27.80 and 29.20Hz are longitudinal modes.

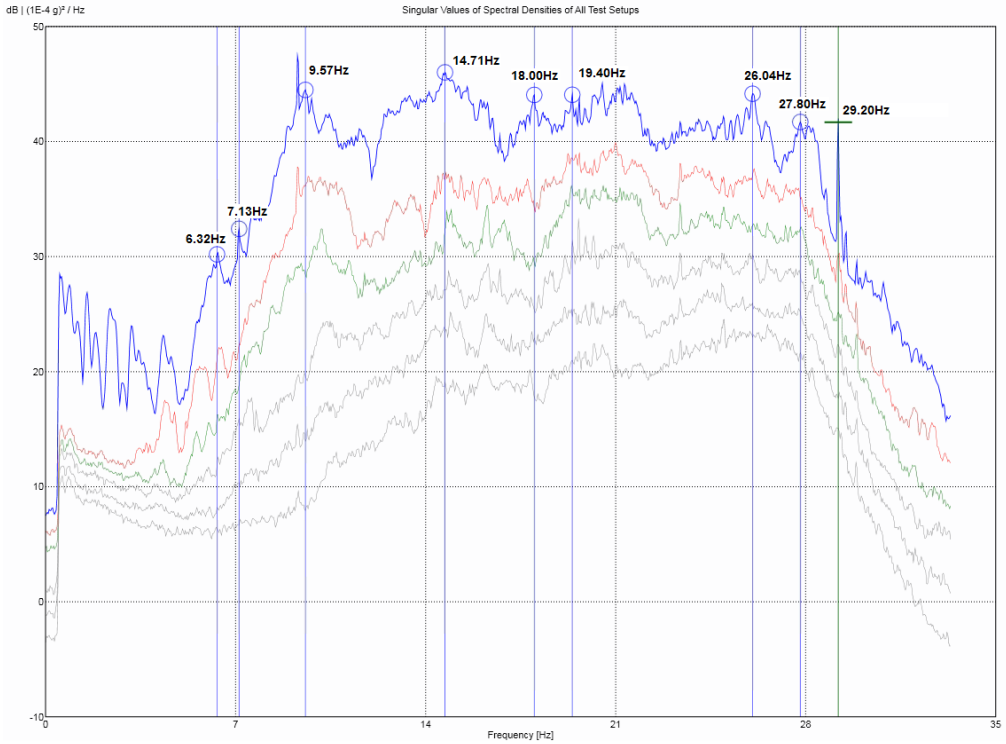

Figure 72 – Singular value of spectral densities of all setups of the vault over the *foyer* (FDD method)

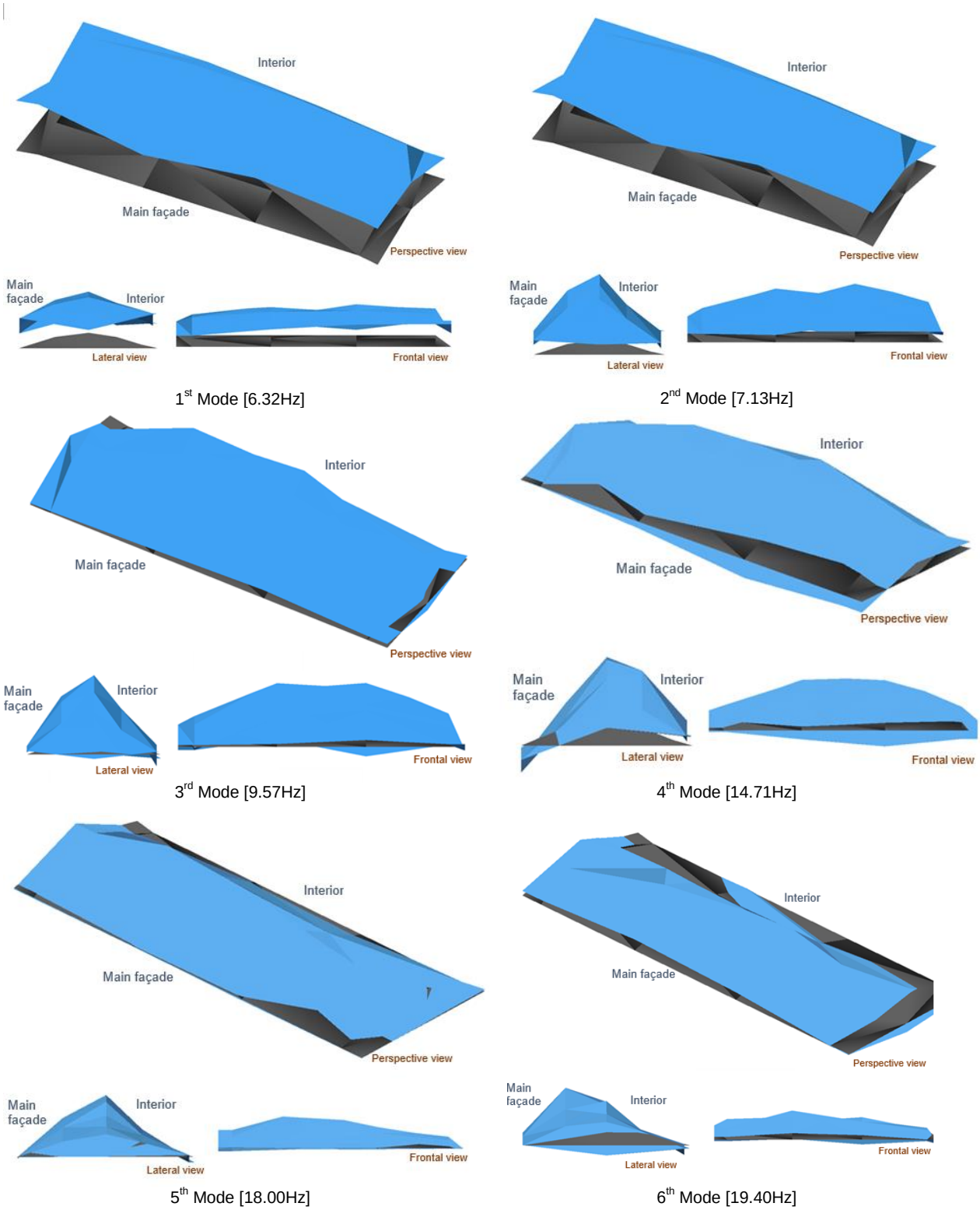

Figure 73 – Local mode shapes of the vault over the *foyer*: 1st do 6th Modes

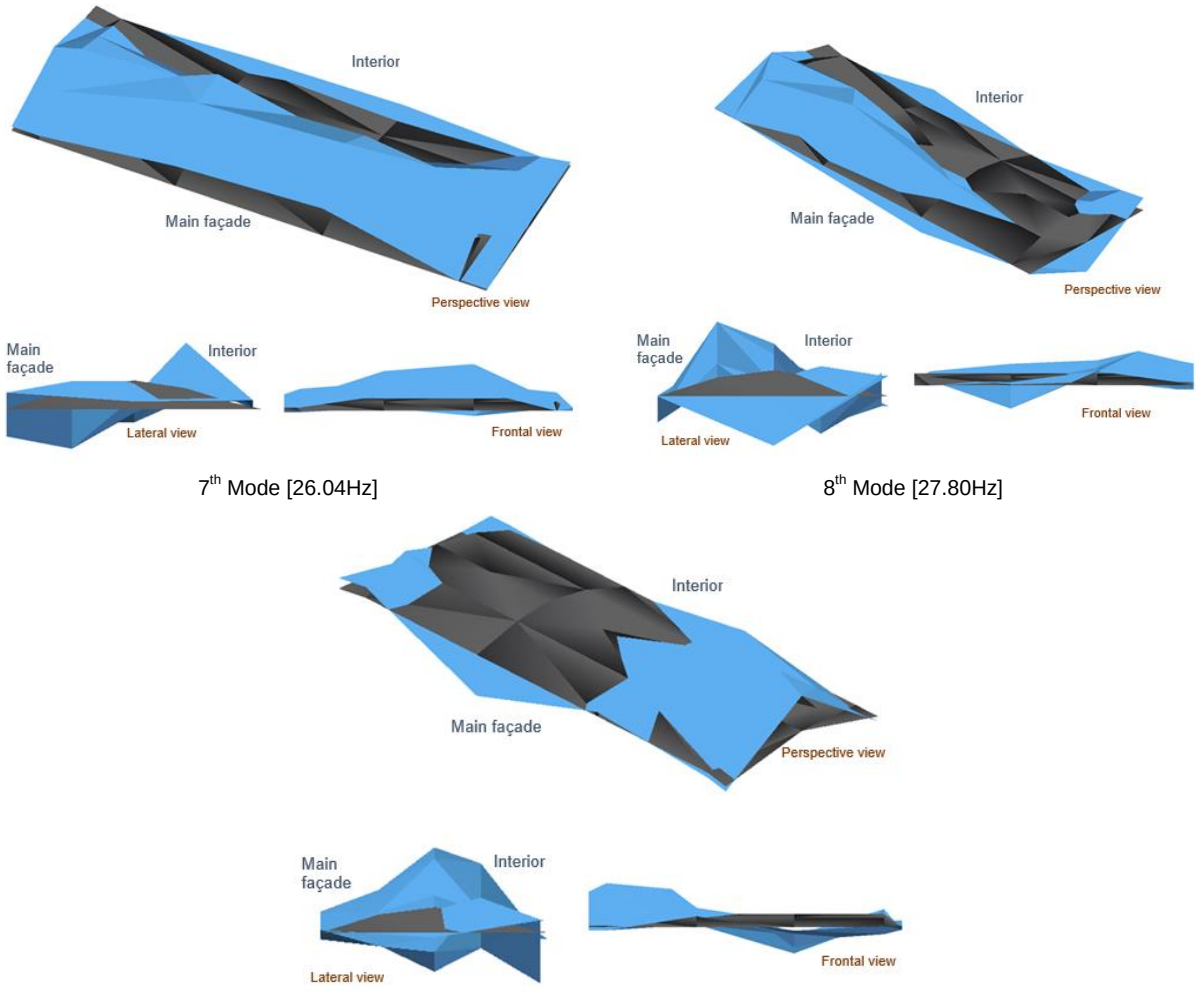

7th Mode [26.04Hz]

8th Mode [27.80Hz]

9th Mode [29.20Hz]

Figure 74 – Local mode shapes of the vault over the *foyer*: 7th do 9th Modes

- **Local modes of the lateral dome**

In the lateral dome, four modes of vibration were identified (Figure 75). The mode shapes of each frequency are presented in Figure 76, in which the grey color represents the undeformed element while the blue the deformed shape. Since this shell element is much more rigid than the *foyer*, the analysis was performed until 100Hz to guarantee that the main mode shapes are analyzed. Furthermore, it is noted that the dome was strengthened with a reinforced concrete layer at the extrados.

As can be observed in Figure 76, the first two mode shapes, with frequencies equal to 4.49 and 29.88Hz, are related to the global behavior of the structure, since there is almost no relative movement between the points of the vault. For the frequency equal to 4.49Hz, the movement is vertical while for the 29.88Hz it is transversal. The mode with frequency equal to 51.66Hz presents local movements of the vault. Only at a frequency of 77.93Hz that the local mode shape of the vault is relevant, even though there is still a global movement attached to it. These high frequencies to mobilize local modes are due to the great stiffness of the vault, since it has a small span and was

reinforced in the 1970s with a layer of reinforced concrete. Higher frequencies should be analyzed in order to verify other local mode of the domes. However, the Nyquist frequency for these dynamic tests is equal to 100Hz, since the sampling frequency adopted was of 200Hz. It is noted that the Nyquist frequency corresponds to the maximum frequency value that the system can correctly analyzed from discrete-time series (Ramos, 2007).

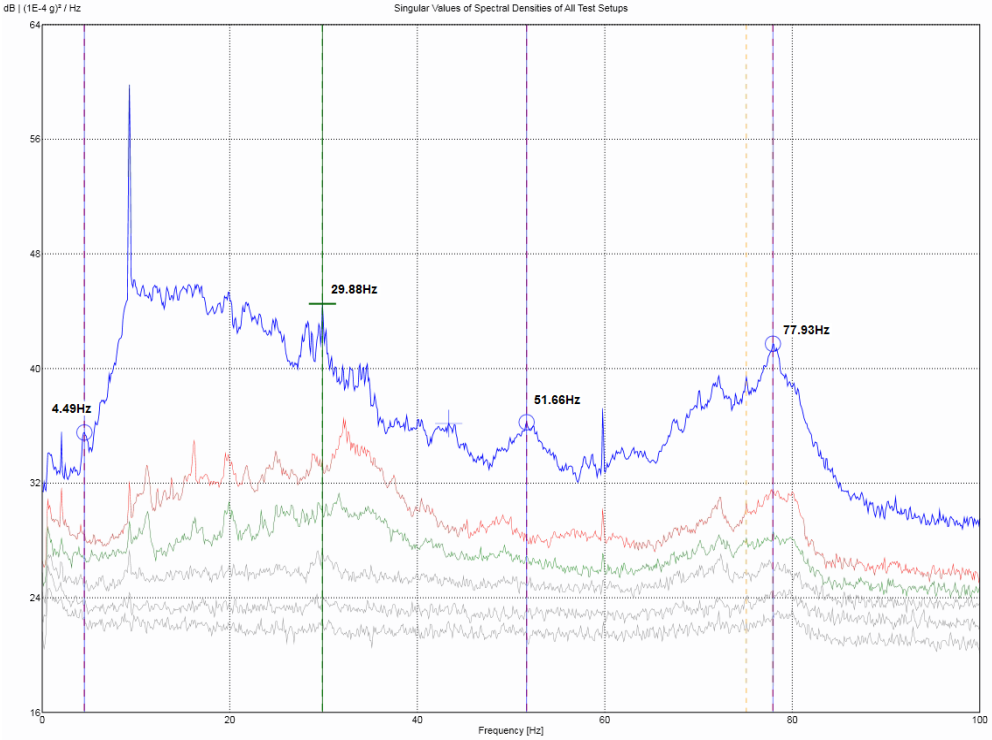

Figure 75 – Singular value of spectral densities of all setups of the lateral dome (FDD method)

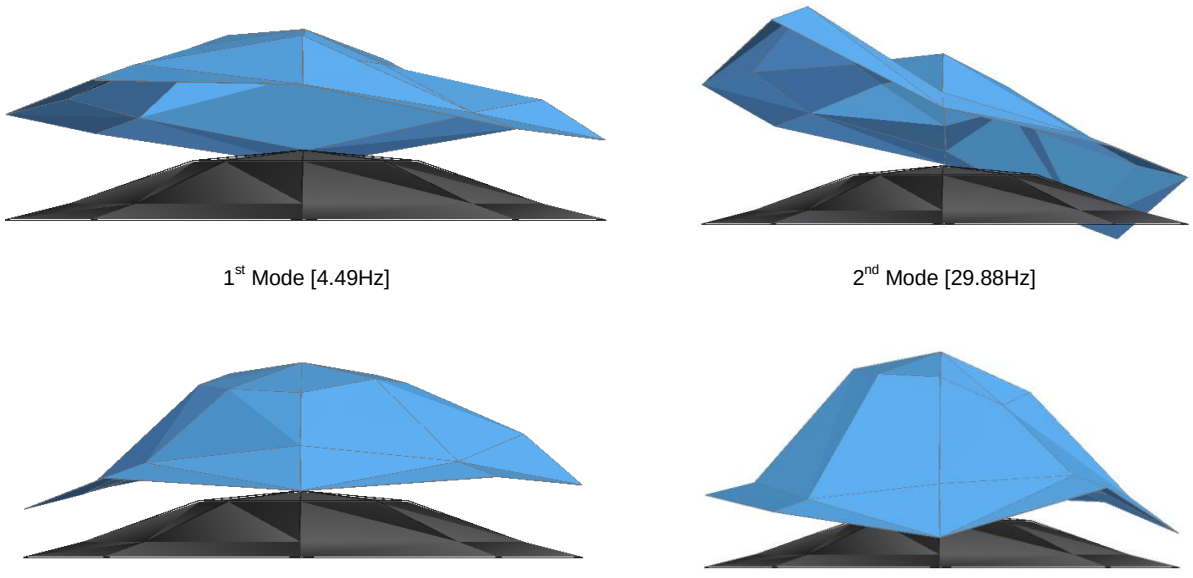

1st Mode [4.49Hz]

2nd Mode [29.88Hz]

3rd Mode [51.66Hz]

4tht Mode [77.93Hz]

Figure 76 – Local mode shapes of the lateral dome

5. NUMERICAL MODELLING

5.1 Introduction

Numerical modelling is a powerful tool that allows a better understanding of structural behaviour. It provides information such as stresses, damage and deformation. For new constructions, this information is used to design the structural elements required in the construction, while for historical construction it is used for diagnosis, safety assessment and definition of intervention. Different actions can be simulated (e.g. gravity, wind, earthquake loading), helping to understand the causes of existing damage and structural capacity. Besides, different types of strengthening techniques can be evaluated, aiming at improving the structural performance of the structure.

In the case of historical structures, the numerical modelling is a challenging task since these constructions usually present highly complex shapes, such as arches and vaults, which can involve 3D analysis with solid elements. Another difficulty is the lack of data regarding the structure, such as material properties, morphology, together with information concerning the geometry and existing damage. In cases of masonry construction, non-linear analysis is required because of the characteristics of the material, which presents high compressive strength and almost null tensile strength. This leads to a considerable increase of computational effort, which is aggravated by the use of 3D models.

A numerical model was developed for the structural analysis of shells in the Municipal Theatre of Rio de Janeiro. Three shells are analysed in this study: a barrel vault and two lateral domes, located in the front part of the theatre. Since the theatre is a massive construction with several different elements, it was decided to model only the front part of the structure, involving the *foyer* room, under the barrel vault and the two lateral towers, under the domes, as presented in Figure 77.

The model was calibrated according to results of dynamic identification tests performed in the structure and the non-linear analysis was performed. In order to reduce the computational cost for the non-linear analysis, the symmetry of the structure was considered for the non-linear analysis, with only half of the structure being modelled and the results mirrored for the rest of it. Furthermore, a partial model with only the top part of the structure (shells and lintels) was prepared, aiming at evaluating the load capacity of the shells. It is noted that in this model the masonry walls and columns were replaced by rigid boundary conditions. In addition, a 2D model representing a section of the barrel vault was performed for both strengthened and unstrenghtened configurations, in order to evaluate the contribution of the concrete layer to the load carrying capacity of the vault. The numerical analyses were carried out in the FEM software DIANA 10.1 (TNO DIANA BV., 2017). Details on the elements considered and modelling strategies are presented in the next Sections.

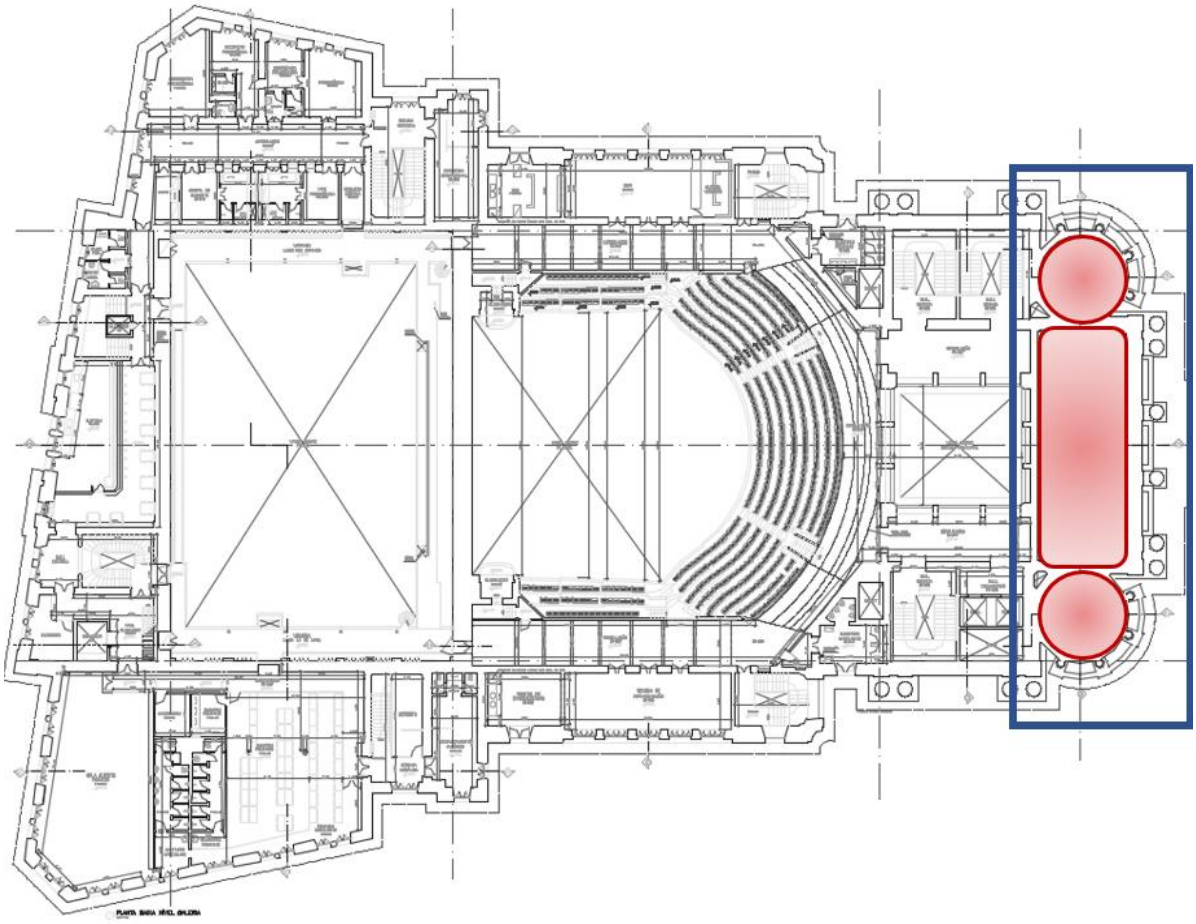

Figure 77 – Part of the structure, including the shells, considered in the numerical modelling (Addapted from Fundação Theatro Municipal do Rio de Janeiro, 2006)

5.2 Geometric properties

The geometry was created based on the architecture drawings provided by Fundação Theatro Municipal do Rio de Janeiro (2006), information acquired in historical and architectural research and in-situ investigation as presented in Section 4.

The horizontal diaphragms are mainly composed by masonry slabs with metallic beams, which are supported in load bearing masonry walls and piers. The walls are made of brick masonry, with the bottom floor in stone masonry, while the piers are made of massive marble, as presented previously. Both masonry and piers have different dimensions according to the location in the structure. The slabs are made also of brick masonry, in small vaults supported by metallic beams. Since there is few information regarding the thickness of these elements, it is assumed that all of them are similar, according to the front bottom slab, which is the only one detailed in the drawings (Figure 78). In order to simplify the shape, the slabs were modelled with a constant thickness of 0.35m, with the beams placed in contact with the bottom surface of the slab. The lateral towers present small spans, hence for these elements the metallic beams were not considered.

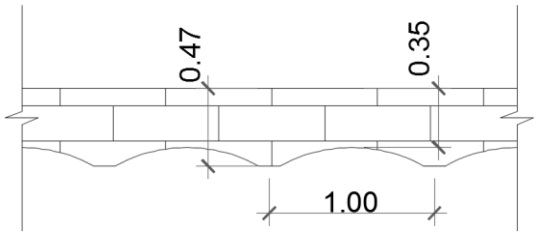

Figure 78 – Section of the slabs (dimensions in meters)

The slabs are supported by the masonry walls and girders. In the first floor, the girder is made of an I profile with approximately 0.60m height, as presented in the architecture drawings, while for the second floor consists in a double I profile, according to the original drawings of the construction (Figure 61). In addition to these girders, there are also two beams joined by an arched masonry element that connects the internal piers around the main stairs. Pachometry tests also indicate the presence of beams over the openings at the towers and at the *foyer*. The lack of information regarding the section of the slab beams and the beams over the openings led to assumptions, hence profiles existing in other parts of the structure were adopted for these cases.

The dimensions of the beams were estimated according to the drawings, but the precise dimensions were defined from commercial profiles available in Europe in the end of 19th century (Bates, 1987), as it is known that the metallic structure of the theatre came from England and Belgium. The profiles considered in the model are presented in Figure 79 and Figure 80.

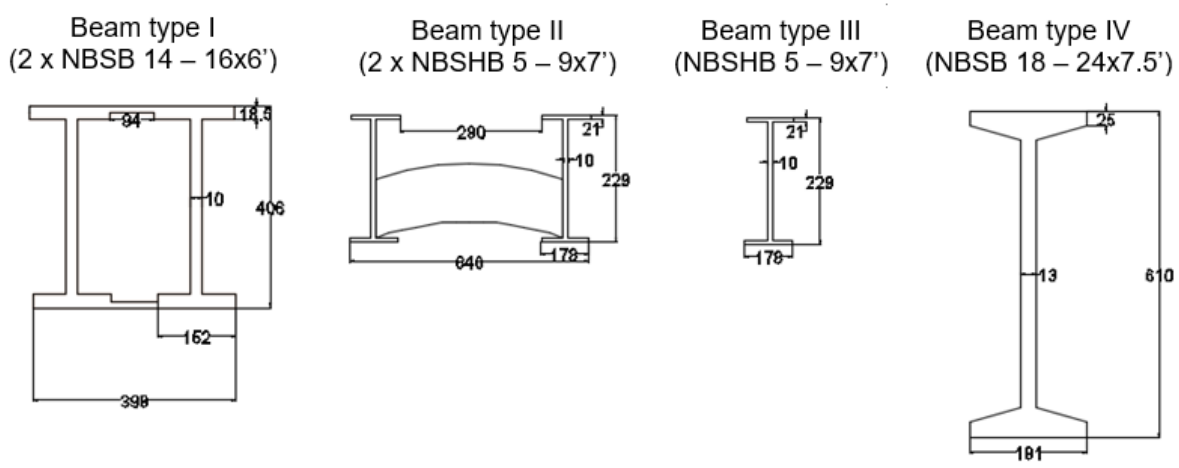

Figure 79 – Beam sections (dimensions in millimetres)

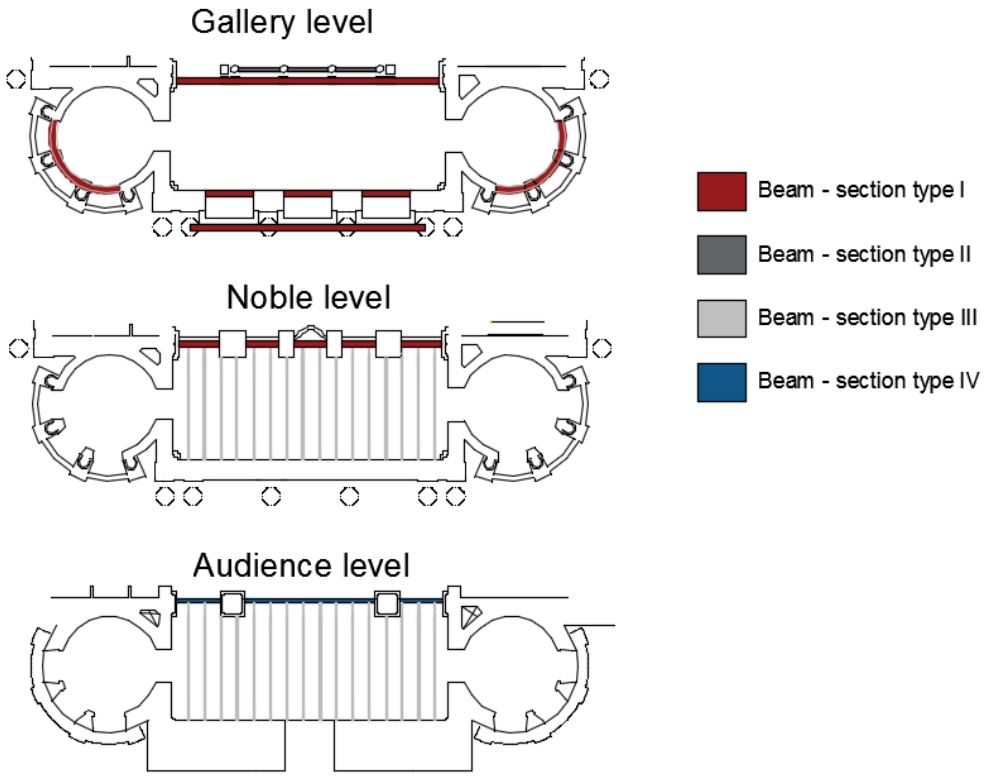

Figure 80 – Location of embedded beams

The barrel vault has constant thickness of 0.23m, with backing in the laterals. It was considered that both the vault and the backing are made of the same material, namely solid brick masonry. The intervention of 1970s added a layer of reinforced concrete with variable curvature on the top of the vault, together with two beams in the laterals over the backings. The reinforcement inside the concrete is made with a mesh of 3mm rebars every 0.10m in both directions in two layers. There is no information regarding the reinforcement of the beams, hence three rebars of 12.5mm were considered on top and bottom faces of the beam.

There is few information regarding the structure of the dome, hence it is assumed that it was built with similar technique as the barrel vault, however with thickness of 0.10m. Even though there is no historical information regarding reinforcement of this element, there is evidence of reinforced concrete also on top of the dome, which was probably added in the same intervention as for the barrel vault. Hence, similar material and construction techniques were considered.

5.3 Material properties

The initial mechanical properties for the masonry materials present in the structure were defined according to the Italian guideline for historic masonry (NTC-08, 2008), presented in Section 2.4. Due to the uncertainties, these values will be calibrated based on the results of dynamic identification tests.

The concrete was made with 500kg/m^3 of cement, which was considered a high strength concrete for the time (Schiros, 1975). Table 3 presents the initial values for the mechanical properties of the materials considered in the modelling, while Figure 81 presents the distribution of the materials in each part of the structure.

Table 3 – Initial material properties

Material	Elastic Modulus [E] (MPa)	Poisson Ratio [v]	Density [ρ] (kN/m^3)
Stone masonry	1500	0.25	21
Brick masonry	1200	0.25	18
Marble	3200	0.25	22
Steel	200000	0.30	78
Concrete	35400	0.20	25
Reinforcement	200000	0.30	78

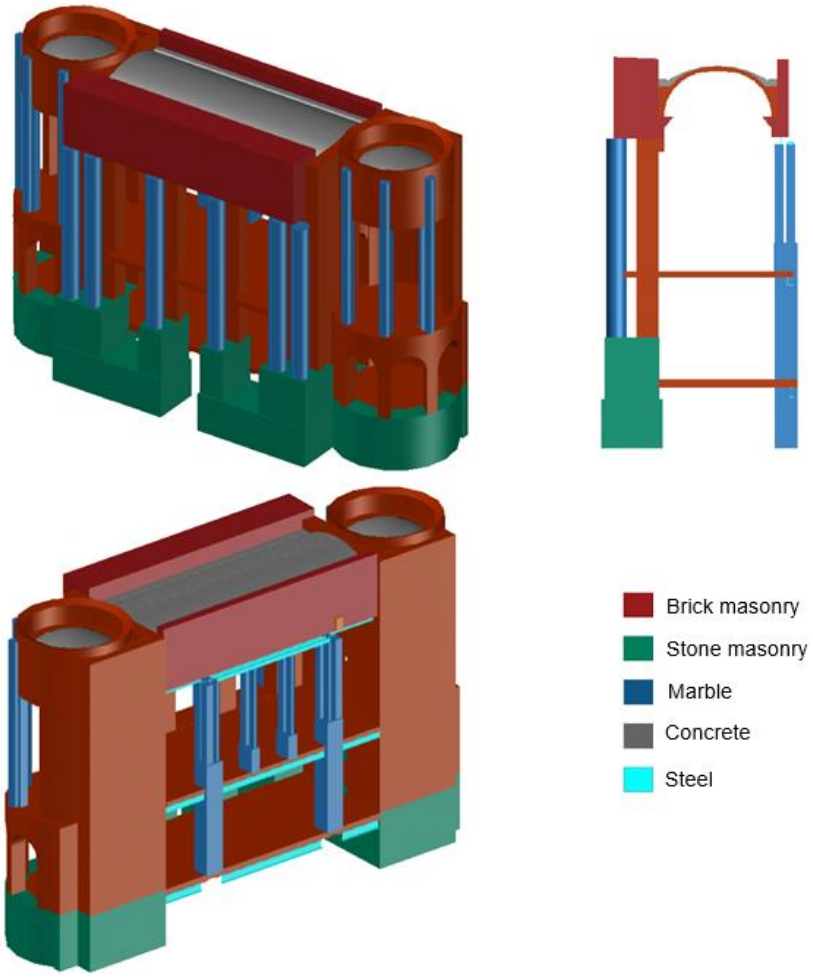

Figure 81 – Distribution of materials in the structure

5.4 Modelling strategy

5.4.1. 3D Model

The complexity of the structural geometry of the Municipal Theatre of Rio de Janeiro leads to a high number of degrees of freedom (DOFs) for a detailed numerical model. Hence, some assumptions were made in order to decrease the computational effort for the non-linear analysis, which are detailed in the next Sections.

- **Element description**

The main element used in the numerical model was the solid element tetrahedron (TE12L), which is a four-node, three-side isoparametric solid. This element was used in walls, piers and vaults. For the slabs, 2D triangular elements of curved shell (T15SH) were considered, while beams were modelled by 1D element L12BE, which is a 2 node three dimensional element (TNO DIANA BV., 2017). Figure 82 presents the three types of elements adopted for the numerical model.

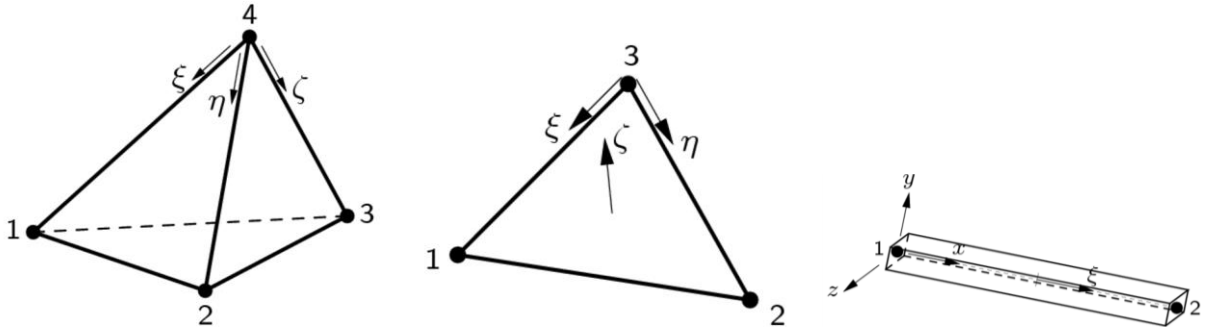

3D element – TE12L 2D element – T15SH 1D element – L12BE

Figure 82 – Elements used in the numerical model (TNO DIANA BV., 2017)

- **Mesh discretization**

Vaults are slender structures with one of the dimensions much smaller than the others. One possibility is to model it with 2D curved elements (2D model). In this case, due to geometry complexity, with variable thickness, presence of backing in the laterals and different boundary conditions, solid elements were chosen to characterize them in order to have a better description of its 3D behaviour.

Vaults are usually connected to massive structures such as walls, hence it must be taken into account that a good discretization on the thickness of vaults will lead to a huge number of nodes in the boundary elements, if care is taken to avoid bad aspect ratios in the elements with small angles. The masonry barrel vault was discretized with elements of 0.10m, while the concrete elements with elements of 0.05m. For the dome elements with 0.05m were used in the masonry part, while 0.03m was adopted for the concrete.

The mesh of the boundary elements grows continuously, until reaching a maximum size of 0.40m. For the marble piers, with smaller sections, a mesh with element size of 0.20m was applied. The slabs also present elements with size of 0.40m, while the beams were meshed according to the elements on

its boundaries. Table 4 presents a summary of the element types and sizes for each part of the structure.

Table 4 – Mesh size and element types

Elements	Mesh size (m)	Element type
Masonry barrel vault	0.1	TE12L
Concrete barrel vault	0.05	TE12L
Backing barrel vault	0.1 to 0.2	TE12L
Masonry dome	0.05	TE12L
Concrete dome	0.03	TE12L
Backing dome	0.05 to 0.2	TE12L
Load bearing walls	0.2 to 0.4	TE12L
Marble piers	0.2	TE12L
Slabs	0.4	T15SH
Beams	0.4	L12BE

With this strategy, the larger model (with the lateral towers) has a total of 315,333 nodes and 1,472,109 elements, being 1,463,992 solid elements, 5,304 shell elements and 2,813 beam elements, which results in more than 4,415,496 DOF. As mentioned previously, for the non-linear analysis, the symmetry in the transversal direction is considered, and the model was cut by half, reducing the number of nodes and consequently the computational effort.

- **Boundary conditions**

From historical survey, it is known that the foundations of the structure are made of timber piles, but no further details on their position was obtained. Hence, it was considered that the walls are one meter deep under the ground level, and rigid pinned supports were defined at to the nodes of the base, restricting the displacements in the three directions.

The points of the structure in contact with other parts not included in the model (Figure 83) were simulated by spring elements acting in the normal direction of the element, for which the stiffness was defined according to the axial stiffness of each element. This stiffness was calculated taking into account the contact area, material and length of the element in contact, and a correction factor (CF) to consider the existence of openings or voids in the elements (Ramírez, 2016). Table 5 presents the stiffness for each element in contact.

$$k_n = \frac{EA}{L} CF \tag{1}$$

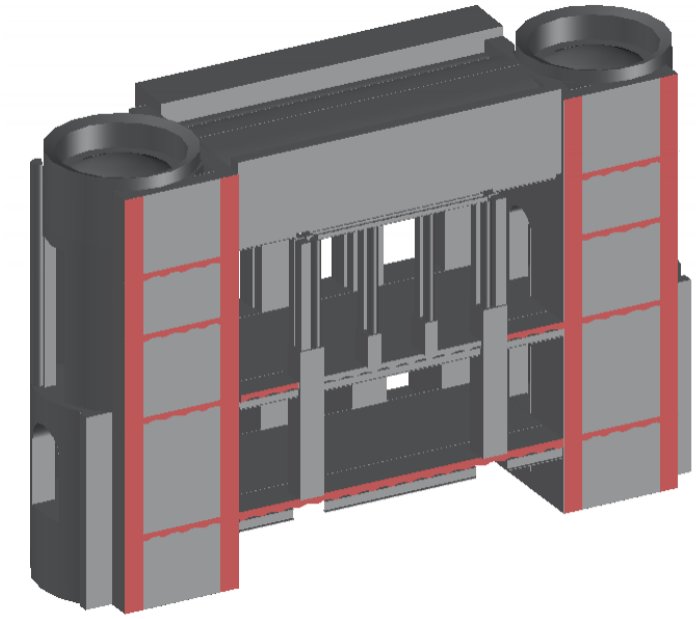

Figure 83 – Parts of the model in contact with other elements of the structure

Table 5 – Normal stiffness provided by the adjacent perpendicular elements

Part in contact	h (m)	t (m)	A (m^2)	L (m)	E (kPa)	CF	k_n.m (kN/m)	Mesh size (m)	k_n.node (kN/m)
External wall	1.00	1.00	1.00	10.96	1200000	90%	98540	0.40	39416
Internal wall	1.00	0.80	0.80	10.96	1200000	90%	78832	0.40	31533
Slabs	1.00	0.35	0.35	10.96	1200000	90%	34489	0.40	13796

In the case of the non-linear model, the symmetry condition is simulated by boundary conditions that constrains the movement in the axial direction (X axis) and the rotation in the perpendicular direction (Y axis). For the model which considers only the top part of the structure, supports in three directions were considered for the tower under the dome, while the supports in the laterals of the barrel vault restrict the movement in vertical direction, but allow it to move horizontally.

- **Loads**

In this study, only vertical gravitational loads were considered. For the elements in the model, the self-weight was considered as body forces automatically by DIANA, based on the density values presented in Table 3.

The self-weight of the roof was calculated considering the copper tiles with metallic structure, with an average weight of 0.6kN/m^2. Since the roof of the dome has a big relation between the span and the height, a correction factor was applied (+50%). These loads were applied as mass elements to the nodes of the mesh of the load bearing walls. Table 6 presents the addopted mass values for each part of the roof.

Table 6 – Weight of the roof

Part of the roof	Area (m^2)	Height factor	Total area (m^2)	Density (kN/m^2)	Total weight (kN)	Number of nodes	Weight/node (kN)
Dome	30.97	1.50	46.46	0.58	26.95	8.00	3.37
Barrel vault	129.77	1	129.77	0.58	75.27	90	0.84

5.4.2. 2D Model

Due to the high computational effort demanded by the 3D model, the use of simpler 2D models for the analysis of the effectiveness of the layer of concrete added in 1075 was adopted. A section of the barrel vault was considered, including the supporting piers on both sides. In this Section details on the main aspects of the model are presented.

- **Element description and mesh discretization**

Since the model represents a section of a continuous structure, shell elements with plane stress state analysis was considered. Hence, the shells were modelled with quadrilateral elements CQ16M, which are eight-node isoparametric plane stress elements (Figure 84). This element was used for the brick masonry and for the layer of concrete. In addition, the mesh of steel reinforced inside the concrete was modelled as the reinforcement element – bar inside plane stress shell, which is automatically considered embedded in the shell elements (TNO DIANA BV., 2017). Figure 85 presents schematically how Diana considers embedded reinforcement elements in shells.

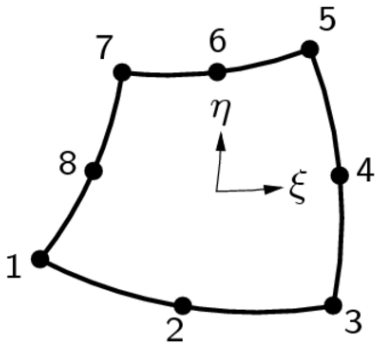

Figure 84 – Quadrilateral element (CQ16M)

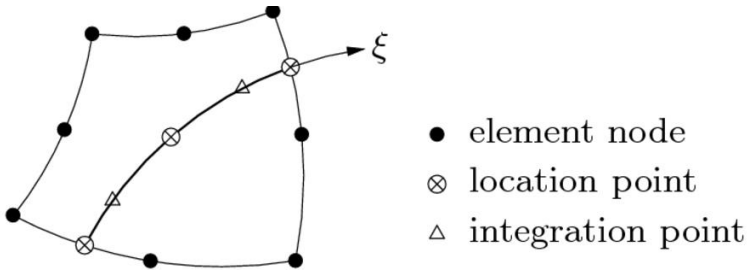

Figure 85 – Bar reinforcement inside plane stress shell element

The mesh presents a discretization of 0.05m for both the masonry and the concrete, resulting in a total of 15,910 nodes, 5,079 elements for the unreinforced model (Figure 86), and a total of 18,499 nodes, 5,854 elements for the reinforced model (Figure 87).

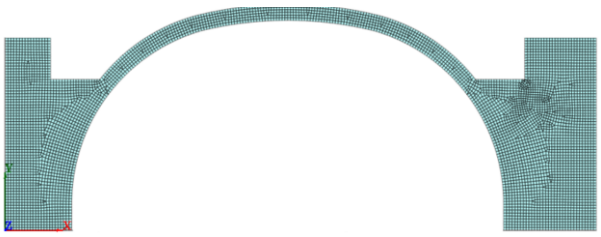

Figure 86 – 2D unstrengthened model

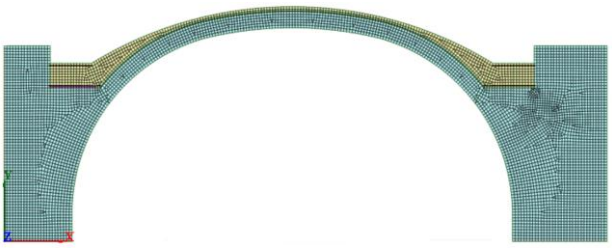

Figure 87 **–** 2D strengthened model

- **Boundary conditions**

The section of the vault is considered to be supported on both sides. On the internal side (left) the translations are constrained in both directions, while for the external side (right), only the vertical direction was constrained, allowing translation in the transversal direction of the vault. The boundary conditions were applied to all nodes of the base on each side.

- **Loads**

The first load considered in the model is the self-weight, considered automatically as body forces by the Diana software, according to the material properties presented in Table 3. Additionally, prescribed displacements were applied to the base nodes on the right side of the vault. The value of the displacements is increased up to the collapse of the vault.

5.5 Linear static analysis

A preliminary linear elastic analysis was performed for the large 3D model in order to have an overview of the results, aiming to check that there were no irregularities in the model, such as geometric, material or loading inconsistencies. This analysis considered only the dead-load (self-weight) of the structure as body forces.

The total amount of vertical loads calculated by the sum of vertical reaction (FBZ) was 39399.78kN, which is in agreement with a by hand calculation. Figure 88 presents the vertical displacements, where the maximum displacement is present in the barrel vault, close to the internal support, with a value of 7.2mm, representing 1% of the transversal span. Lastly, the resultant vertical stresses are presented in Figure 89, where it can be observed that the maximum stresses in the base are close to 0.5MPa, which is less than the compression strength for the stone masonry considered in the model (2.6MPa), according to the Italian guideline (NTC-08, 2008). The maximum stress is close to 0.7MPa, which is lower than the compression strength of 5.3MPa for marble, considering that the compression strength calculated by (NTC-08, 2008):

$$E = 600 f_k \quad (2)$$

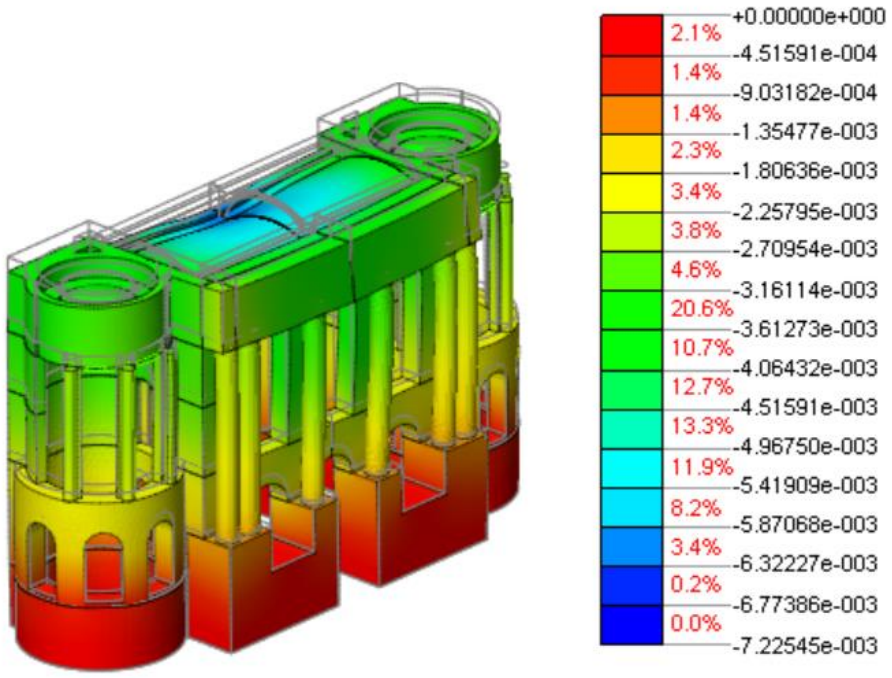

Figure 88 – Vertical displacements due to dead-load [m] (slabs were not represented)

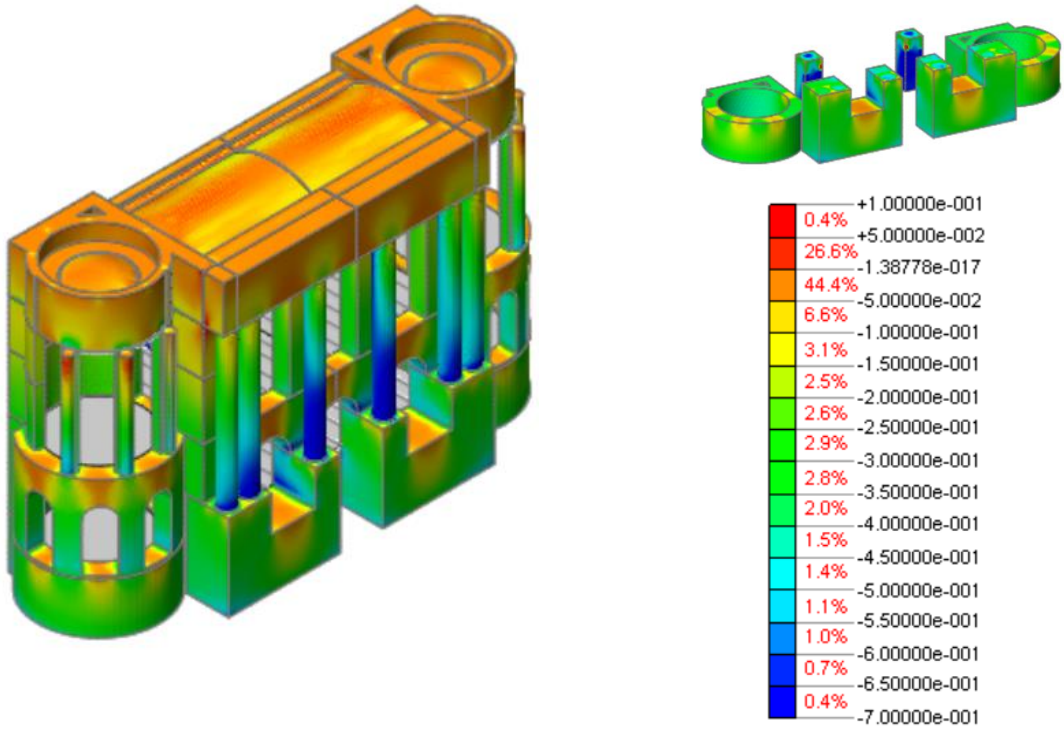

Figure 89 – Vertical stresses due to dead-load [MPa]

5.6 Eigenvalue analysis

The eigenvalue analysis aims to identify the natural frequencies and mode shapes of a structure. In order to evaluate the numerical model, an initial eigenvalue analysis was carried out using the linear mechanical properties previously defined. Four mode shapes were considered relevant for the description of the behaviour of the structure (Figure 90): the first mode (2.90Hz) is transversal; the second mode shape (5.88Hz) is longitudinal, indicating a movement only of the middle of the building, while the laterals – connected to the back part of the structure – are still; the third mode shape (7.00Hz) is in the vertical direction and is also the first local mode shape of the barrel vault; the fourth mode shape is also a vertical local mode for the lateral domes. Even though this mode shape is not clear in the global behaviour of the structure, it can be seen when the dome is analysed alone.

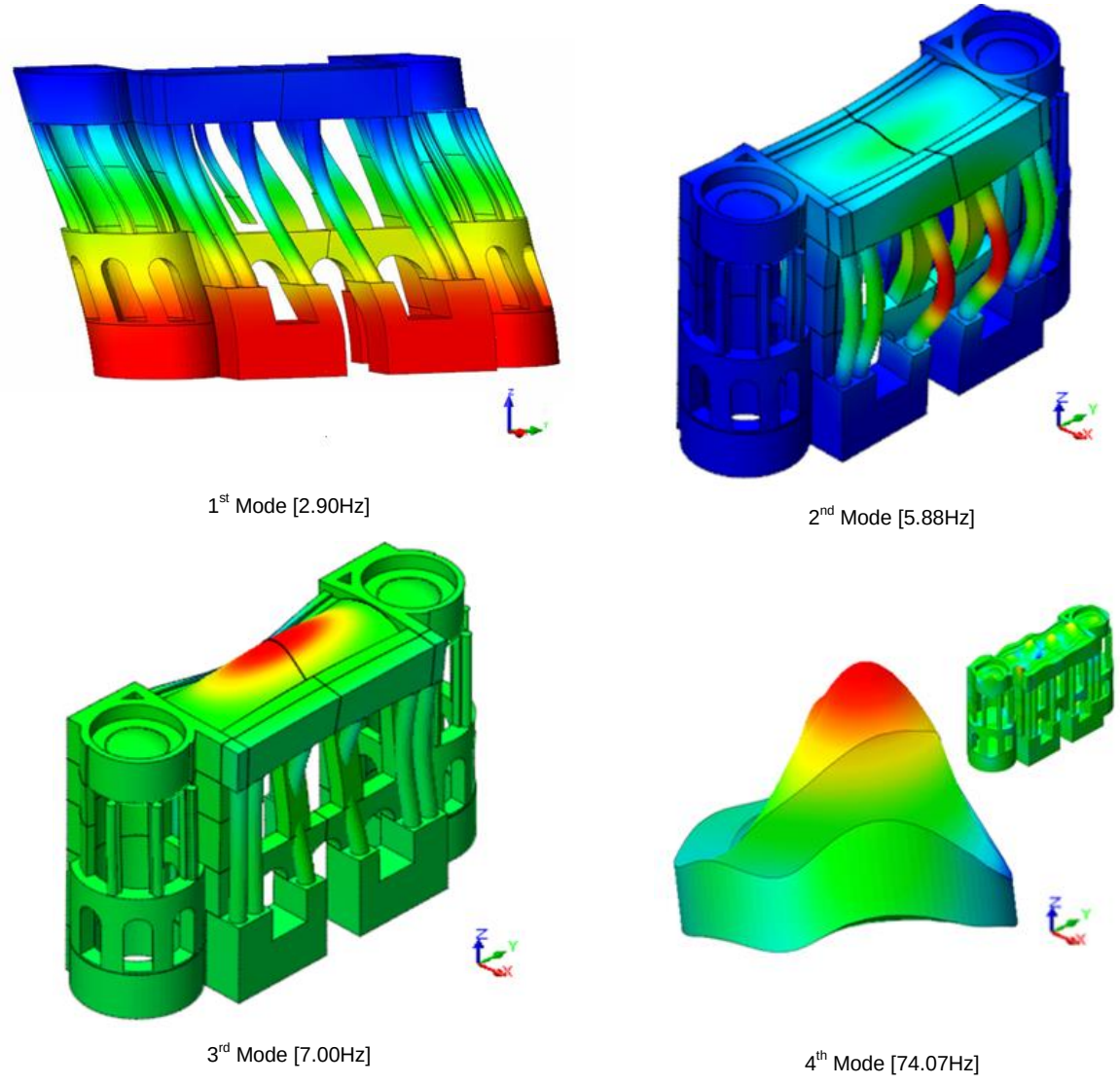

1st Mode [2.90Hz]

2nd Mode [5.88Hz]

3rd Mode [7.00Hz]

4th Mode [74.07Hz]

Figure 90 – Four mode shapes of the structure (slabs were not represented)

The first, third and fourth mode shapes are similar to the results obtained from the dynamic identification tests (Section 4.4). The second mode shape was not identified experimentally, which can be associated to the lack of acceleration measurements in the longitudinal direction at points located in the middle of the *foyer* room.

Table 7 presents the numerical results for the eigenvalue analysis. The first mode shape is clearly the main mode in the transversal direction, mobilizing 54% of the effective mass in transversal direction and none in the other directions. The second mode shape mobilizes 29% of the effective mass in the longitudinal direction and has no contribution to other directions. The third and fourth mode shapes are local and they have almost null impact in the total mass of the structure.

Table 7 – Results of eigenvalue analysis

Mode	F [Hz]	Mass part. in X [%]	Mass part. in Y [%]	Mass part. in Z [%]
1	2.91	0	54	0
2	5.88	29	0	0
3	7.01	2	0	3
4	74.07	0	1	1

5.7 Calibration of dynamic properties

The dynamic properties of the numerical model should agree with the experimental results. As mentioned previously, the first, third and fourth mode shapes for the numerical modes were also identified experimentally. Table 8 presents a comparison between the numerical and experimental frequency values, while Figure 91 presents the comparison between the experimental and numerical mode for the material properties with initial values.

Table 8 – Comparison between experimental and numerical results for the material properties with initial values

Mode shape	f_{exp} [Hz]	f_{num} [Hz]	Error [%]	Average error [%]
1	2.82	2.91	3.09	
3	7.13	7.01	1.71	3.34
4	77.93	74.07	5.21	

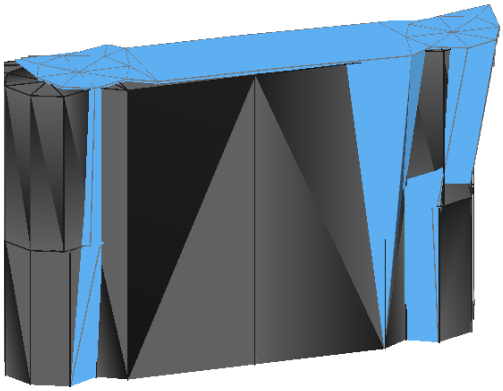

1st Mode - Experimental [2.82Hz]

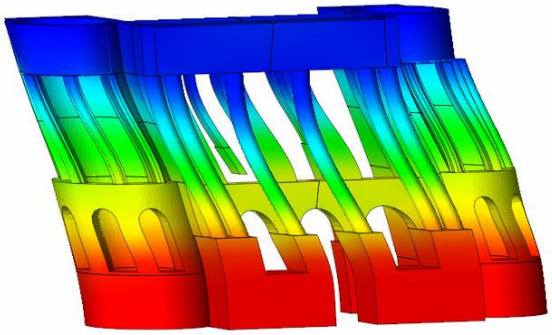

1st Mode - Numerical [2.90Hz]

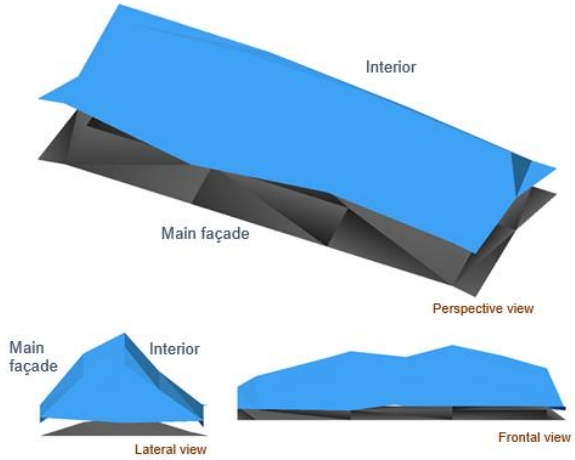

3rd Mode - Experimental [7.13 Hz]

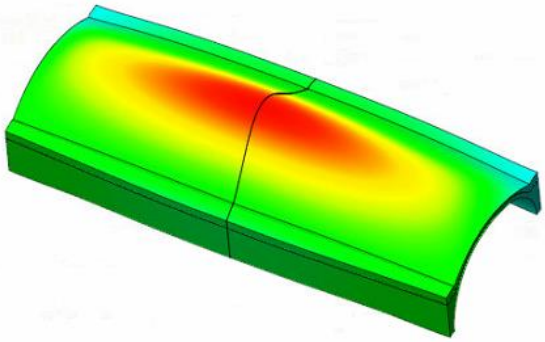

3rd Mode - Numerical [7.00Hz]

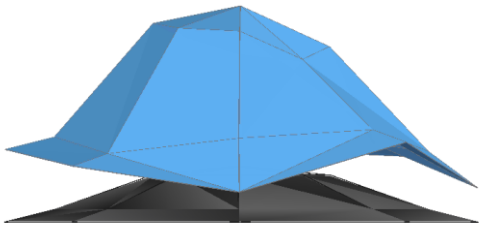

4th Mode – Experimental [77.93Hz]

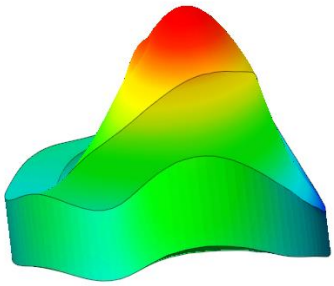

4th Mode - Numerical [74.07Hz]

Figure 91 – Comparison between experimental and numerical modes for the material properties with initial values

The numerical model was then calibrated based on the frequencies of these modes, in order to have a better correlation between the dynamic properties for the numerical and experimental results. The calibration is an updating process based on an optimization process that minimizes the difference between the experimental and mathematical responses (N. A. L. Mendes, 2012). The calibration of the numerical frequencies is performed following the Douglas-Reid (Douglas & Reid, 1982) method that considers the natural frequencies according to the following expression:

$$f_i^N(X_1, X_2, \dots, X_n) = C_i + \sum_{k=1}^{n} [A_{ik} X_k + B_{ik} (X_k)^2] \tag{3}$$

where $f_i{}^N$ represents the frequencies of the numerical model, X_k (k = 1,2, … , n) are the variables to calibrate and A_{ik} , B_{ik} and C_i are constants. To satisfy the expression, (2n + 1) constants must be calculated, according to the following expression:

$$\begin{cases} f_i^N({X^B}_1, {X^B}_2, \dots, {X^B}_n) = C_i + \sum_{k=1}^{n} [A_{ik} {X^B}_k + B_{ik} ({X^B}_k)^2] \\ f_i^N({X^L}_1, {X^B}_2, \dots, {X^B}_n) = C_i + \sum_{k=1}^{n} [A_{ik} {X^L}_k + B_{ik} ({X^B}_k)^2] \\ f_i^N({X^U}_1, {X^B}_2, \dots, {X^B}_n) = C_i + \sum_{k=1}^{n} [A_{ik} {X^U}_k + B_{ik} ({X^B}_k)^2] \\ \dots \\ f_i^N({X^B}_1, {X^B}_2, \dots, {X^L}_n) = C_i + \sum_{k=1}^{n} [A_{ik} {X^L}_k + B_{ik} ({X^L}_k)^2] \\ f_i^N({X^B}_1, {X^B}_2, \dots, {X^U}_n) = C_i + \sum_{k=1}^{n} [A_{ik} {X^U}_k + B_{ik} ({X^U}_k)^2] \end{cases} \tag{4}$$

where ${X_B}^k$ are the reference values of the variable to calibrate (initial or base values), and ${X_L}^k$ and ${X_U}^k$ are the respective lower limit and upper limit values. Once the constants are defined, a least square minimization of the difference between the numerical frequencies $f_i{}^N$ and the experimental frequencies $f_i{}^E$ is used:

$$\pi = \sum_{i=1}^{m} w_i {\varepsilon_i}^2 \tag{5}$$

$$\varepsilon_i = \sum_{i=1}^{m} f_i{}^E - f_i{}^N(X_1, X_2, \dots, X_N) \tag{6}$$

where π is the objective function, ε is the residual function, w is the weight for the constants and m is the number of frequencies considered in the updating.

Two variables were considered in the calibration, namely the elastic modulus of the brick masonry and the elastic modulus of the marble, which are the main constitutive materials of the structure. Firstly, the initial values used for the linear analysis were manually updated until reaching the values of E=2100kPa for elastic modulus of masonry brick and E=7000kPa as elastic modulus for marble, leading to frequencies closer to the experimental results (Table 9). These values were then considered as base for the more accurate calibration, which can be observed in Table 10. This Table presents also the reference, maximum and minimum values considered in the calibration process together with the results. Table 11 shows the calibrated frequencies after the modal updating, for which an average of about 0.3% was obtained. Table 12 presents the reduction of the errors during the calibration of the frequencies.

Table 9 – Comparison between experimental results and numerical results considering base values

Mode shape	f_{exp} [Hz]	f_{num} [Hz]	Error [%]	Average error [%]
1	2.82	2.88	2.10	1.34
3	7.13	7.23	1.34	
4	77.93	77.48	0.58	

Table 10 – Variable values assumed for the calibration

Variable	Base values [MPa]	Lower values [MPa]	Upper values [MPa]	Updated values [MPa]
$E_{masonry}$	2100	2000	3000	2053
E_{marble}	7000	5000	15000	6262

Table 11 – Comparison between experimental and numerical results for the calibrated model

Mode	f_{exp} [Hz]	f_{num} [Hz]	Error [%]	Average error [%]
1	2.82	2.82	0.00	0.34
3	7.13	7.14	0.14	
4	77.93	77.24	0.89	

Table 12 – Reduction of error during the calibration process

Model	Error for Mode 1 [%]	Error for Mode 2 [%]	Error for Mode 3 [%]	Average error [%]
Initial	3.09	1.71	5.21	3.34
Base values	2.10	1.34	0.58	1.34
Calibrated	0.00	0.14	0.89	0.34

6. STRUCTURAL ANALYSIS

6.1 Introduction

Once the model has been calibrated and validated, it can be considered trustworthy to describe the structural behaviour of the theatre. As mentioned previously, the linear analysis is not suitable for analysing masonry construction due to its highly non-linear behaviour, being required the use of non-linear analysis in the numerical study of such type of material.

In this study, non-linear analysis was performed to describe the structural behaviour of the shells located in the front part of the Municipal Theatre of Rio de Janeiro. The non-linear response was calculated according to the Newton-Raphson iterative method, in which a new tangent stiffness matrix is calculated within each iteration. The analysis convergence criterion was defined by the energy control with a tolerance equal to 10^{-3}.

The non-linear analysis was carried out in three different models as described in Section 5, aiming to analyse three distinct aspects of the structural behaviour. Firstly, the interaction between soil and structure was analyse under different soil conditions, in order to estimate the possible cause of cracks that led to the intervention in 1975. Secondly, a study of the load capacity of the structure prior to the 1975 intervention was performed. Lastly, the increase of the structural capacity due to the addition of the reinforced concrete layer was evaluated. This Section presents the analysis performed, including the main assumptions considered and the results obtained.

6.2 Non-linear material properties

The non-linear behaviour of masonry was modelled using the Total Strain Crack Model (TSCM), which describes the tensile and compressive behaviour of a material with a stress-strain relationship. A Rotating Crack model was adopted, where the stress-strain relationship is evaluated based on the principal strains, defining also the direction of the crack opening (TNO DIANA BV., 2017). For the Rotating Crack model, it is not necessary to define the shear behaviour, since in this material model a unique shear term is evaluated and updated, based on the current damage occurred during the analysis.

The compression behaviour is described as a non-linear parabolic function (Figure 92), defined from the relation between fracture energy in compression and crack bandwidth of the mesh elements. The crack bandwidth value is automatically considered by DIANA according to the volume ($h = \sqrt[3]{V}$ for solid elements). For 2D elements the crack bandwidth is equal to $\sqrt[2]{A}$, in which *A* is the area of the element (TNO DIANA BV., 2017). The compressive strength of the different masonry types was

defined based on the elastic modulus. The parameter α for masonry, which relates the compressive strength with the elastic modulus, may ranges from 200 to 1000 (Tomazevic, 1999). In this study, a α = 600 was adopted (f_c = E/600). The compressive fracture energy was defined according to the relation between the ductility index and the compressive strength ($d_{u,c}$=G_c/f_c, where ductility index was assumed to be 1.6 mm, as recommended value for a compressive strength lower than 12 MPa (CEB, 1991).

The tensile behaviour was defined by an exponential softening curve (Figure 93), based on the tensile fracture energy, the crack bandwidth of the elements and the tensile strength of the material. The crack bandwidth value was automatically calculated by the software, the tensile strength is considered 150KPa for the stone and brick masonry, and 500KPa for the marble, approximately 5% of the compressive strength. Lastly, the fracture energy was considered 0.05kN/m for the brick and stone masonry and 0.10kN/m for the marble.

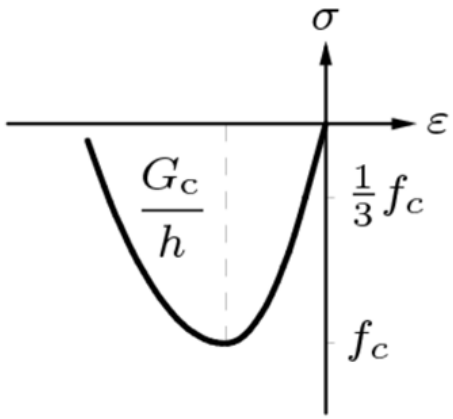

Figure 92 – Parabolic diagram for compressive behaviour of masonry

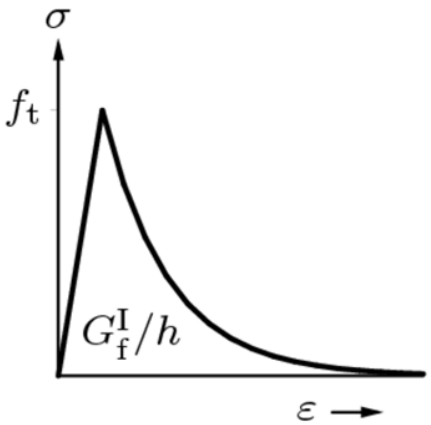

Figure 93 – Exponential diagram for tensile behaviour of masonry

The non-linear properties of the concrete are automatically defined by Diana 10.1, according to the CEB-FIP Model Code 1990 (CEB, 1991), also considering the TSCM. Concrete class C40 was considered in this analysis, since it is known that a high-quality concrete was applied in the intervention. Additionally, a model considering a current concrete, class C25, was evaluated. The behaviour of the rebars and steel grid of the concrete was also analysed according two criteria, namely the Von-Mises model and non-linear elasticity, with almost null strength under compression and linear behaviour for tension. The steel considered is class CA25 (Brazilian standards) with a tensile strength of 217MPa. The steel of the beams was considered to behave as linear-elastic.

The linear-elastic parameters where defined according to Section 5.3, including the updated values of the elastic modulus of the brick masonry and the marble, obtained in the calibration (Section 5.7). Table 13 and Table 14 present the final values for the linear-elastic and non-linear parameters for each material considered in the analysis, respectively.

Table 13 – Linear-elastic material parameters

Material	Elastic Modulus [E] (MPa)	Poisson Ratio [ν]	Density [ρ] (kN/m^3)
Stone Masonry	1500	0.25	21
Brick Masonry	2053	0.25	18
Marble	6262	0.25	22
Steel	200000	0.30	78
Concrete (C40)	35400	0.20	25
Concrete (C25)	28000	0.20	25
Reinforcement	200000	0.30	78

Table 14 – Non-linear parameters of the masonry materials

Material	Tensile Strength [f_t] (kPa)	Tensile Fracture Energy [G_t] (kN/m)	Compressive Strength [f_c] (kPa)	Compressive Fracture Energy [G_c] (kN/m)
Stone Masonry	150	0.05	2500	4.00
Brick Masonry	150	0.05	3420	5.47
Marble	500	0.10	10430	16.67

6.3 Analysis for the soil structure interaction

As mentioned in Section 3.3, in the 1970s the barrel vault and the lateral domes presented serious cracks that led to the need of intervention in the structure. A continuous longitudinal crack was observed at the intrados of the barrel vault, located in the middle of the section, together with transversal cracks. A vertical displacement of the central part of the element was detected, causing a reduction in the vault rise. Cracks were also observed in the intrados of the lateral domes, crossing them diagonally. There is no information regarding the presence of cracks in the extrados of the vault. One possible cause for these cracks can be differential soil settlements in the structure (Schiros, 1975). This settlement may have happened due to different causes, such as the construction of the metro station nearby, the high and unstable level of water table, carriage of fine particles of the soil among others.

In this Section, the interaction between soil and structure is evaluated, in order to identify the possible cause for the cracks. It must be noted that the existence of timber piles as foundation is known. However, limited information was found regarding their location in the structure, height or state of conservation. Hence, it was assumed foundations with same cross section as the external walls and piers with a depth of one meter.

Firstly, an analysis of the original state of the structure was carried out. In order to simulate the construction process of the structure, a phased analysis was performed, in which the first phase consists in the structure up to the level of the top of the piers (22.48m). Then, in the second phase the

vaults, beams and walls were added (Figure 94). The phased analysis is relevant in this case because the central piers at the internal side are not in contact with the soil (Figure 95), being susceptible to cause deformation of the second-floor slab. If the phased analysis is not performed, the structure will load equally, and the slab will deform, causing tensile stresses at the top pier and consequently deformations at the vault. With the phased analysis, a compression state of stresses is created in the pier previously to loading it with the self-weight of the vaults, improving its behaviour. The displacements resultant from the first phase were not considered for the second phase, however the state of stresses was kept in the elements. The support condition in these two phases is considered rigid.

Figure 96 presents the displacements of the structure together with its deformed shape. It can be noted that the main displacement occurs at the middle of the barrel vault, with a value of approximately equal to 3mm. No damage could be observed for this phase (self-weight loading).

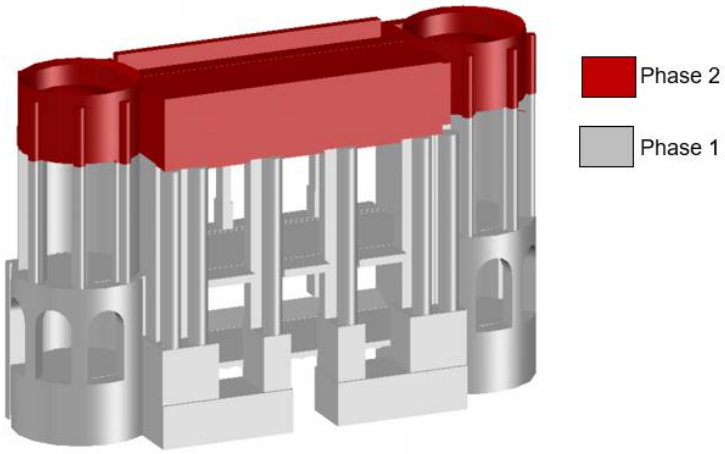

Figure 94 – Distinct parts of the structure considered in the phased analysis

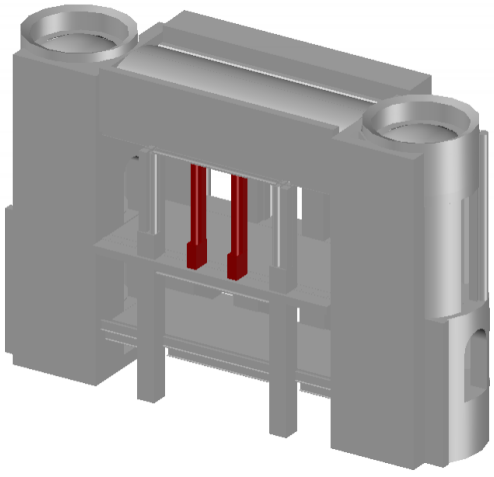

Figure 95 – Piers without connection with the soil

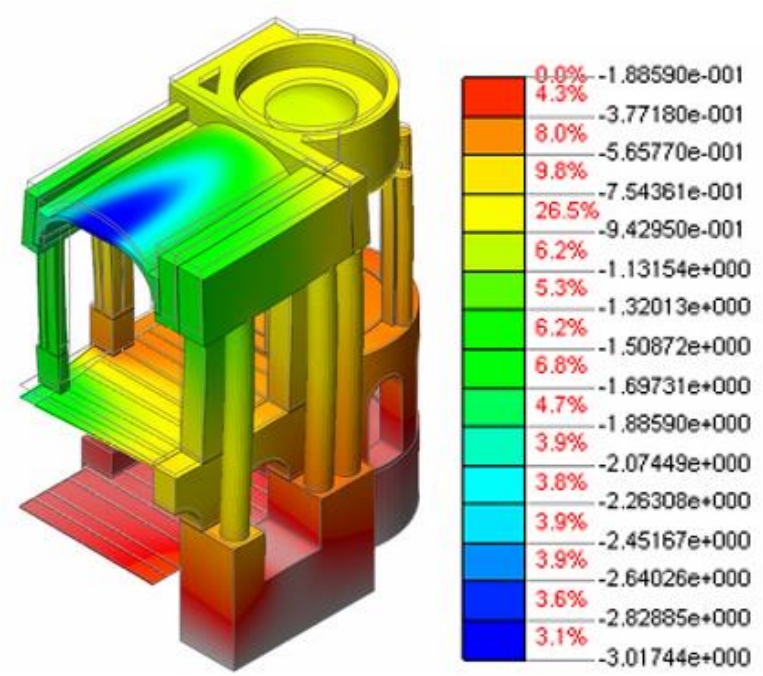

Figure 96 – Displacements for the self-weight of the structure after Phase 1 and Phase 2 (scale in mm)

Phase three consists in the simulation of changes in the soil conditions after the construction of the theatre. Three different scenarios were analysed, aiming at evaluating the situation that better matches the damages described: (i) the soil stiffness decreases uniformly in the whole building, (ii) the decrease of soil stiffness is concentrated in the main façade, (iii) the decrease of soil stiffness decreases in the main façade and lateral tower together (Figure 97).

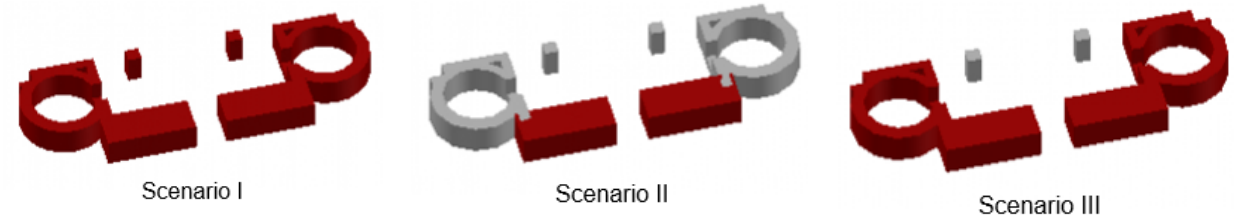

Figure 97 – Scenarios for decrease in soil stiffness

In order to simulate the stiffness of the soil, interface elements were created at the base of the structure with a stiffness value for normal and shear behaviour. Since there is few information regarding the soil properties in the region of the theatre, a simplified approach was adopted (very stiff soil/structure interface) to start analysis (type I), with a systematic decrease in the stiffness to simulate the decrease in soil stiffness. Four different values of stiffness were considered in this study. The first stiffness simulates the very stiff soil while the others vary according to the case studied, as presented in Table 15. The different values assumed for each analysis together of the results are presented in this Section.

Table 15 – Normal and shear stiffness in the interface elements (base of the model)

Type of interface	Normal stiffness (kN/m)
I	1000000
II	50000
III	35000
IV	20000

6.3.1. Uniform decrease of soil stiffness

The first assumption considers that the soil stiffness decreases uniformly in all the building. The decrease on the stiffness on interface elements was applied gradually, with interfaces type two to four being applied in each analysis for all the elements.

Figure 98 and Figure 99 present the results of displacement and crack width for each of the analysis, respectively. The settlement of the internal pier is higher than in the other elements of the foundation. This is due to the difference in area of such elements, causing higher stresses in the soil under the pier, which has smaller contact area. It must be noted that the properties of the foundation are not known and the area of the foundation can be larger than the area considered in this model.

In the Figure 99, it can be observed that the severity of the damage is low and occurs at the interior side on top of the piers, mainly at the lateral support with the back wall, which spreads through the vault with the decrease of soil conditions. The damage at the top of the internal piers can be not realistic, since this model considers full connection between the piers and the lateral supports of the vault. Probably, in reality this connection only works under compressive stresses. The displacement of the piers cause bending on the upper element, making it work as a cantilever, which causes tensile stresses on the upper part of the support (connection with the masonry wall).

The damage in the vault occurs mainly at the intrados, close to the interior supports. A longitudinal crack is formed located in the beginning of the internal backing, where there is a significant reduction on the transversal section of the element. This crack pattern differs in some aspects from the damage described previously to the intervention, particularly in the location of the longitudinal crack, which was formed at the middle of the vault, while in this hypothesis is located in the lateral.

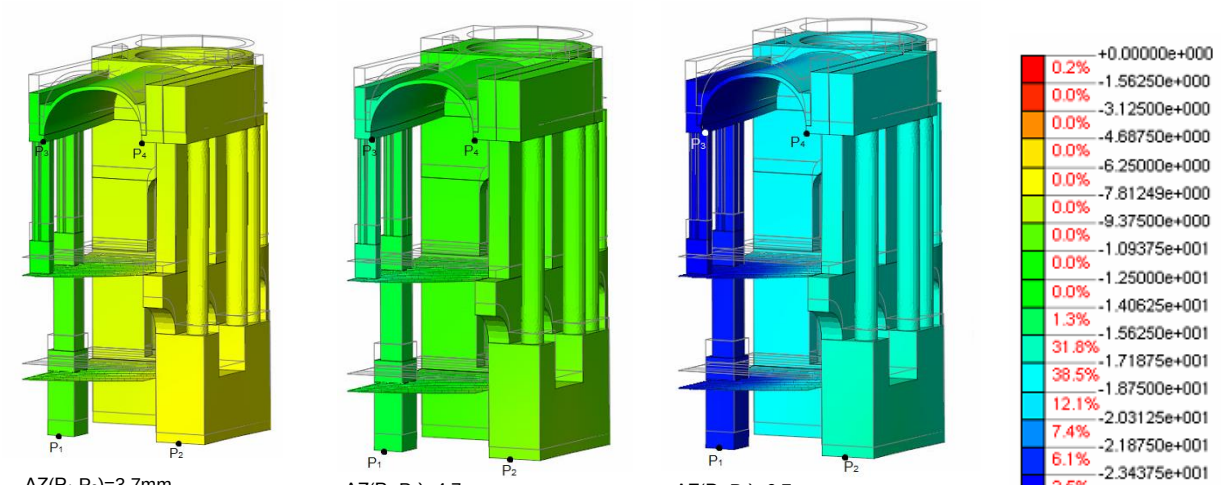

$\Delta Z(P_1,P_2)$=3.7mm
$\Delta X(P_3,P_4)$=0.6mm

Interface type II

$\Delta Z(P_1,P_2)$=4.7mm
$\Delta X(P_3,P_4)$=0.3mm

Interface type III

$\Delta Z(P_1,P_2)$=6.7mm
$\Delta X(P_3,P_4)$=0.2mm

Interface type IV

Figure 98 – Vertical displacements for settlements at the base of all model (scale in mm)

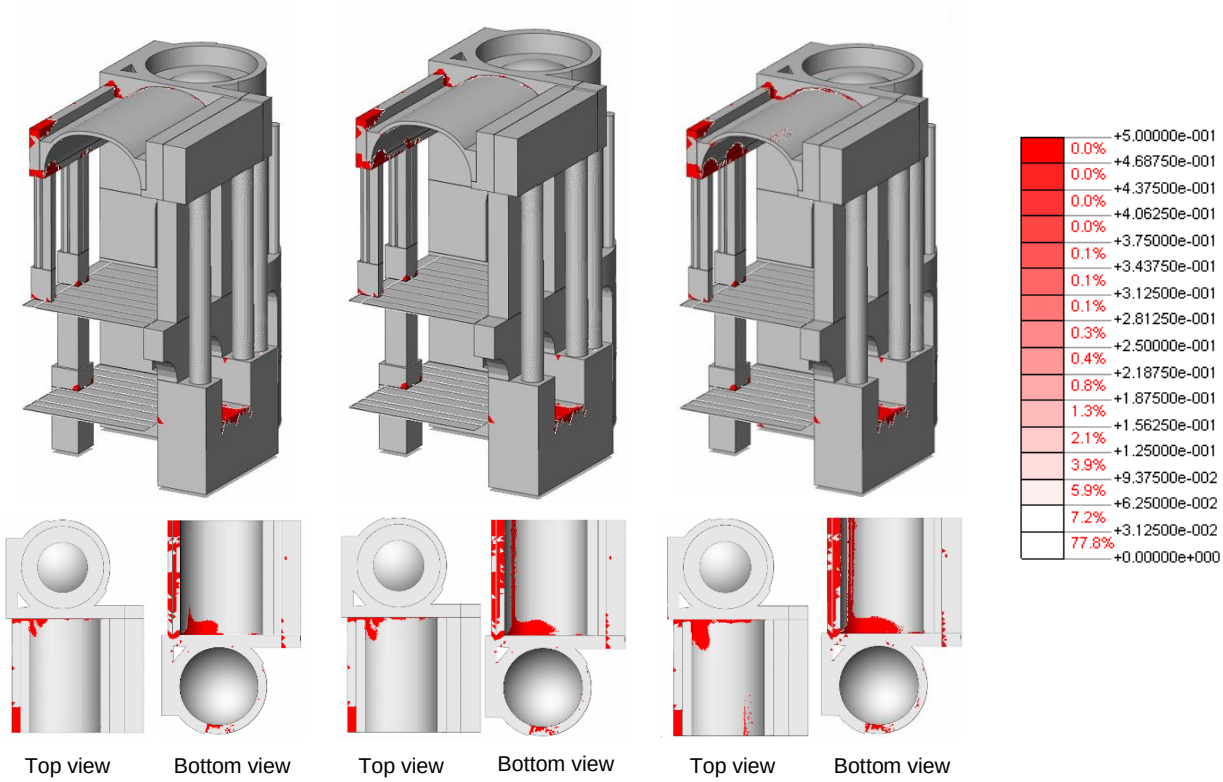

Top view Bottom view

Interface type II

Top view Bottom view

Interface type III

Top view Bottom view

Interface type IV

Figure 99 – Crack width for settlements at the base of all model (scale in mm)

6.3.2. Decrease of soil stiffness at the main façade

This scenario simulates the assumption where only the main façade settles, while the rest of the supports remain in the original condition. With this purpose, a very stiff interface element was applied to the base of the internal pier and the tower (interface type I). The interface elements under the façade were described with interface elements type II, III and IV, simulating the systematic reduction of the soil stiffness under this part of the structure.

Figure 100 presents the displacements for this hypothesis. Differential soil settlement between the façade and both the tower and pier can be observed. Since the pier and the tower are supported on very stiff elements, the differential settlement between these elements is minimum.

The damage associated to this hypothesis is presented in Figure 101, where the evolution of the damage can be observed. The main damage is located close to the piers of the façade, mainly at the middle of the span. A crack between the wall and the vault is also formed, and can be observed from both the intrados and extrados, indicating that the vault may detach from the wall. In this model, it was assumed fully connection between those elements. However, it is possible that this connection is made only by a layer of mortar, which would crack under low stresses, allowing the displacements between these parts without damaging the masonry vault.

The formation of a longitudinal crack can be observed in the middle of the vault. For the case with lower stiffness of the interface element, not only the crack in the intrados can be observed, but also two cracks in the extrados close to the beginning of the backing, characterizing the beginning of formation of hinges.

The third simulation also presents the formation of cracks at the dome, both in the intrados and the extrados. These cracks are mainly distributed around the ring formed by the presence of backing and spreads through the side of the wall that connects the dome to the vault. It must be highlighted that the severity of the damage is low and only a beginning of damage is identified.

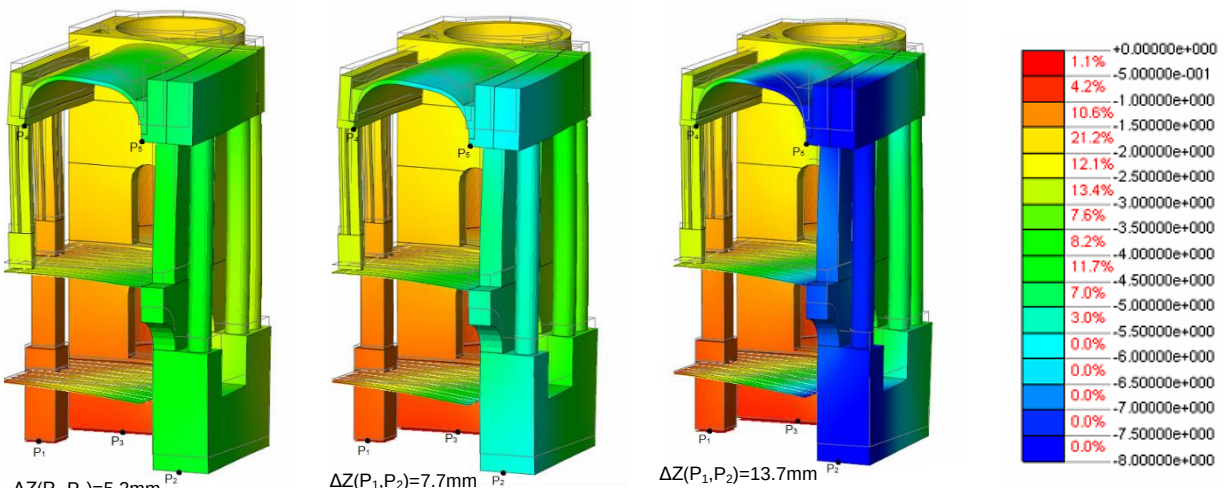

$\Delta Z(P_1,P_2)$=5.2mm
$\Delta Z(P_1,P_3)$=0.1mm
$\Delta Z(P_2,P_3)$=5.3mm
$\Delta X(P_4,P_5)$=0.5mm

Interface type II

$\Delta Z(P_1,P_2)$=7.7mm
$\Delta Z(P_1,P_3)$=0.3mm
$\Delta Z(P_2,P_3)$=7.9mm
$\Delta X(P_4,P_5)$=0.5mm

Interface type III

$\Delta Z(P_1,P_2)$=13.7mm
$\Delta Z(P_1,P_3)$=0.9mm
$\Delta Z(P_2,P_3)$=14.6mm
$\Delta X(P_4,P_5)$=0.5mm

Interface type IV

Figure 100 – Vertical displacements for settlement at the base of the façade (scale in mm)

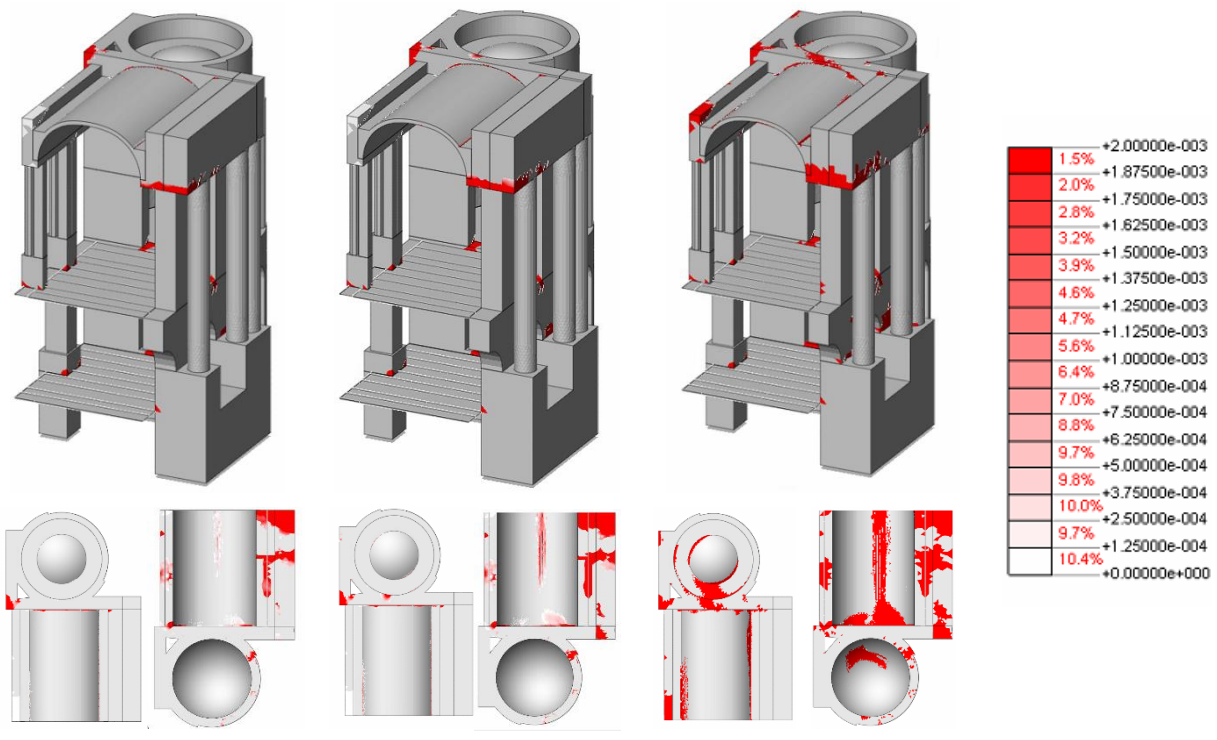

Top view Bottom view

Interface type II

Top view Bottom view

Interface type III

Top view Bottom view

Interface type IV

Figure 101 – Crack width for settlement of the façade (scale in mm)

6.3.3. Decrease of soil stiffness at the main façade and tower

The third scenario consider the hypothesis of settlement the base on both main façade and tower. This scenario is likely to occur due to the massive elements in these locations, increasing considerably the weight, and low vertical stress at the base of the pier. For this case, interface elements type I (very stiff) were applied at the base of the internal pier, while the stiffness of the interface elements under the main façade and the tower varied with elements type II to IV, decreasing successively the soil stiffness.

The results for this scenario are presented in terms of displacements and crack width in Figure 102 and Figure 103, respectively. The main façade and the tower settle almost uniformly, with small relative displacements between these elements. The differential settlement is also associated to the internal pier, which has very low deformation in comparison with the other two elements. In this case, the deformation leads to increase of the vault span (ΔX), indicating flattening effect in the vault shape.

The support presenting the most relevant damage is the internal pier connected to the ground, where cracks appear on top of the section, indicating an inflexion point in the deformed shape of the vault. This damage spreads quickly into the vault, and can be observed in both intrados and extrados. Furthermore, a crack between the vault and the wall is observed.

The formation of a longitudinal crack in the vault is observed, that connects with the transversal crack from the pier for the worse soil conditions. From the extrados, a crack close to the internal backing is observed, while in the external side no damage is observed. Once again, the severity of the damage is low and only the beginning of the damage is identified.

The dome also present cracks, in both intrados and extrados, located close the ring that marks the beginning of the backing. These cracks are clear only for the third stiffness of soil simulated in this analysis.

This scenario presents a crack pattern similar to the damage described by Schiros (1975), where the longitudinal crack in the middle of the vault can be observed, together with the transversal cracks in the laterals. No information is presented regarding the damage conditions in the extrados of the vault. The cracks observed in the dome are quite different, since the cracks described crossed the dome diagonally, while the cracks observed in this study are mainly at the beginning of the backing. The dome also presents damage at the centre with very low severity (interface type IV).

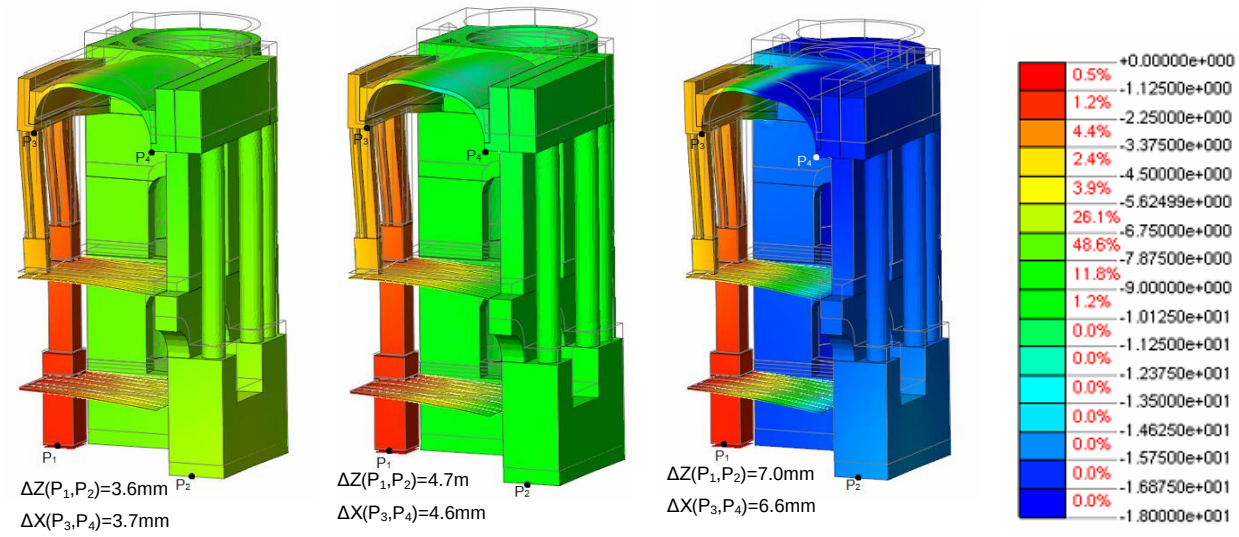

Interface type II | Interface type III | Interface type IV

Figure 102 – Vertical displacements for settlement at the base of the façade and tower (scale in mm)

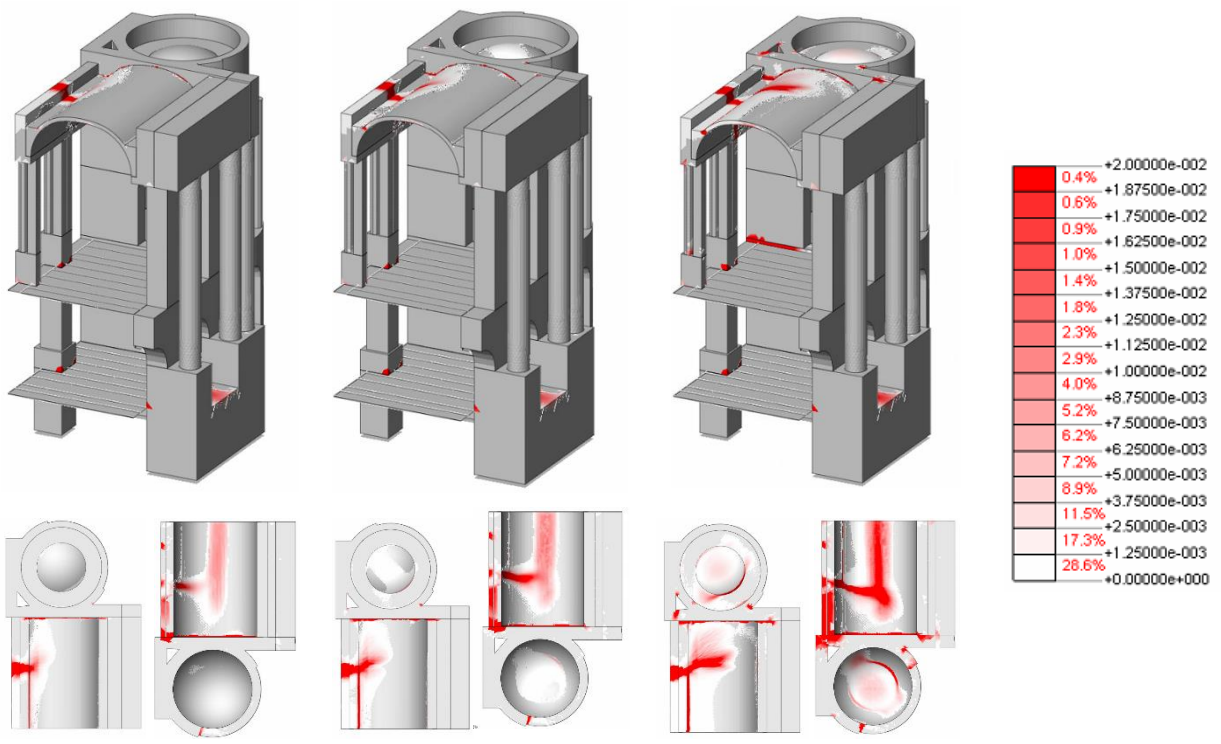

Top view | Bottom view | Top view | Bottom view | Top view | Bottom view

Interface type II | Interface type III | Interface type IV

Figure 103 – Crack width for settlement at the base of the façade and tower (scale in mm)

6.4 Load capacity assessment of the shells

As mentioned previously, in order to evaluate the load capacity of the shells under study, namely the barrel vault and the two lateral domes, a partial model was created, considering only the top part of the structure and the symmetry. In this model, the supporting piers and walls being simulated as rigid boundary conditions (vertical supports), with the movement in the horizontal direction being allowed. A static non-linear analysis was performed, in which the self-weight was increased systematically by steps of 10%. Figure 104 presents the displacements after the application of the self-weight loads, in which the highest displacements occurs at the centre of the barrel vault (1.9mm). The displacements of the dome, however, are almost null.

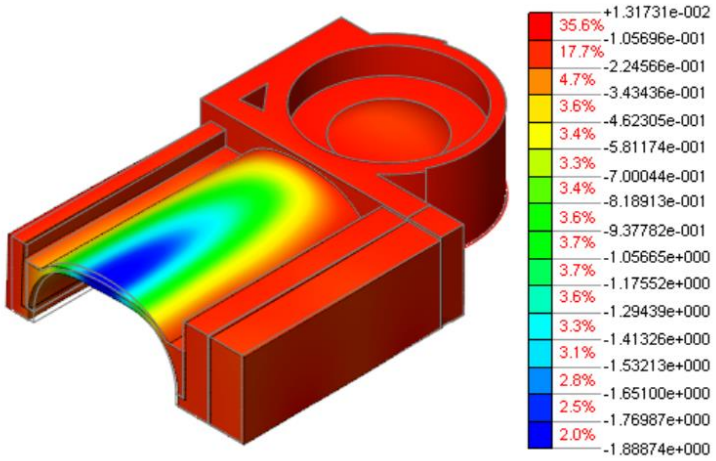

Figure 104 – Vertical displacements for the self-weight load (scale in mm)

After reaching the value of 100% of the self-weight, two distinct cases are analysed. The first case is related to the collapse of the barrel vault, hence the structure continued to be loaded with systematic increments of self-weight. Only the self-weight related to the vault and backing elements were included. The second case simulates only the increase of the self-weight for dome elements.

6.4.1. Barrel vault

In this case, the self-weight of the vault and the backing is systematically increased until reaching the collapse. A load factor is defined by the relation between the applied load and the self-weight of the vault. Due to the strong non-linear behaviour of this kind of structure, the line-search algorithm and arc-length method was adopted in the analysis of the barrel vault, aiming stabilise the convergence in the iteration process. In the final part of the analysis, two control points located in the thirds of the vault span were considered for the arc-length method, with the displacements controlled in the vertical direction.

Figure 105 presents the capacity curve of the structure in terms of vertical displacements of the central node of the dome and in terms of base opening. The damage pattern formed during the loading

process is also presented in terms of crack width. In the curves, a change in the response can be observed for the load factor of approximately 3.9. This behaviour represents the loss of stiffness due to formation of hinges. Analysing damage pattern for this load, the formation of two hinges can be observed, namely one at the intrados (middle of the vault) and a second at the extrados (connection between the internal backing and the vault). Another stiffness decrease is also presented close for the load factor equal to 7.5, characterizing the formation of the third hinge, also located at the extrados (connection between the vault and the external backing). Finally, the fourth hinge occurs for a load factor of 10.0, located at the base of the vault (internal side), indicating the loss of connection between the vault and the supporting piers. Without this connection, the rotation of the vault base is allowed.

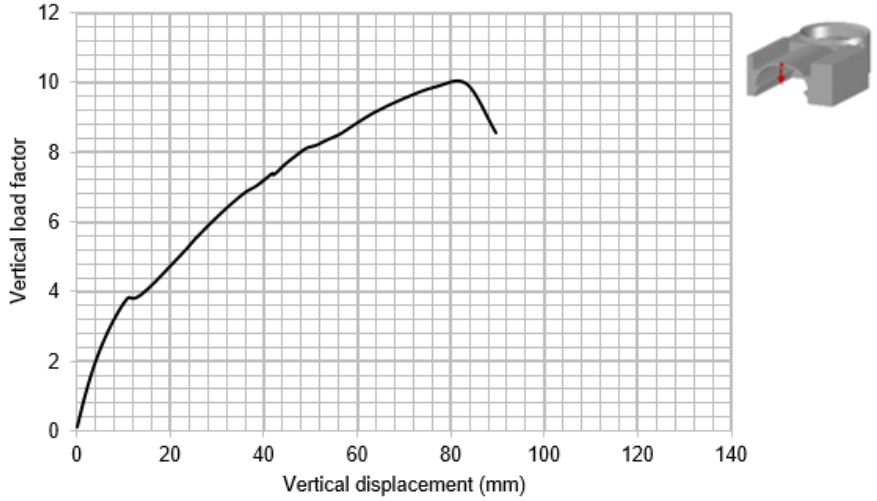

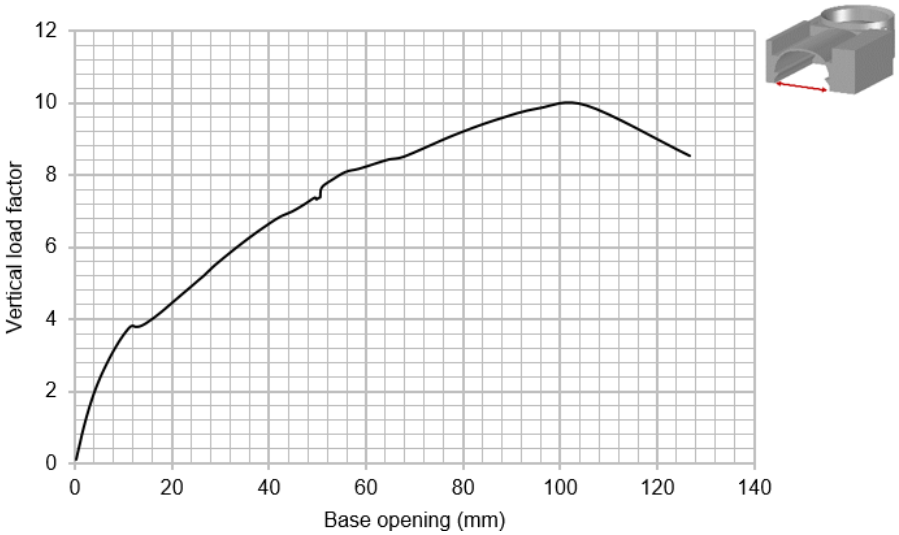

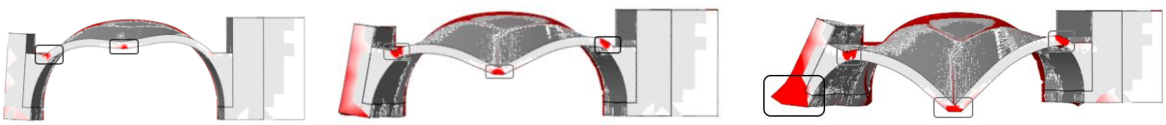

Two hinges are formed together (Load factor ~ 3.9)

Third hinge is formed (Load factor ~ 7.5)

Fourth hinge is formed - collapse (Load factor = 9.93)

Figure 105 – Capacity curve of the barrel vault (damage represented in red)

Since the vault has different supporting conditions on each side, the structure is not symmetric. Hence, four hinges are necessary to characterize a kinematic acceptable collapse mechanism, which can be observed in Figure 105. The crack pattern for the collapse is presented in Figure 106. The cracks related to the hinge formation can be observed. Furthermore, the crack at the middle of the vault separates in two diagonal cracks close to the wall. This is due to the difference of stiffness between the two elements (high in-plane stiffness of the masonry wall). A crack over the external pier and another crack separating the lateral external wall to the wall of the tower are also observed.

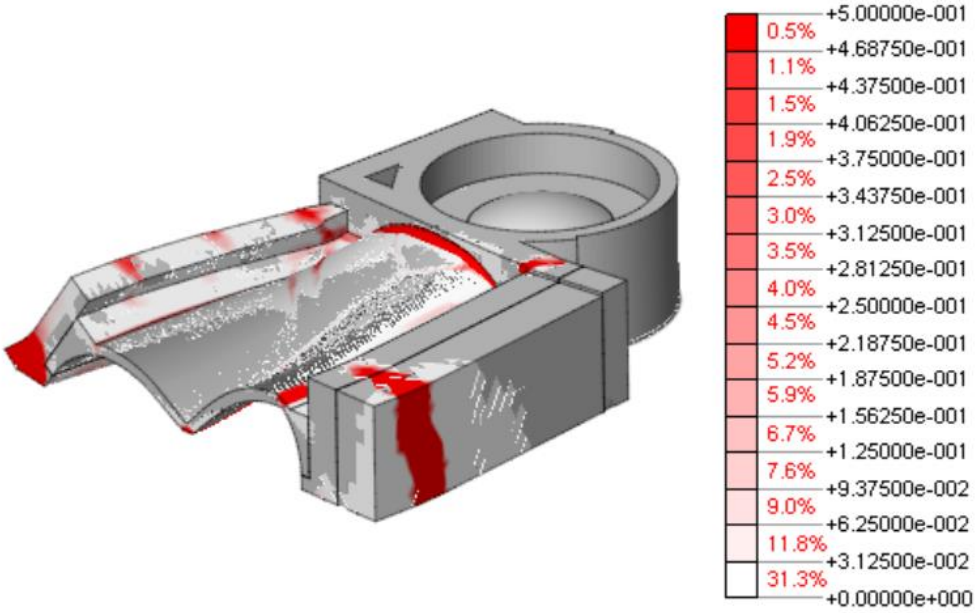

Figure 106 – Damage pattern for the collapse of the barrel vault (scale in mm)

6.4.2. Domes

The domes were firstly analysed with load increments due to self-weight of both shell and backing. However, the structure reached a load factor of approximately 20 and the damage was formed at the ring that marks the connection between the shell and the backing. Hence, a different strategy was assumed, considering only the self-weight of the shell, meaning the free span without considering the backing elements.

Figure 107 presents the capacity curve for the dome in terms of vertical displacements of a point located at the middle of the span. It is possible to observe a continuous decrease in the stiffness until reaching the value of approximately 104 of load factor. In this point, the change on the response is clear, showing a strongly reduction in the stiffness of the structure. Subsequently to this point, the structure is no longer able to absorb more vertical load. However, it must be noted that the structure is highly resistant to vertical loads, able of resisting more than 100 times its self-weight (self-weight of the free span).

The crack pattern for the collapse can be observed in Figure 108. Even for the case of increment of loads applied only in the shell elements, the damage is formed at the external ring of the dome, in the connection between the backing and the shell. The curved shape of the dome generates only compressive stresses under distributed load. Being masonry capable of resisting high compression stresses, the failure occurs in the connection between the dome and the backing, which is a horizontal element with stresses caused by shear and bending.

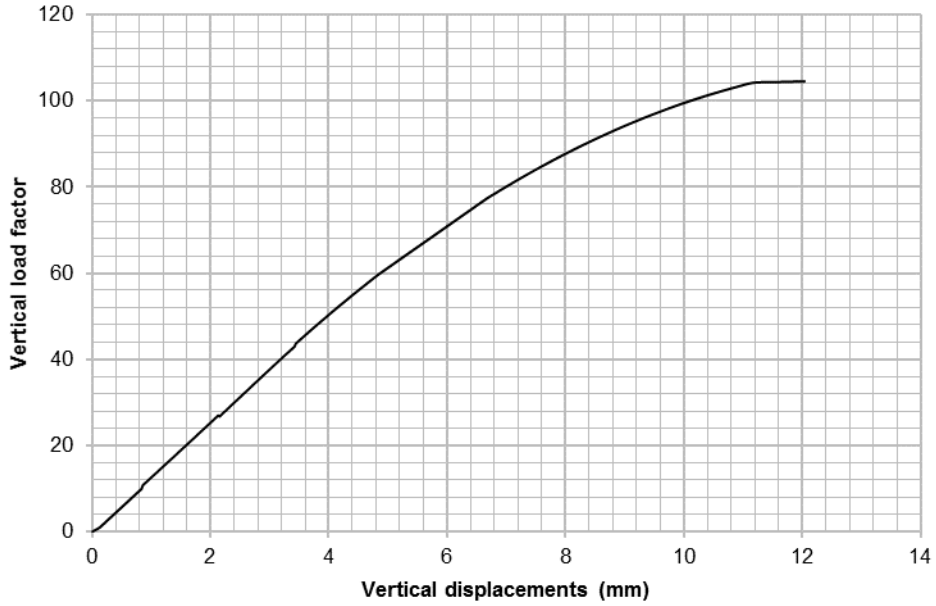

Figure 107 – Capacity curve of the dome

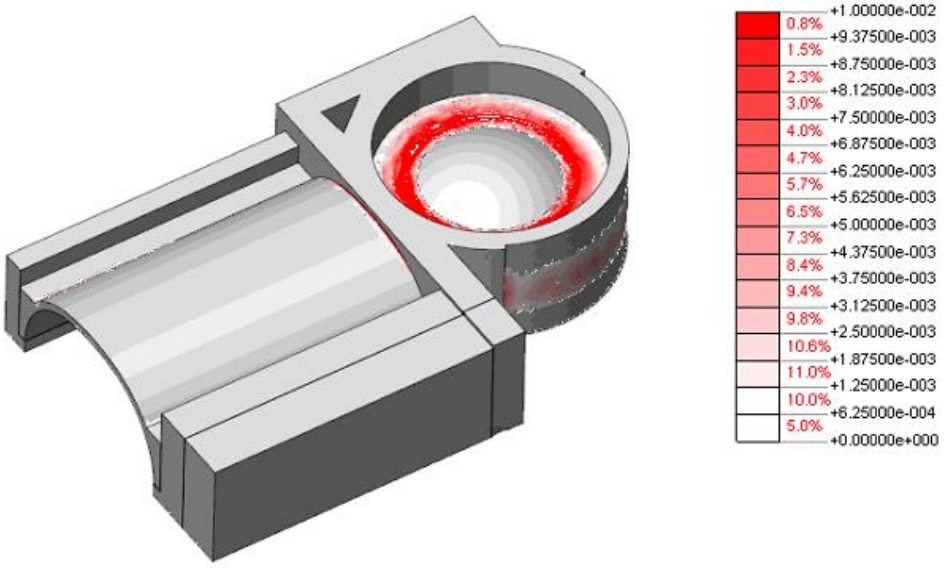

Figure 108 – Damage pattern for the collapse of the dome (scale in mm)

6.5 Evaluation on the effectiveness of the strengthening intervention

A strengthening intervention was performed in the shells under study in 1975 (Section 3.3), in which a layer of reinforced concrete was applied in the extrados of the shell, aiming at increasing its resistance. The study will be performed only for the barrel vault, since it presented lower load capacity than the domes (Section 6.4).

This section presents an evaluation on the effectiveness of such intervention, by applying a horizontal displacement at the external lateral support of the vault (span opening). Firstly, the dead load is applied. Then, the displacement in the base was increased monotonically until reaching the collapse of the structure. For this analysis, 2D models simulating a section of the vault were considered, for both unstrengthened and strengthened situations.

6.5.1. Unstrengthened model

Figure 109 presents the capacity curve in terms of vertical displacement of the node at the centre of the span and the horizontal loads associated to the applied displacement (horizontal reactions resultant from the prescribed displacements). The capacity curve in terms of horizontal displacements at the base is also present. Furthermore, Figure 109 shows the formation of hinges related to the changes in the path of the capacity curve.

In the capacity curve, a change on the response is observed for a load of approximately 5.1kN, representing a loss in the stiffness. In this point, the horizontal displacement at the base is 5mm. This phenomenon is related to the formation of two hinges in the connection between the shell element and the backings (extrados). From this point, the structure is no longer capable of absorbing higher loads. However, it is still presents capacity in terms of displacement. Hence, the horizontal displacement at the base is increased until approximately 7mm, the third hinge occurs at the middle of the span (intrados). The collapse mechanism of the unstrengthened model corresponds to a local failure of the vault with three hinges (curved shell at free span).

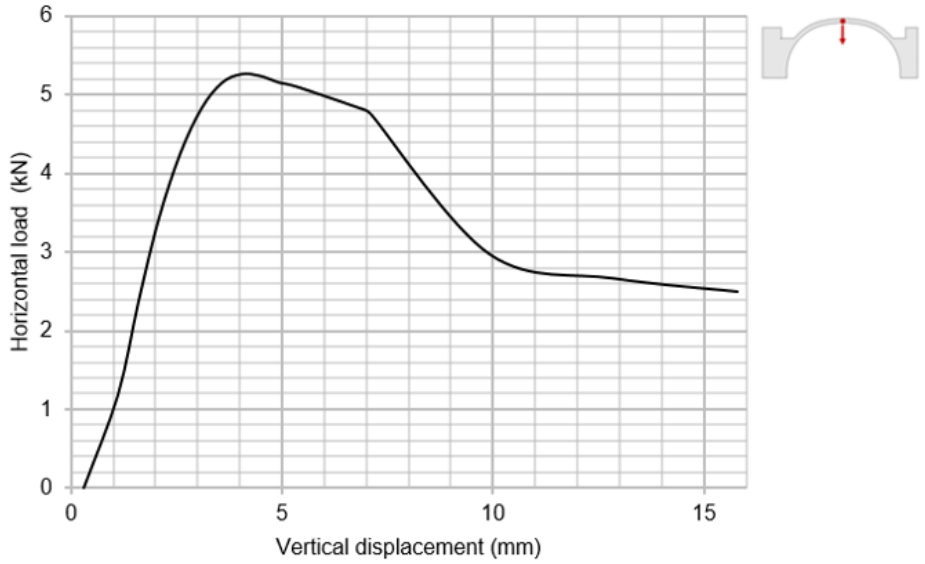

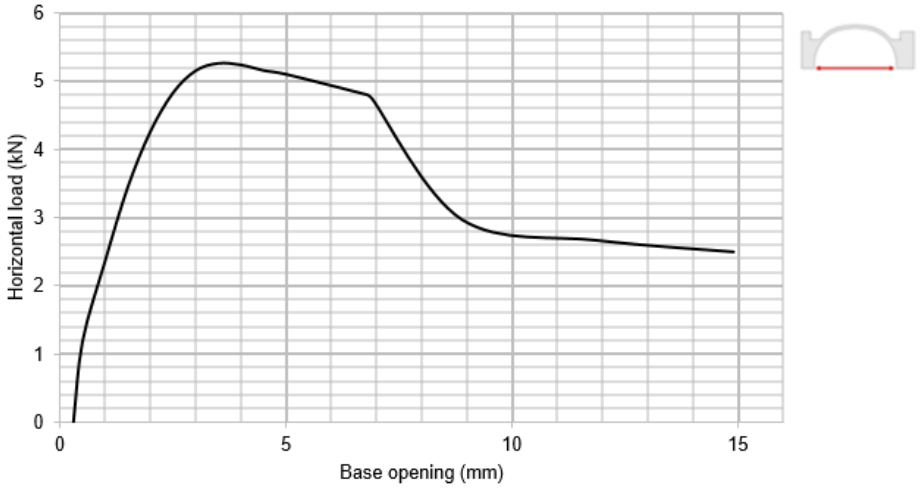

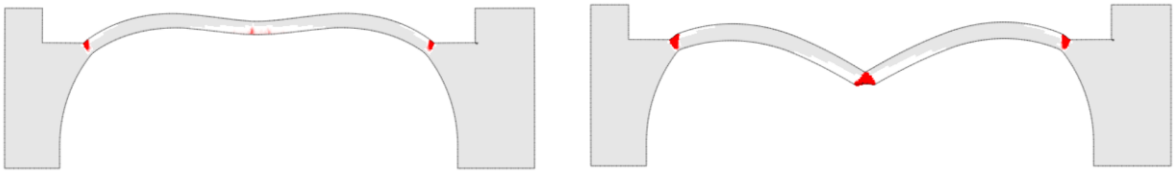

Two hinges are formed together
(Horizontal load ~ 5.1kN)
(Horizontal displacement ~ 5mm)

Third hinge is formed
(Horizontal load ~ 2.9kN)
(Horizontal displacement ~ 7mm)

Figure 109 - Formation of hinges in the unstrengthened model

6.5.2. Strengthened model

The concrete applied in the intervention is described as a high quality material (Schiros, 1975). However, little information is given related to the mechanical properties. Thus, two distinct classes of concrete were evaluated, namely concrete class C40, which is considered a high strength concrete for the time, and a regular C25 concrete. Additionally, the rebars of the reinforced concrete (vault and beams) were considered based on Von Mises failure criterion. However, the results of the non-linear analysis presented compressive stresses acting on the rebars. It is unlikely that the mesh works under compression, since it is made of very thin rebars, causing possible inappropriate results. Hence, a second material behaviour was considered for the rebars, in which null compressive strength was assumed. It was considered that the bond-split between the concrete and the rebars, and between concrete and masonry do not occur.

Figure 110 presents the capacity curve for the four situations described, namely the vault strengthened with concrete class C40 and class C25 and the two different material behaviours for the rebars. The capacity curve is presented in terms of base opening and the horizontal load at the right support (forces associated to the prescribed displacement). It can be observed that the response of the structure is very similar for the four cases analysed, until reaching the maximum load capacity of the structure. Until this point, the vault behaves with low and progressive damage, reaching a peak of approximately 25kN (span opening of 3mm). From this point on, the response of the structure differs mainly according due to different steel behaviour. For the Von Mises behaviour, the rebar present compressive stresses at the right beam, improving the capacity of this part of the model. As consequence of this behaviour, a crack occurs at the extrados of the right part of the vault. On the other hand, when a null compressive strength is assumed for the rebars, the damage at the connection between the right beam and the masonry increase its severity and no cracks are observed at the extrados of the vault. The different properties of the concretes assumed in this study have low influence on the response of the model, since the maximum compressive stress observed in the model is significantly lower than the compressive strength of both concretes. It is noted that in the post-peak response large steps were adopted for the analyses assuming that the rebars do not have compressive strength.

Figure 111 presents a comparison between the evolution of the crack pattern for the two types of steel behaviour. As mentioned previously, within the elastic range the behaviour of the two cases is similar. The damage is concentrated in two points: the centre of the vault from the intrados and the base on the left-side. This damage spreads in the post-peak situation forming hinges in these locations. After the peak-point, the structure behaves differently for the different behaviour of the steel. For the case with only tensile stresses on the rebars, cracks are formed at the connection between the right concrete beam and the masonry. These cracks spreads towards the intrados of the vault with the increase of displacements forming a third hinge in the model. In the Von-Mises behaviour, the rebars in the lateral beams work under compression, improving the response of the model at the section. For

this case, the damage appears firstly in an intermediate point of the vault (extrados). If the displacement increases, the damage at the connection between the right concrete beam and the masonry also appears.

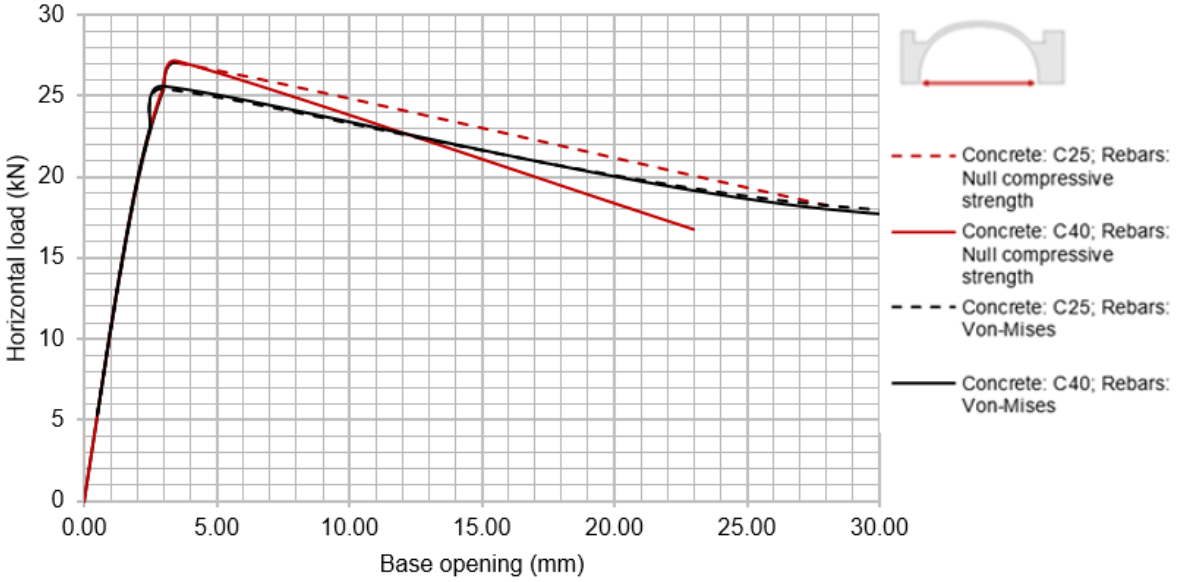

Figure 110 - Capacity curve of the strengthened vault using different assumptions for the rebars and concrete

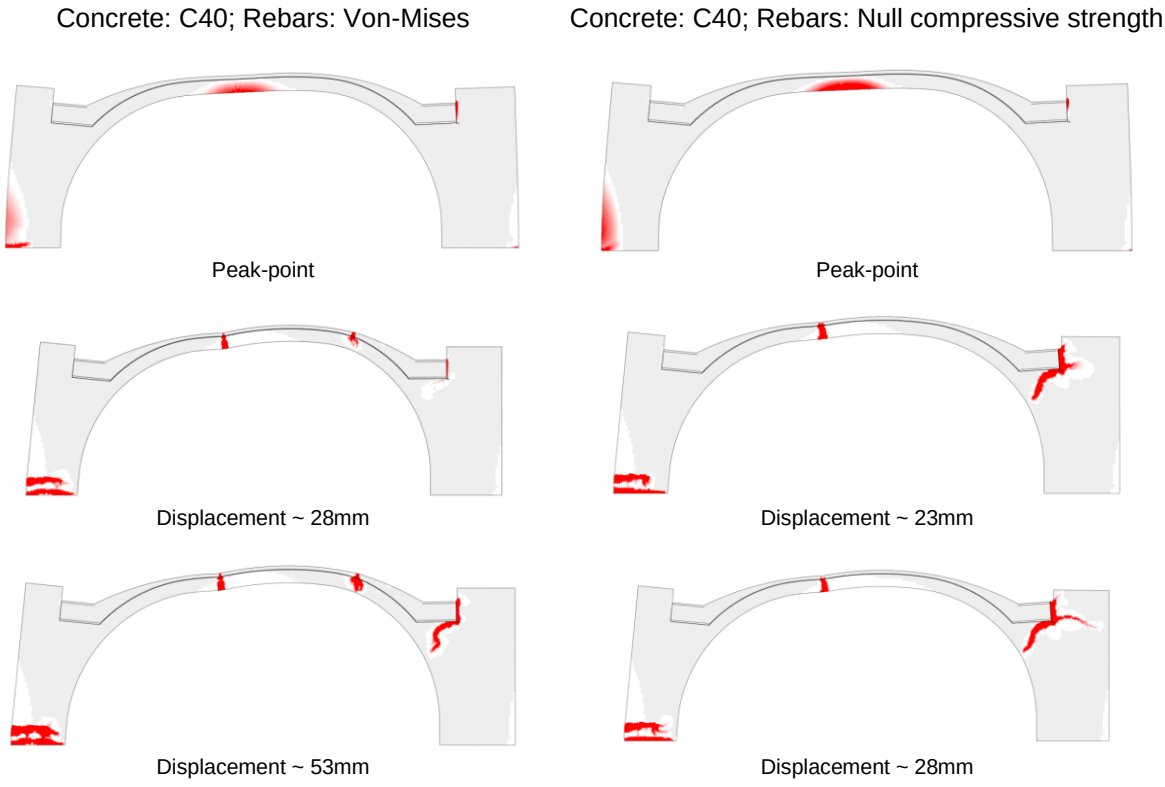

Figure 111 – Schematic evolution of crack pattern for the strenghtened vault

Figure 112 presents a comparison between the capacity curve of the strengthened and the unstrengthened models. The results show that the strengthening technique improve significantly the capacity of the structure (500%) and is able to prevent the two hinges at the extrados observed in the unstrengthened model (Figure 109). However, the strengthened vault presents a more brittle failure than the unstrengthened configuration.

Finally, the following aspects of the contribution of the reinforcement are highlighted:

- The increase of thickness in the connection between the backing and the shell, making a smooth variation of thickness and stiffness where previously there was a sudden change in the cross section. This was the first point where hinges were formed for the unstrengthened model.
- The increase of section at middle of the vault with a new layer improved the response, postponing the formation of hinge at this location for a higher load and horizontal displacement;
- The introduction of a tensile resistant component by the application of steel elements prevented the formation of the hinge at the extrados.

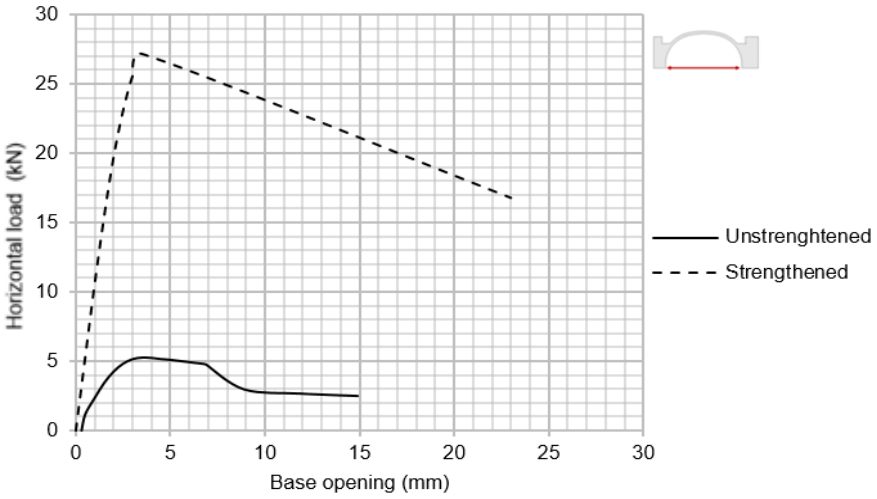

Figure 112 - Comparison between the capacity curves of the strengthened and unstrengthened models

7. CONCLUSIONS AND RECOMMENDATIONS

This thesis presented a detailed study on the behaviour of shells in the Municipal Theatre of Rio de Janeiro. In the development of this work, four main phases were carried out. The first phase consists in the literature review on the state of art of structural behaviour and numerical analysis of shell elements, together with historical and architectural research on the structure under study. The second step involved in-situ investigation on the structure, including visual inspection and NDT tests, such as dynamic identification tests. The information gathered in the first and second parts of the study were fundamental for the preparation of a numerical model (fourth task of the work). An eigenvalue analysis was carried out and the model was calibrated by comparing the numerical results with the experimental data obtained from the dynamic identification tests. Finally, a non-linear analysis was performed for the structure, aiming evaluate three main objectives: (i) the possible cause for the damage reported in the 1970s, taking into account the soil-structure interaction, (ii) the assessment of the load capacity under vertical loads and (iii) the evaluation of the strengthening intervention applied in 1975, by the analysis of the unstrengthened and strengthened conditions under a prescribed base displacement. As a result of the these works, the following conclusions and recommendations for further studies are presented:

- The inspection and diagnosis campaign allowed to identify important facets of the structural conditions. However, there are still several aspects that should be clarified, mainly regarding the soil properties, foundation elements and steel elements embedded in the masonry. Further studies should also be performed in order to confirm the hypothesis assumed in this study concerning the morphology of the shells, such as GPR, impact echo and sonic tests.
- The dynamic identification tests performed in this study allowed to estimate the elastic modulus of masonry materials by the calibration of the numerical model with the experimental results. However, these results should be validated by other methods. NDT and MDT tests could be carried out for this purpose, such as sonic tests and double flat jack tests.
- The numerical model prepared in this study considers only the front part of the theatre where the shells are located. The contact with other parts of the structure was simulated by elements with normal stiffness. A global model of the structure should be made in order to have a full understanding on the global behaviour of the structure. Furthermore, with a full model it is possible to calibrate the other global modes that are not clear in the partial model.
- The non-linear analysis carried out to study the soil-structure interaction presented relevant results in terms of crack pattern related to each scenario of differential settlement, identifying possible causes for the damages in the structure. The assumption of a decrease of the stiffness of the soil at the base of main façade and tower presents the crack pattern more

similar to the damage that led to the intervention in 1975. However, this analysis reached only the beginning of damage pattern. Due to lack of information regarding the foundation and soil conditions, a simplified approach for simulating the foundation conditions was adopted. It is recommended further studies in this assumption, including the foundation elements in the 3D model, as well as the soil characteristics, in order to properly determine the severity caused by possible differential settlements for which the structure may have been submitted. An analysis considering differential settlement between the side facing Treze de Maio Avenue and the side facing Rio Branco Avenue should also be performed, to evaluate possible decrease on soil stiffness due to the opening of the ditch during the construction of the metro in the 1970s.

- The structural capacity of the shells was assessed for self-weight loading, leading to the conclusion that the structure is able of resisting high levels of vertical loads. These shells, mainly the dome, are curved elements that act mainly under compressive stresses. Distributed loads increase the confinement of these elements, increasing their behaviour. Other types of loads could be applied for the shell such as horizontal forces or point loads, in order to have a full estimation on the structural capacity.
- The analysis of the unstrengthened and strengthened models of the dome showed that the reinforced concrete layer and beams applied in 1975 improved significantly the performance of the dome, in which an increase of about 500% on the load capacity for a prescribed horizontal displacement at the base was observed. The strengthening technique presented a different collapse mechanism with respect to the unstrengthened model, preventing the two hinges at the connection with the backing (cracking at the extrados). One again, other types of loading should be evaluated, such as point loads.

REREFENCES

Andreu, A., Gil, L., & Roca, P. (2006). Limit Analysis of Masonry Constructions by 3D Funicular Modelling. *Structural Analysis of Historical Constructions*, 1135–1142.

Arun, G. (2006). Behaviour of Masonry Vaults and Domes : Geometrical Considerations.

Azevedo, J., Sincraian, G., & Lemos, J. V. (2000). Seismic behavior of blocky masonry structures. *Earthquake Spectra*, *16*(2), 337–365.

Barthel, R. (1993). *Structural preservation of the architectural heritage*. Zürich: IABSE.

Bates, W. (1987). *Historical Structural Handbok - Steelwork*. (T. C. P. Limited, Ed.) (4th ed.). London.

Binda, L., Chesi, C., & Parisi, M. A. (2010). Seismic damage to churches: observations from the L'Aquila, Italy, earthquake and considerations on a case-study. *Advanced Materials Research*, *133–134*, 641–646.

Block, P. (2005). Equilibrium systems. *Architectural Engineering*, 1–42.

Block, P., & Lachauer, L. (2014). Three-Dimensional (3D) Equilibrium Analysis of Gothic Masonry Vaults. *International Journal of Architectural Heritage*, *8*(3), 312–335.

Blondel, F. (1675). *Cours d'architecture*. (L. Roulland, Ed.). Paris.

Borri, A., Corradi, M., & Castori, G. (2015). A method for the analysis and classification of historic masonry. *Bulletin of Earthquake Engineering*, 2647–2665.

Brunelleschi's Dome: Florence Cathedral, Florence Duomo. (n.d.). Retrieved from http://www.brunelleschisdome.com/

Calderini, C. (2004). The effect of the masonry pattern on the global behaviour of vaults. *Proceedings of the 4th International Conference on Structural Analysis of Historic Construction*, 619–628.

Canhão, R. (n.d.). *Dynamic Analysis of the Masonry Arch The Effect of the Extrados Filling*. Instituto Superior Técnico.

Cattari, S., Resemini, S., & Lagomarsino, S. (2008). Modelling of vaults as equivalent diaphragms in 3D seismic analysis of masonry buildings. *Structural Analysis of Historic Construction*.

Cauvin, A., & Stagnitto, G. (1993). Problems concerning strength assessment and repair of Historical Vaulted Structures. In: Public assembly structures from antiquity to the present. In *Public assembly structures from antiquity to the present*. Istanbul: IASS.

CEB. CEB-FIP Model code 1990 (1991). Lausanne, Switzerland: Comite Euro-International du Beton.

Cerne Engenharia e Projetos. (2006a). Restauração da Cobertura de Cobre - Fase 1 - Levantamento da estrutura da cobertura - Cúpula. Fundação Theatro Municipal do Rio de Janeiro.

Cerne Engenharia e Projetos. (2006b). Restauração da Cobertura de Cobre - Fase 1 - Levantamento da estrutura da cobertura - Rotunda Rio Branco. Fundação Theatro Municipal do Rio de Janeiro.

Cerne Engenharia e Projetos. (2006c). Restauração da Cobertura de Cobre - Fase 1 - Levantamento da estrutura da cobertura - Telhado Frontal. Fundação Theatro Municipal do Rio de Janeiro.

Cerne Engenharia e Projetos. (2006d). Restauração da Cobertura de Cobre - Fase 2 - Levantamento e análise estrutural da área nobre - Corte Longitudinal. Fundação Theatro Municipal do Rio de Janeiro.

Cerne Engenharia e Projetos. (2006e). *Restauração da cobertura de cobre e modernização das intalações – Fase II Volume I Relatório de Vistoria* (Vol. I).

Cintra, D. C. B. (2018). *Monitoramento estrutural de cascas históricas*. To be edited by PUC-Rio, 2018, Rio de Janeiro, Brazil.

Cintra, D. C. B., Roehl, D. M., Filho, E. S. S., Santos, M. F. S. F., Filizola, G., & Assumpção, M. S. (2017). Structural Intervention Case in the Theatro Municipal do Rio de Janeiro. In

3rd International Conference on Protection of Historical Constructions. Lisbon.
Coulomb, C. A. (1773). Essai sur une application des régles de maximis et minimis à quelques problémes de statique relatifs à l'architecture. *Mémoires de Mathématique et de Physique, Présentés À l'Académie Royale Des Sciences Par Divers Savants et Lus Dans Ses Assemblées (Paris)*, *7*, 343–382.
Couplet, P. (1729). De la poussée des voûtes. In *émoires de l'Académie Royale des Sciences de Paris* (pp. 79–117).
Croci, G. (1998). The Basilica of St Francis of Assisi after the September 1997 earthquake. *Struct Eng Int*, *8*(1), 56–58.
Croci, G. (2006). Seismic behaviour of masonry domes and vaults Hagia Sophia in Istanbul and St. Francis in Assisi. *First European Conference on Earthquake Engineering and Seismology*, (September), 1–21.
Cundall, P. A., & Hart, P. (1971). Computer model for simulating progressive large scale movements in blocky rock systems. In *Symposium of the international society of rock mechanics*. Nancy.
D'Ayala, D., & Casapulla, C. (2001). Limit state analysis of hemispheri-cal domes with finite friction. In *Structural Analysis of Historical Constructions*. Guimarães.
De La Hire, P. (1712). Sur la construction des voûtes dans les édifices. *Mémoires de l'Académie Royale Des Sciences de Paris*, 70–78.
Derand, F. (1643). *L'architecture des voûtes, ou l'art des traits et coupes des voûtes*. Paris.
Douglas, B. M., & Reid., W. H. (1982). Dynamic tests and system identification of bridges. *Journal Struct. Div. (ASCE)*, *108*, 2295–2312.
Eder Santos Carvalho. (2012). Iluminação devolve glamour ao Teatro Municipal do Rio de Janeiro. Retrieved April 11, 2017, from http://historiaearquitetura.blogspot.pt/2012_12_01_archive.html
Eliseu Visconti - Site oficial do pintor. (n.d.). Retrieved April 10, 2017, from http://www.eliseuvisconti.com.br/Site/Obra/PrimeiroAto.aspx
Elyamani, A. (2015). *Integrated monitoring and structural analysis strategies for the study of large historical construction. Application to Mallorca cathedral*. Universitat Poltecnica de Catalunya.
Feilden, B. M. (1982). *Conservation of Historic Buildings*. London: Butterworth Scientific.
Fray Lorenzo. (1639). *Arte y uso de architectura*.
Fundação de Teatros do Rio de Janeiro (FUNTERJ). (1977). Vistoria do prédio do Theatro Municipal do Rio de Janeiro – Considerações Gerais. Rio de Janeiro.
Fundação Theatro Municipal do Rio de Janeiro. (2006). Levantamento métrico e digitalização das plantas e cortes. Fundação Theatro Municipal do Rio de Janeiro.
Fundação Theatro Municipal do Rio de Janeiro. (2016). História – Theatro Municipal do Rio de Janeiro. Retrieved April 7, 2017, from http://www.theatromunicipal.rj.gov.br/sobre/historia/
Gaetani, A. (2016). *Seismic Performance of Masonry Cross Vaults : Learning from Historical Developments and Experimental Testing*. Universidade do Minho and Sapienza Università di Roma.
Gelms, M. (2015). Origin and Use of Roman Engineering. Retrieved April 18, 2017, from https://engineeringrome.wikispaces.com/Origin+and+Use+of+Roman+Engineering
Gilbert, M., Casapulla, C., & Ahmed, H. M. (2006). Limit analysis of masonry block structures with non-associative frictional joints us-ing linear programming. *Comput. Struct.*, *84*, 873–887.
Giovanetti. (2000). *Manuale del recupero del Comune di Città di Castello*. Rome.
Google Maps. (2017). Retrieved April 10, 2017, from https://www.google.pt/maps/@-22.9098987,-43.1762254,538m/data=!3m1!1e3?hl=pt-BR
Great Buildings Image - Pantheon. (n.d.). Retrieved from http://www.greatbuildings.com/cgi-

bin/gbi.cgi/Pantheon.html/cid_1202711678_pantheon_0005.html
Heyman, J. (1966). The stone skeleton. *International Journal of Solids and Structures*, *2*, 249–279.
Heyman, J. (1982). *The Masonry Arch*. (John Wiley & Sons Inc., Ed.), *Structural Analysis*. New York. https://doi.org/10.1017/CBO9780511529580.006
Heyman, J. (1995). *The stone skeleton: Structural engineering of masonry architecture*. Cambridge University Press.
Hojdys, Ł., & Krajewski, P. (2014). Buried vaults with different types of extrados finishes – Experimental tests. In *SAHC* (pp. 14–17).
Hooke, R. (1675). *Description of helioscopes, and some other instruments*. London.
Hourihane, C. (2012). *The Grove encyclopedia of medieval art and architecture*. Oxford University Press.
Huerta, S. (2001). Mechanics of masonry vaults: The equilibrium approach. *3rd International Seminar in Historical Constructions, Guimarães, Portugal*, (February), 47–70.
Huerta, S. (2004). *Arcos, bóvedas y cúpulas. Geometría y equilibrio en el cálculo tradicional de estructuras de fábrica*. (I. J. de Herrera, Ed.). Madrid.
Huerta, S. (2007). Oval Domes: History, Geometry and Mechanics. *Nexus Network Journal*, *9*(2), 211–248. Retrieved from http://link.springer.com/10.1007/s00004-007-0040-3
Humanities I Test 1 Images. (n.d.). Retrieved April 18, 2017, from http://www.humanitiesresource.com/lecture/hum2210_test1.htm
Lemos, J. V. (1998). Discrete element modeling of the seismic behavior of stone masonry arches. *Pande G et Al (Eds) Computer Methods in Structural Masonry*, *4*, 220– 227.
Long Life of Catenary. (n.d.). Retrieved from https://www.schillerinstitute.org/fid_02-06/031_long_life_catenary.html
Lopez, J., Oller, S., Oñate, E., & Lubliner, J. (1999). A homogeneous constitutive model for masonry. *Int J Numer Methods Eng*, *46*, 1651–1671.
Lourenço, P. B. (1996). *Computational strategies for masonry structures*. *PhD Thesis* (Vol. 70). https://doi.org/ISBN 90-407-1221-2
Lourenço, P. B. (1997). An anisotropic macro-model for masonry plates and shells: implementation and validation. *TU-DELFT Report No. 03.21.1.31.07*, (3), 102.
Low, K. N. (2011). Engineering the Pantheon - Architectural, Construction, & Structural Analysis. Retrieved April 18, 2017, from https://engineeringrome.wikispaces.com/Engineering+the+Pantheon+-+Architectural,+Construction,+%26+Structural+Analysis
Lucchesi, M., Padovani, C., Pasquinelli, G., & Zani, N. (2007). Statics of masonry vaults, constitutive model and numerical analysis. *J Mech Mater Struct*, *2*(2), 221–244.
Machado, E. P. (2012). *A cobertura do Theatro Municipal do Rio de Janeiro : restauração ou reconstrução?* Instituto do Patrimônio Histótico e Artístico Nacional.
Mainstone, R. J. (Rowland J. . (2001). *Developments in structural form* (2nd ed.). Abingdon, England: Architectural Press. Retrieved from https://books.google.com/books?id=l6fLIUFJhxwC
Mamaghani, I. H. P., Aydan, O., & Kajikawa, Y. (1999). Analysis of masonry structures under static and dynamic loading by discrete finite element method. *Struct Eng/Earthq Eng JSCE*, *16*(2), 75–86.
Mapa de Cultura RJ. (n.d.). Theatro Municipal do Rio de Janeiro | Mapa de Cultura RJ. Retrieved April 10, 2017, from http://mapadecultura.rj.gov.br/manchete/theatro-municipal-do-rio-de-janeiro-2#prettyPhoto
Maynou, J. (2001). *Estudi estructural del pòrtic tipus de la Catedral de Mallorca mitjançan l'estàtica gràfica*. Universitat Politècnica de Catalunya.
Mazziotti, A. (2016). *Structural Analysis of Historic Masonry Buildings*. University of Naples Federico II.
Mendes, N. A. L. (2012). *Seismic Assessment of Ancient Masonry Buildings : Shaking Table*

Tests and Numerical Analysis. University of Minho.
Mendes, N., Costa, A. A., Lourenço, P. B., Bento, R., Felice, G. De, Gams, M., … Felice, G. De. (2017). Methods and Approaches for Blind Test Predictions of Out-of-Plane Behavior of Masonry Walls : A Numerical Comparative Study Methods and Approaches for Blind Test Predictions of Out-of-Plane Behavior of Masonry Walls : A Numerical Comparative Study. *International Journal of Architectural Heritage*, *11*(1), 59–71.
Méry, E. (1840). Mémoire sur l'equilibre des voûtes en berceau. In *Annales des Ponts et Chaussées* (pp. 50–70).
Milani, E., Milani, G., & Tralli, A. (2008). Limit analysis of masonry vaults by means of curved shell finite elements and homogenization. *International Journal of Solids and Structures*, *45*(20), 5258–5288.
Milani, G., Lourenço, P., & Tralli, A. (2007). 3D homogenized limit analysis of masonry buildings under horizontal loads. *Engineering Structures*, *29*(11), 3134–3148.
Misseri, G., Rovero, L., & Feo, L. (2016). Experimental investigation on masonry arches strengthened with PBO-FRCM composite. *Composites Part B*, *100*(July), 228–239.
Moseley, H. (1833). On a new principle in statics, called the principle of least pressure. *Philosophical Magazine*, *3*, 285–288.
Navascués Palacio, P. (1974). *El libro de arquitectura de Hernán Ruiz el Joven. Estudio y edición crítica*. Madrid: Escuela Técnica Superior de Arquitectura.
NTC-08. (2008). Decreto Ministeriale 14 gennaio 2008: Nuove Norme Tecniche per le Costruzioni.
O'Dwyer, D. (1999). Funicular analysis of masonry vaults. *Computers and Structures*, *73*(1–5), 187–197. https://doi.org/10.1016/S0045-7949(98)00279-X
O Globo. (1996). Construção do metrô do Rio | Acervo. Retrieved April 19, 2017, from http://acervo.oglobo.globo.com/fotogalerias/construcao-do-metro-do-rio-9372304
Oñate, E., Hanganu, A., Barbat, A., Oller, S., Vitaliani, R., Saetta, A., & Scotta, R. (1995). Structural analysis and durability assessment of historical constructions using a Finite Element Damage Model. *Structural Analysis of Historic Construction: Possibilities of Numerical and Experimental Techniques*, *111*, 189–224.
Onion Dome Creator | SketchUp Extension Warehouse. (n.d.). Retrieved from https://extensions.sketchup.com/ru/content/onion-dome-creator
Orduña, A., & Lourenço, P. B. (2005). Three-dimensional limit analysis of rigid blocks assemblages. Part I: Torsion failure on frictional interfaces and limit analysis formulation. *International Journal of Solids and Structures*, *42*(18–19), 5140–5160.
Ottoni, F., Coïsson, E., & Blasi, C. (2010). The crack pattern in Brunelleschi's dome in Florence: damage evolution from historical to modern monitoring system analysis. *Advanced Materials Research*, *133–134*, 53–64.
Pagnoni, T. (1994). Seismic analysis of masonry and block structures with the discrete element method. In *10th European conference on earthquake engineering* (pp. 1674–1694).
Palladio, A. (1570). *Quattro libri dell'Architettura* (Dominico d). Venice.
Panoramio. (2014). Panoramio - Photo of Theatro Municipal do Rio de Janeiro - Fachada lateral. Retrieved April 10, 2017, from http://www.panoramio.com/photo/109211696
Pelà, L. (2009). *Continuum Damage Model for Nonlinear Analysis of Masonry Structures*. echnical University of Catalonia, University of Ferrara.
Pettraca, M. (2016). *Computational multiscale analysis of masonry structures*. Thecnical University of Catalonia.
Pluijm, R. van der. (1999). *Out-of-Plane Bending of Masonry Behaviour and Strength*. (T. U. Eindhoven, Ed.). Eindhoven.
Ràfols, J. F. (1929). Gaudí. Barcelona.
Ramírez, R. (2016). *Structural analysis of the church of the Monastery of São Miguel de*

Refojos. University of Minho.
Ramos, J. L. F. da S. (2007). *Damage Identification on Masonry Structures Based on Vibration Signatures*. University of Minho.
Rankine, W. J. M. (1858). *Manual of Applied Mechanics*. (C. Griffin, Ed.) (3a ed.). London.
Roca, P., Cervera, M., Gariup, G., & Pela, L. (2010). Structural analysis of masonry historical constructions. Classical and advanced approaches. *Archives of Computational Methods in Engineering*, *17*(3), 299–325. https://doi.org/10.1007/s11831-010-9046-1
Sainte Chapelle: The Radiating Cathedral. (n.d.). Retrieved June 12, 2017, from https://shan4.wordpress.com/tag/rib-vault/
Santos, J. M. M. dos. (2014). Constructive and Structural Behaviour of Tiled Vaults, (October).
Schiros, L. M. (1975). Recuperação estrutural das cúpulas do foyer do Theatro Municipal do Rio de Janeiro. In *Colóquio sobre Patologia do concreto e recuperação estrutural* (pp. 189–204). São Paulo: IBRACON.
Secretaria de Cultura. (2017). Cultura.rj | Espaços Culturais - Theatro Municipal do Rio de Janeiro. Retrieved April 10, 2017, from http://www.cultura.rj.gov.br/apresentacao-espaco/theatro-municipal-do-rio-de-janeiro
Simeone, A. (2002). Teatro Municipal do Rio de Janeiro: uma leitura representativa. *SIGraDi - Iberoamerican Congress of Digital Graphics*, 67–70.
Sincraian, G. E. (2001). *Seismic behaviour of blocky masonry structures. A discrete element method approach*. IST.
SkyscraperCity. (2011). Theatro Municipal do Rio de Janeiro - 1909/2011 - 102 Aanos de glórias. Retrieved April 10, 2017, from http://www.skyscrapercity.com/showthread.php?t=905790
Structural geometry | Geometrica. (n.d.). Retrieved from http://geometrica.com/en/arquitectonico/geometry
SVS. (2014). ARTeMIS Extractor Pro User Manual, Release 5.0, Structural Vibration Solutions. Aalborg, Denmark.
TNO DIANA BV. (2017). DIANA Finite Element Analysis User's Manual Release 10.1. Delft.
Tomazevic, M. (1999). *Earthquake-resistant and design of masonry buildings*. London: Imperial College Press.
Tralli, A., Alessandri, C., & Milani, G. (2014). Computational methods for masonry vaults: A review of recent results. *Open Civil Engineering Journal*, *8*(1), 272–287. Retrieved from http://www.scopus.com/inward/record.url?eid=2-s2.0-84923118587&partnerID=tZOtx3y1
Vouga, E., Höbinger, M., Wallner, J., & Pottmann, H. (2012). Design of self-supporting surfaces. *ACM Transactions on Graphics*, *31*(4), 1–11.
What is saucer dome? definition and image. (n.d.). Retrieved from http://www.dictionaryofconstruction.com/definition/saucer-dome.html
Winkler, E. (1880). Die Lage der Stützlinie im Gewölbe. *Deutsche Bauzeitung*, *13*, 117–119, 127–128, 130.
Wren, C. (1750). *Parentalia: or, Memoirs of the Family of the Wrens*. London: Stephen Wren.
Zucchini, A., & Lourenço, P. B. (2009). A micro-mechanical homogenisation model for masonry: Application to shear walls. *International Journal of Solids and Structures*, *46*(3–4), 871–886.